DOCTORAL THESIS

Phase Equilibria of Complex Mixture in the Context of Unconventional Fuel Resources

Parsa Mozaffari

TALLINN UNIVERSITY OF TECHNOLOGY
DOCTORAL THESIS
61/2022

Phase Equilibria of Complex Mixture in the Context of Unconventional Fuel Resources

PARSA MOZAFFARI

TAL
TECH
PRESS

TALLINN UNIVERSITY OF TECHNOLOGY
School of Engineering
Department of Energy Technology
This dissertation was accepted for the defense of the degree 22/09/2022

Supervisor: Senior Researcher Oliver Järvik
School of Engineering
Tallinn University of Technology
Tallinn, Estonia

Co-supervisor: Researcher Zachariah Steven Baird
School of Engineering
Tallinn University of Technology
Tallinn, Estonia

Opponents: Prof. Omar S. Al-Ayed
Department of Chemical Engineering
Faculty of Engineering Technology
Al-Balqa Applied University
Amman, Jordan

Dr. Indrek Aarna
Head of Development Department
Viru Keemia Grupp
Kohtla Järve, Estonia

Defence of the thesis: 25/10/2022, Tallinn

Declaration:
Hereby I declare that this doctoral thesis, my original investigation and achievement, submitted for the doctoral degree at Tallinn University of Technology has not been submitted for doctoral or equivalent academic degree.

Parsa Mozaffari

_____
signature

Komplekssete segude faaside tasakaalud mittekonventsionaalsete energiaallikate tehnoloogiates

PARSA MOZAFFARI

Contents

List of publications

The list of author's publications, in which this thesis has been prepared:

I   Mozaffari, P.; Baird, Z. S.; Listak, M.; Oja, V. (2020). Vapor pressures of narrow gasoline fractions of oil from industrial retorting of Kukersite oil shale. Oil Shale. 37(4), 288–303.

II   Mozaffari, P.; Järvik, O.; Baird, Z. S. (2020). Vapor Pressures of Phenolic compounds Found in Pyrolysis Oil. Journal of Chemical & Engineering data, 65 (11), 5559–5566.

III Mozaffari, P.; Baird, Z. S.; Järvik, O. (2022). A Predictive Approach towards Using PC-SAFT for Modeling the Properties of Shale Oil. Materials, 15 (12), 4221.

Author's contribution to the publications

Contribution to the papers in this thesis are:

I The author carried out the experiments, analyzed the data and contributed to writing the article.

II The author carried out the experiments, analyzed the data and wrote the article.

III The author contributed to developing the procedure, analyzed the data and writing the article.

Introduction

Oil shale is a type of rock that contains organic matter. Organic component of oil shale is mostly kerogen (macromolecular matter of oil shale) which, can be converted into valuable products such as fuel and industrial chemicals, etc. (Dyni, 2003). This conversion is usually achieved using thermal treatment (pyrolysis) at temperatures around 500 °C (Vahur Oja et al., 2016; Vahur Oja & Suuberg, 2012). Conventional crude oils have been widely studied and therefore, important thermodynamic data required for product development as well as transportation properties have been comprehensively investigated. While global shale oil deposits are vast, these reserves were mostly remained unrecovered due to challenges that exist both technically and environmentally.

In order to economically exploit the shale oil deposits, characteristic of shale and thermodynamic properties of shale oil are of importance (Baird, Zachariah et al., 2015). These data can be employed in design and operation of oil production plants and refineries as well as storage, transportation and environmental protection evaluation (Pichler & Lutz, 2014; Raj, 2016; Mohammad R. Riazi & Al-Enezi, 1999). In this regard, compared with conventional crude oil, considerably less shale oil properties data is available in literature (Ge et al., 2019a; S. Lee, 1990; Vahur Oja & Suuberg, 2012; Yu et al., 2019). Estonian Kukersite shale oil is not an exception. Comparatively, while the presence of olefin is not common in crude oil, shale oil has a significant amount of olefin in addition to aromatic compounds. Moreover, shale oil produced from Kukersite oil shale contains great amount of hetroatomic compounds. The heteroatoms were observed to be less in lighter fractions (gasoline fractions up to 200 °C) and similarly, phenolic compounds were considered to be insignificant in light portions of oil. Therefore, for analysis, the presence of phenolic compounds were considered negligible for fractions up to 180 °C (Zachariah Steven Baird et al., 2021).

These complex mixtures (shale oil) and vaporization target compounds from these complex matrices were selected for studies. This work carried out for studying and modelling industrial Kukersite shale oil fractions that were produced through solid heat carrier pyrolysis process (Galoter).

Modelling shale oil has not gained much attention despite the fact that shale oil composition and properties differ from conventional oil and therefore, correlations, and models developed for conventional oil most likely are not applicable to shale oil and more specifically Kukersite shale oil (Zachariah S Baird et al., 2017; Zachariah Steven Baird et al., 2015; R Rannaveski & Listak, 2018; Rivo Rannaveski, 2018). As explained before, due to compositional difference, different approaches have to be used to develop a model for this type of oil. Moreover, the composition of classes of compounds are varying so much that suggested correlations unlikely be of use for these types of shale oils. In general, compositions of Kukesite shale oil were provided previously elsewhere (Aarna et al., 1953; Barschevski et al., 1963; Blinova et al., 1974; O. G. Eisen & Rang, 1968; V. Oja et al., 2006). In this regard, several properties of narrow boiling range Kukersite shale oil fractions (as pseudocomponents) obtained experimentally were used for modelling. To model the Kukersite shale oil, PC-SAFT equation of state was used at which, measured properties (vapor pressure, liquid density) could be used to fit the PC-SAFT parameters to propose a model for predicting the phase behavior of these types of oils.

Thus, in this study, primarily, the applicability of vapor pressure correlations developed for conventional oil were assessed for Kukersite shale gasoline. In this respect, Kukersite shale oil gasoline was distilled into fractions with average boiling point from

about 40 to 180 °C. Then, these fractions were as well used for modelling the Kukersite shale oil gasoline and further on, Kukersite shale oil as a whole using PC-SAFT equation of state independently, considering that the presence of phenolic compounds in gasoline fractions up to 180 °C can be neglected and the composition of other classes of compounds varies. For heavier fractions, the interaction parameter between phenolic compounds was also considered and found through optimization. In general, for crude oils non-associating term were not considered. Besides, characterization was mostly performed using SARA analysis (Saturates, Aromatics, Resins, Asphaltenes) based approach which is more commonly used method in characterization of crude oil for PC-SAFT asphaltene precipitation modeling. It was also seen that aromaticity parameter were also taken into account in various correlations developed for such oils (Seitmaganbetov et al., 2021). While modeling the conventional oils have already been assessed for a longer period, developing a distinct model for Kukersite shale oil was not studied as much broadly.

Abbreviations

ABP	Average Boiling Point
API	American Petroleum Institute
ARD	Average Relative Deviation
ASTM	American Society for Testing and Materials
CAS RN	Chemical Abstracts Service Registry Number
DSC	Differential Scanning Calorimetry
EoS	Equation of State
GC	Gas Chromatography
H/C	Hydrogen-Carbon ratio
MW	Molecular Weight
PC-SAFT	Perturbed Chain-Statistical Associating Fluid Theory
RD	Relative Deviation
RI	Refractive Index
RMSE	Root Mean Square Error
SARA	Saturates, Aromatics, Resins, Asphaltenes
UOP	Universal Oil Product
VKG	Viru Keemia Grupp

1 Literature review

1.1 Overview of Estonian oil shale

The need of exploration for additional energy resources has drawn attentions to utilization of unconventional alternatives and therefore, shale oil was no exception in this rule particularly over the last decades (Vahur Oja, 2007). It was estimated about 2 decades ago that global oil shale reserves are approximately 3 trillion barrels of crude oil (Dyne, 2003). Despite the large supplies of oil shale around the world, only limited number of countries use oil shale deposits for fuel, power production and industrial products (Dyni, 2003; Vahur Oja & Suuberg, 2012). For instance, Unites States, Russia, Brazil, China and Estonia are among those countries known to have major deposits of oil shales and exploit these resources (Knaus et al., 2010).

In 2020, according to the data published in Estonian oil shale yearbook, around 1.6 million tonnes of oil shale produced in Estonia. The production rate started downward trend in 2019, as the rate was hovering around 15 million tonnes per year on average between 2014 to 2019. Oil shale produces about 75% of the main energy in about 80 to 90% of the electricity in the country (Sillak & Kanger, 2020). Shale oil resources in Estonia are estimated to be near 1000 million tons and by 2012, the rate of oil shale production was close to 18 million ton per year (Raukas & Siirde, 2012).

Shale oil is produced from pyrolysis of oil shale – sedimentary rock that contains naturally occurring, cross-linked macromolecular organic matters (also called kerogen) (Hruljova & Oja, 2015; U. Lille, 2004; Speight, 2014). Kerogen is forming major share of organic matters in oil shale. In pyrolysis process, which is also called retorting, oil shale is heated to temperature around 500 °C and kerogen decomposes and coverts to crude shale oil, gas and solid residue. This process occurs in the absence of oxygen (Vahur Oja & Suuberg, 2012; Tissot et al., 1978). The purified vapor-gas mixture obtained from retorting process goes through multistage condensation in order to obtain different shale oil fraction which could also be referred to as wide technical fractions (such as gasoline, middle oil and heavy oil) (Neshumayev et al., 2019).

There are two main pyrolysis (retorting) technologies used to produce shale oil: Kiviter and Gaolter process. Kiviter refers to gaseous heat carrier process, while Galoter relates to solid heat carrier process (Eldermann et al., 2016). Currently, solid heat carrier process is used to process oil shale in Estonia. This technology that has undergone several modifications in recent decades (Neshumayev et al., 2019) is more efficient in energy utilization and surpass the other technology in meeting the climate and environmental regulation and policies (Reinik et al., 2015; Siirde et al., 2013).

The crude shale oils produced from different processes were seen to be a complex mixture of hydrocarbons in which physical and chemical properties are different (Vahur Oja et al., 2016). The composition and properties of shale oils from different retorts differ. In general, the industrial shale oil is separated into three wide fractions. Shale gasoline that made up to about 20% of total shale oil, is considered mixture of compounds with boiling points below 200 °C. This light fraction contains mainly olefins followed by paraffins (about two third). Although aromatic compounds are also present, they are lesser in comparison with heavier fractions. Compared with conventional oil, Kukersite shale contains more olefin and aromatics hydrocarbons and less paraffins (M R Riazi, 2005). Additionally, phenolic compounds make up about one third of Kukersite shale oil (Baird, Zachariah et al., 2015; Vahur Oja et al., 2016).

1.2 Kukersite shale oil characterization

Considering the production, transportation and storage of oil, physical and thermodynamic properties of oil such as volatility characteristic (vapor pressure), evaporative losses, flammability etc., are of foremost importance (Pichler & Lutz, 2014; Raj, 2016; Mohammad R. Riazi & Al-Enezi, 1999).

These properties are essential parameters to be employed in refinery designs and operations, transportation as well as environmental protection. While the most accurate method to obtain these properties is through experimental measurement, this is not always possible because measurements are time-consuming, uneconomical, or sometimes impractical. Therefore, some sort of prediction model is required to enable us to calculate the important parameters that are unknown.

Shale oil were seen to have more aromatic and olefin contents than conventional oil (Vahur Oja et al., 2016; Qian & Yin, 2010) and they contain heteroatomic compounds in abundance (Urov & Sumberg, 1999). Differently, for Kukersite shale oil as a mainstream of this thesis, the amount of phenolic compounds is high and they have large quantities of oxygenated compounds with majority being alkylphenolic. (Baird, Zachariah et al., 2015; Derenne et al., 1990; Kogerman & Kõll, 1930). These properties places Kukersite shale oil in different class from petroleum and biofuel and therefore a choice for developing a model or assessing other thermodynamic correlations used for liquid fuels such as conventional oils. (Zachariah S. Baird et al., 2018). Therefore, the experimental data of vapor pressure measured for Kukersite shale oil gasoline fractions were also used to evaluate several available vapor pressure correlations, which are convenient to use. As mentioned earlier, Kukersite shale oil is rich in oxygen-containing compounds including phenolic compounds. In the structure model suggested by Lille et al. (Ü. Lille et al., 2003), these compounds have mostly aliphatic side chains bound to them.

Phenolic compounds can also be found in bio oil obtained through pyrolysis from lignocellulosic biomass (Effendi et al., 2008; Xiu & Shahbazi, 2012). Because these dry matters contain large amount of oxygen, many oxygen-containing compounds such as phenolic compounds are formed in bio-oil. Phenolic compounds are produced through dephenolation process and due to their favorable properties, they received much attention for different industrial purposes. For instance, compounds and/or mixture obtained from Kukersite shale oil such as 5-methylresorcinol and its derivatives as well Honeyol (alkylresorcinol mixture containing around 50% 5-methylresorcinol) are used in, cosmetic, dyes etc. (Järvik et al., 2014; Perez-Caballero et al., 2008).

To precisely estimate the property of shale oil, the compositions of all the components in the mixture should be known and, with current techniques, it is not yet truly achievable (Quann, 1998). One approach to characterize a compound is through its composition. If the composition of all the constituents in a mixture is exactly known, compound is a "defined mixture" otherwise; it is "undefined mixture". Therefore, oil is considered an undefined mixture whose composition is unidentified.

Defining crude oil properties with single average property value is far from being helpful. In order to characterize and estimate the properties of an oil mixture, pseudocompoent concept is a common approach to be used (M R Riazi, 2005). In this method, oil can be defined as a mixture of several but limited pseudocomponents that behave similarly. These pseudocomponents can be considered as a single compound and the properties of each pseudocomponent can be independently defined.

In order to characterize undefined mixtures (oil fractions) or psedocomponents, bulk parameters such as density, molecular weight, carbon to hydrogen atomic ratio, refractive

index or distillation boiling point (true boiling point) is estimated. This approach enables to better comprehend and predict the behavior of oil while knowledge of compositions is not needed. One approach to characterize the oil is to separate them into narrow boiling range fractions. Each narrow boiling range fraction is considered as a pseudocomponent and the characteristic (bulk properties) of each fraction is estimated separately regardless of the composition of the compounds in fraction. Moreover, some of the pure hydrocarbon correlations could be applicable to these pseudocomponent fractions.

When existing, these properties data could be used for developing prediction models to correlate the basic properties of oils and accordingly, this type of shale oils. For that, at least two easy-to-measure properties could be related. Most of the available correlations for thermodynamic properties require two parameters. These correlations were mostly developed for narrow boiling range fractions with atmospheric boiling point and molecular weight below 350 °C and 300 g mol^{-1}, respectively. One parameter refers to molecular weight of the fraction such as refractive index and specific gravity, while the other parameter is selected according to the molecular size such as average molecular weight or average boiling point. Therefore, following the proposed methods followed in the past decades, for these empirical correlations to estimate average boiling point, specific gravity or average molecular weight were used (M R Riazi, 2005).

In this thesis and related studies, the industrial gasoline shale oil was separated into narrow boiling range fractions through distillation and each narrow boiling range fraction was considered as pesudocomponent.

1.3 Kukersite shale oil studies

While Estonian Kukersite shale oil has been broadly studied for many decades, (Johannes et al., 2012; Vahur Oja, 2007) and is the most important resource of its kind in Estonia in the last century, (Savest & Oja, 2013) the available data for oil extracted from shale is minimal (Kollerov, 1951; Vahur Oja et al., 2016). Moreover, thermodynamic properties information regarding retorting oil shale including Kukersite, is not existed or limited such that, they are not applicable or systematic (Zachariah S. Baird et al., 2018; Zachariah S Baird et al., 2017; Rivo Rannaveski et al., 2018; Savest & Oja, 2013).

These properties data could be used for developing prediction models to correlate the basic properties of oils and accordingly, this type of shale oils. For that, at least two easy-to-measure properties could be related.

Alternatively, these data allow assessing the correlations that were previously developed for conventional oils. Therefore, the applicability of petroleum prediction correlations could be evaluated for some set of systematic shale oil data. Oja and coworkers (Vahur Oja et al., 2016) reviewed that most systematic experimental data of thermodynamics and physical properties for Kukersite shale oil were measured mostly by Kogerman and Kõll in the book "Physical properties of Estonian shale oil" published in 1930 (Kogerman & Kõll, 1930). However, the data were given for fractions with average boiling points about 150 to 300 °C with 25 °C boiling point increment and the book did not include any developed correlation.

Additionally, most of the data related to the physicochemical properties of Kukersite shale oil were compiled by Kollerov in the book "Fiziko-khimicheskie svojstva zhidkikh slantsevykh i kamenougol'nykh produktov" written in Russian in 1951 (Kollerov, 1951) or in the book "Der estländische Brennschiefer-Kukersit, seine Chemie, Tehnologie und Analyse" published by Luts in 1934 in German (Luts, 1934). In addition to containing some

thermodynamic and physical properties for shale oil, some correlations were also developed based on the measurable basic properties of shale oil. In the book, wide technical fractions were obtained from 30–300 °C. These fractions were distilled similar to industrial fractions. For instance, for gasoline fractions boiling range 40 to 205 °C or for diesel fuel boiling range 250 to 350 °C were considered to be a range for such fraction. Additional data and correlations could also be found in several other works (Skrynnikova, 1954; Watson & Nelson, 1933; Zelenin, N. I., Fainberg, V. S., Chernysheva, 1968).

The published data mostly dates to earlier than 1970s and yet to be considered sufficiently systematic experimental data for the purpose of prediction model development. Prior to 1970, in which computer-aided analytical correlations started to develop, the correlations were mostly presented in graphical form.

Even though the basic thermodynamic and physical properties of shale oil, such as normal boiling point, molecular weight and temperature dependent properties such as vapor pressure, heat capacity, viscosity and specific gravity were published and become available. It should be noted that, these data are not systematically robust for presenting a prediction model for shale oil properties or evaluating the suitability of conventional oil prediction methods (M R Riazi, 2005).

In summary, while major studies have already been done on conventional oil, as mentioned earlier, limited volume of data are systematically available for alternative oils such as shale oils and so are inadequately investigated. For this purpose, shale oil was separated into several pseudcomponents and using bulk properties method, further analyses were performed.

1.4 Property correlations for Kukersite shale oil

Although basic properties data such as molecular weight, atmospheric boiling point, vapor pressure, and vaporization enthalpy are available, these data dated more than a century ago and more detailed and systematic data is needed for robust correlation for shale oil bulk properties. As reviewed earlier, there are only three records in which, correlations for Kukersite shale oil were presented (Kogerman & Kõll, 1930; Kollerov, 1951; Luts, 1934). These correlations were either graphical or simple relationship mostly based on limited number of experimental data.

Correlations for vaporization characteristics (such as vapor pressure) are extensively studied and hence, they are available for conventional oils. For instance, correlations developed by Van Nes and Van Westen that have also been used in this thesis employ normal boiling point and experimental temperature to calculate the vapor pressure of specific fraction. These correlations could be used to predict the vapor pressure using input parameters from basic properties of oil (Andersen et al., 2010; Nji et al., 2008; Tsonopoulos, C, Heidman, J L, & Hwang, 1986). However, limited data for shale oils hindered developing a robust correlation for predicting the fraction vapor pressure (Ge et al., 2019b; S. Lee, 1990; Vahur Oja & Suuberg, 2012; Yu et al., 2019). Due to presence of polar compounds in these oils, developing a correlation is a complex task (Akalin et al., 2019; Akash, 2010; Vahur Oja, 2015; Qian & Yin, 2010; Siitsman & Oja, 2016; Urov & Sumberg, 1999).

In general, while developing correlation for Kukersite shale oil was which is one of the objectives of this thesis, no vapor pressure data for Kukersite shale oil gasoline were published or availabe in the literature. Therefore, according to the ASTM D6378-10 standard test method (ASTM D6378-10, 2016) and using ERAVAP analyzer, the vapor pressures of gasoline fractions were measured. These data in addition to other available

gasoline data that have been measured along with characteristics were used to develop a prediction model for Kukersite shale oil gasolines vapor pressures. The procedure towards developing a correlation for Kukersite shale oil gasoline vapor pressure data should be considered as a base to further develop a correlation for Kukersite shale oil vapor pressure as a whole up to 500 °C. In this sense, additional fractions (pseudocomponents) were used and their basic thermodynamic and physical properties were estimated.

The necessary procedure to develop a method for estimating Kukersite shale gasoline vapor pressure data were deliberated such that, these steps are consistent with subsequent progressions to refine the correlation with additional fractions up to 500 °C. While these correlations were developed primarily for Kukersite shale oil gasoline vapor pressure estimation and then Kukersite shale oil altogether, the applicability of these correlations is debatable for other types of shale oils since shale oil composition is dependent on the type of oil shale in the reserve and the process in which shale oil is produced (Guo, 2009).

Phenolic compounds are not desirable in fuels due to the their particular characteristics such causticity and instability (Lyu et al., 2015; Yang et al., 2009; Zhang et al., 2013). Likewise, they are considered as potential environmental hazards (Kahru et al., 1994). Therefore, knowledge of vaporization properties and other thermodynamic characteristics of these compounds are useful for designing the operating system and conversion process. Nevertheless, these properties are not adequately available and therefore, the available data are minor. Moreover, the correlations presented for these properties do not satisfactorily model these compounds and possibly phenol-rich mixtures.

Hence, in this thesis, some of the vapor pressure and other physical properties data for a few phenolic compounds/mixtures determined or estimated from oil shale pyrolysis experiment were provided. The earlier-mentioned phenolic compounds/mixtures properties or vapor pressure data, i.e., 5-methylresorcinol and Honeyol were selected as by product of Kukersite shale oil. Additionally, another compound chosen for this purpose is bio based phenolic compound, which is 4-ethyl-2-methoxyphenol (4-ethylguaiacol). This compound which can also be extracted from petroleum sources, is extensively used as a chemical intermediate in pharmaceutical and petrochemical industries (Ye et al., 2012).

1.5 Kukersite shale oil modelling

Equation of state (EoS) was essentially employed to predict thermophysical properties and phase equilibria oil fractions. The use of this approach has been used in estimation of thermphysical properties of simple fluids. This led to an increasing interest in finding alternate approach to model various complex mixtures such polymers or compounds with particular molecular interactions such as association (hydrogen bonding) or polar interactions. Therefore, characteristics of molecules and their effect on thermodynamic properties of the compounds requires different approach for modelling of compounds that have more complex systems (Tumakaka et al., 2005). This approach was based on statistical thermodynamics.

One way to model the thermodynamic properties of hydrocarbon is Perturbed Chain Statistical Associating Fluid Theory (PC-SAFT). PC-SAFT based method which was first developed by Gross and Sadowski, (Gross & Sadowski, 2001) has advantage over cubic equation of state in which takes into account the interactions that occur between molecules of the mixture and on contrary to cubic Equation of States in which, the knowledge of critical properties is not required. This equation was primarily developed

to model non-associating fluids and system with long-chain molecules such as polymers. In this approach, pure fluids are considered as hard-spheres (or segments). For PC-SAFT equation, the non-associating model parameters to characterize the fluids are segment number (m), segment dimeter (σ) and segment energy parameter (ε/k) and these parameters are obtained by fitting experimental vapor pressure and liquid density data. Applicability of this method is investigated better for pure compounds than undefined complex mixtures such oils.

While such modelling and developments were mostly proposed for petroleum fractions, shale oils were not received much consideration for this purpose. Models developed for petroleum unlikely be applicable to shale oil (Zachariah S Baird et al., 2017; Zachariah Steven Baird et al., 2015; R Rannaveski & Listak, 2018; Rivo Rannaveski, 2018) since the compositions and structures of petroleum and shale oil are different. While the applicability of different petroleum correlations could be assessed for various shale oil deposits, modelling of Kukersite shale oils were of concern of this work.

In summary, measured experimental data for Kukersite shale oil narrow boiling pseudocomponents were employed to develop correlations that could be used to calculate PC-SAFT parameters. These models primarily presented for gasoline fractions up to 180 °C, and then extended to all shale oil fractions up to 500 °C.

1.6 Conclusions

Based on literature review the following conclusions could be drawn:
- Shale oil has been studied in lesser extent compared with crude oil and therefore, available data were found to be much less.
- The availability of vapor pressure data of shale oil-related products or mixtures are no exception as well.
- The correlations for crude oil vapor pressure data were also studied in larger scale and thus the application of some of these correlations for various properties of shale oils is yet to be assessed.
- Despite correlations for Kukersite shale oil developed over five decades ago, the necessity to introduce new model including much larger number of experimental data could be necessary.
- Simple yet robust model with larger number of fractions is continuously valued. In addition, the model given is non-cubic equation of state which is presented differently compared with those published earlier.

1.7 Objectives

It was noted that the Kukersite shale oil properties data were available in a much smaller set, date back to decades ago, and are mostly not systematic. Moreover, a more robust model to predict the properties of Kukersite shale oil using a larger dataset was also of interest. Previous correlations were simple yet only covered much smaller range of oil properties.

The limited availability of Kukersite shale oil properties data and oil by-products in addition to having a predictive model to estimate the properties of shale oil fractions have led to the aim of the thesis to meet several research objectives.

Therefore, the objectives of the thesis are to:

- Provide thermodynamic and physical properties for narrow boiling Kukersite shale oil gasoline fractions. In addition to evaluating the applicability/suitability of several petroleum vapor pressure correlations to shale oil fractions.
- Generate vapor pressure data for pyrolysis oil-derived phenolic compounds for wide range of pressures by DSC.
- Assess the possibility of these pyrolysis oil-derived phenolic compounds to be used as model compound for modelling phenolic compounds of shale oil.
- Develop a correlation to model Kukersite shale oil gasoline fractions using PC-SAFT equation of state
- Extend the development of the model used for shale oil gasoline to all available fractions using PC-SAFT equation which includes the non-associating parameter correlations for aromatic compounds.

This method allows for estimation of Kukersite shale oil properties which could further be considered to develop property prediction method for oil shales from different origins.

2 Experimental and modelling

In this section, pure compounds and oil mixtures used for analysis were listed and preparation of these compounds were described. Experimental procedure developed for vapor pressure measurements, were described and methods used for development of correlations were explained.

2.1 Materials

In this work, several compounds were used for measurements as part of experimental studies.

Pure compounds

List of pure compounds used for studies as well as pure compounds used for performance check of the instruments, supplier, CAS RN., chemical formula, molecular weight, purity, and the purpose were provided in Table 1. For analysis, all pure compounds used as received with no further purification. The purity of 5-methylrescorcinol, biphenyl and 4-ethyl-2-methoxyphenol were measured by Gas chromatography (GC). The reported purities for Toluene and Benzene were also given in Table 1.

Shale oil-derived compounds

Narrow boiling Kukersite shale oil gasoline fractions were obtained from wide Estonian Kukersite shale oil gasoline fraction using distillation method. The wide fraction of shale oil gasoline used in this study produced through Galoter process. While for the first article, wide gasoline fractions distilled for measurements, considerably more narrow boiling range fractions were used for modelling. This was done to meet the objective of third article as more data were needed for developing a model. The additional fractions that have been previously distilled as part of the goal of other project, used in here so that the more properties data fitted for the correlations. Additional wide Kukersite samples used for third article studies were taken from different Eesti Energia plants within 2 years when the bigger project was ongoing. Therefore, the properties of narrow boiling fractions obtained from wide fractions, were measured earlier and used for to model the Kukuesite shale oil fractions.

Table 2 report the measured thermohysical properties of the narrow gasoline fractions (Initial and final boiling points of each fraction, percent distilled, refractive index, densities and molecular weight) used to validate the petroleum vapor pressure correlations. Initial boiling point and end boiling point of distillation temperature range refer to the temperature that first and final drop of specific fraction collected. It was so that the final distillation temperature of earlier fraction is identical to initial distillation temperature of subsequent fraction. These fractions numbered in increasing routine so that former fractions represent the lighter fractions and first fractions of each distillation denote the lightest fraction of respective distillation.

Another compound, Honeyol (CAS No. 799275-41-5 with Molecular weight of 142.8 g/mol – measured in the lab), produced by VKG (Viru Keemia Grupp) Company, used for vapor pressure measurement. The water used is distilled and purified in our laboratory. Using gas chromatography technique, compositional analysis of Honeyol showed that 62.4% of this mixture is 5-methylresorcinol, while 11.4% is 4,5 dimethylresorcinol, 9.4% is 5-ethylresorcinol and 6.7% is 2,5 dimethylresorcinol. These compounds take up to around 90% of Honeyol.

Because Honeyol is highly viscous with sticky consistency, it was slowly heated prior to measurement so that the properties are not affected.

Table 1. Pure compounds properties

Compound	Supplier	CAS RN	Empirical formula	Molecular weight (g mol^{-1})	Purity (mass %)	Purpose
Benzene	Lachner	71-43-2	C_6H_6	78.1	99.9	Used to evaluate the performance of ERAVAP vapor pressure tester
Toluene	Sigma-Aldrich	108-88-3	C_7H_8	92.1	99.7	
4-ethyl-2-methoxyphenol	ACROS Organics	2785-89-9	$C_9H_{12}O_2$	152.2	98.6	Used to provide new sets of vapor pressure data up to atmospheric pressure
5-methylresorcinol	VKG	504-15-4	$C_7H_8O_2$	124.1	99.9	
Biphenyl	Alfa Aesar	92-52-4	$C_{12}H_{10}$	154.2	99.0	Considered to check the DSC measurement accuracy
Water	Purified water in the laboratory	-	H_2O	18.0	Bi-distilled	

Table 2. Properties of the narrow boiling shale gasoline fractions

Fraction	Initial boiling point	Final boiling point	Percent recovered	Refractive Index (20 °C)	Density (20 °C)	Molecular weight
No.	*°C*	*°C*	*wt%*		*g cm^{-3}*	*g mol^{-1}*
1	58	68	1.2%	1.4053	0.7103	103
2	68	86	2.1%	1.4161	0.7301	91
3	86	98	3.1%	1.4235	0.7478	93
4	98	84	5.4%	1.4254	0.7498	106
5	84	94	1.4%	1.4210	0.7419	99
6	94	104	2.3%	1.4299	0.7608	94
7	104	112	3.6%	1.4420	0.7852	97
8	112	118	3.7%	1.4314	0.7660	105
9	118	121	3.9%	1.4298	0.7625	110
10	121	126	3.2%	1.4359	0.7753	112
11	126	134	3.8%	1.4466	0.7960	124
12	134	140	4.4%	1.4524	0.8090	117

Expanded uncertainties (95% level): refractive index = 0.0021, density = 0.0003 g cm^{-3}, molecular weight = 10 g mol^{-1}

2.2 Sample preparation

Technical straight-run gasoline fraction of Estonian Kukersite shale oil was received from Eesti Energia with boiling range from around 40 to 200 °C. The plant uses solid heat carrier technology (Gaolter process). (Elenurm et al., 2008; Golubev, 2003). In this technology, Kukersite shale oil as raw material was used, in which, three wide industrial shale oil fractions were produced: heavy oil, fuel oil and gasoline.

Technical gasoline fraction (density of 0.7848 g cm^{-3} at 20 °C) was used in this work for the column distillation. Elemental composition analysis of literature data confirm that around 3% of the technical gasoline fractions consist of heteroatos (likely sulfur and oxygen compounds) (Qian & Yin, 2010; Urov & Sumberg, 1999).

The technical gasoline fraction was then distilled into narrow boiling fractions using distillation column in accordance with ASTM D2892 (ASTM D2892-15, 2015). For the column distillation, a packed distillation column with reflux ratio 6 to 1 and 24 theoretical trays was used. A mercury thermometer was used to measure the temperature at the top of the column, and the accuracy of this thermometer was checked in boiling water to make sure it showed the correct temperatures. The fractions were separated on the basis on the volume collected. Meaning that once around 20 ml of sample was collected, new bottle was used to collect the next sample. To prevent from losing the volatiles, the gasoline vapors and subsequently liquid samples were collected in cooled glass condenser at approximately –10 °C. During the column distillation, there were some difficulties with keeping the temperature stable and at points, the temperature at the top of the column dropped instead of steadily increasing.

For this distillation, the mass percent recovered in each fraction is given in Table 2. Note that to make the curves comparable the average normal boiling points calculated from the vapor pressure data were used instead of distillation temperatures. The drop in temperature for some of the fractions during the column distillation is due to the difficulty in maintaining a stable temperature increase during that distillation.

2.3 Methods and procedures

In this section, commercial instruments and methods developed to measure thermodynamic and physical properties of various compounds and procedure described to obtain correlations for Kukersite shale oil fractions were given.

Measurement of properties
Properties of pure compounds and oil fractions were measured by means of different methods. These measurement methods are provided in this section of the thesis.

Density
Density of 4-ethyl-2-methoxyphenol and Kukersite shale oil gasoline fractions were obtained by DMA5000M density meter (Anton Paar GmbH). For gasoline fractions, Standard uncertainty was 0.00015 g cm^{-3} and expanded uncertainty (95% level) was estimated to be 0.0003 g cm^{-3} (Zachariah Steven Baird, 2017).

However, the expanded uncertainty for 4-ethyl-2-methoxtphenol was 0.00005 g cm^{-3}. Considering the purity of this compound, the expanded uncertainty (95% level) was 0.0001 g cm^{-3}. The performance of density meter was checked with air and distilled water before and after each measurement. This ensured that the instrument is clean prior to experiment and therefore the accuracy is high. The difference between measured and reference value does not exceed 0.00005 g cm^{-3}.

Molecular weight

The average molecular weight was either measured by cryoscopy method according to ASTM D2224 (ASTM D2224, 1983) or measured using vapor pressure osmometry technique. In cryoscopy measurement, benzene was used as solvent. The method was described thoroughly by Järvik and Oja (Järvik & Oja, 2017). The uncertainty increased with molecular weight, and for the samples given here, the 5 g mol^{-1} standard uncertainty (10 g mol^{-1} expanded uncertainty k = 2) was recorded.

The number average molecular weight of Honeyol was measured using KNAUER K-7000 vapor pressure osmometer (Wissenschaftliche Gerätebau Dr. Ing. Herbert KNAUER GmbH, Germany). Distilled water used as solvent and expanded uncertainty was about 7%.

Refractive index

Abbemat HT refractometer (Anton Paar GmbH) at wavelength 589.592 nm was used to measure the refractive index at 20 °C. The performance check was done before and after measurement and for this purpose, distilled water was used. For gasoline samples, the expanded uncertainty (95% level) was found to be 0.0021.(Zachariah Steven Baird, 2017) Due to high volatility of first few gasoline fractions, and therefore, constant change of RI value, the estimation of average values obtained were taken.

Boiling Point

The average boiling point of gasoline fractions obtained from distillation in which arithmetic mean of temperature calculated when first and final drop of the fraction collected. The boiling point uncertainty was estimated to be 1 °C.

Vapor pressure measurement

Several vapor pressure of pure compounds as well as Honeyol were measured using Differential Scanning Calorimetry (DSC). Vapor pressure of Kukersite gasoline fractions were measured using ERAVAP. The detailed experimental procedure is provided below.

ERAVAP vapor pressure tester

Vapor pressure was measured with ERAVAP (Eralytics GmbH) and 4 to 1 vapor-liquid ratio according to the ASTM D6378 standard (ASTM D6378-10, 2016). This commercial analyzer measures temperature and pressure of up to 120 °C and 1000 kPa, respectively. Prior to measuring the vapor pressure of gasoline fractions, the instrument was cleaned using vacuum pump. This procedure was repeated before each gasoline fraction experiment. Moreover, the instrument reliability was assessed by measuring vapor pressure of toluene and benzene. The values were then compared to those from references for Benzene (Ambrose et al., 1990; Boublik et al., 1984; Connolly & Kandalic, 1962; Dreisbach, 1955; Wilhoit & Zwolinski, 1971) and Toluene (Dean, 1992; Dreisbach, 1955; Wilhoit & Zwolinski, 1971; Willingham et al., 1945). Based on this data, the vapor pressure standard uncertainty was obtained to be 0.3 kPa.

Differential Scanning Calorimeter (DSC)

Vapor pressure of phenolic compounds were measured using Netzsch 204HP Phoenix high pressure Differential Scanning Calorimeter (DSC), in accordance with standard test method ASTM E 1782 "Standard test method for determining vapor pressure by thermal analysis" (ASTM, 2003). To increase the accuracy of pressure measurement, another pressure controller (Brooks instrument Model 5866) and pressure sensor (Omegadune Inc., model PX409-150 AUSB) were connected to the system. The pressure sensor has 0.008% full-scale error. For pressure monitoring, in general two sensors were connected

to the outlet and inlet of the system so that the pressure drop could be recorded. The observed pressure drop value can be considered for final pressure analysis. The significance of minor pressure loss can contribute to likely major calculation error when very low vapor pressure experiments were of interest.

As DSC system shown in Figure 1, for measurement of vapor pressures in vacuum, the system was equipped with membrane vacuum pump (vacuum-brand PC 3001 Vario) with variable motor speed controller CVC 3000. Overall, several modifications were done to better observe the behavior of the system. Vacuum sensor MKS Baraton (type 626B) was added to the outlet of the system to measure the pressure of DSC cell. The calibration of the sensor was performed in metrological center to ensure reliable results. Vacuum sensor has operating range of 0.0133–130 kPa. The accuracy of reading was specified to be 0.25%.

The distance between the outlet pressure sensor and DSC cell was 47 cm and measured pressure drop was 0.003 kPa at atmospheric conditions. The inlet and outlet tubes of DSC cell were modified and immersed in 2L ballast tank cooling fluid connected with Huber CC250 chiller in order to trap the vaporizing samples in the system. Temperature of cooling bath was monitored by Thermocouple thermometer to be not higher than –39 °C.

Experimental vapor pressure carried out within the pressure range between 1 kPa and atmospheric pressure. The heating rate was 5 K min^{-1}. Hermetically sealable 40 μl aluminum pan, which had 50 μm laser drilled pinhole lid was used to place the sample inside the furnace. Inert gas (Nitrogen) with 99.999% purity was used as purge gas for 20–30 min before each experiment to eliminate the possibility of air presence and oxidation in the system during experiment. This procedure was followed during vacuum experiments as well. The nitrogen flow rate was 40 ml min^{-1}. the sample used for the measurements were between 1–5 mg for pressures between 5–101.3 kPa and 3–10 mg for pressures between 1–5 kPa.

The DSC performance test was done using distilled water (Wagner & Pruß, 2002) and biphenyl (99% purity, CAS RN. 92-52-4) (Chipman & Peltier, 1929; Chirico et al., 1989; Garrick, 1927). In this regard, for vapor pressure experiments above 5 kPa, crucibles with 50 μm pinhole lid were used. However, for experiments below 5 kPa, the lid hole was manually enlarged to as much as 180 μm for very low vapor pressure measurements. This recommendations was provided to in order to obtain better curve from DSC analysis software (Brozena, 2013; Butrow & Seyler, 2003).

The temperature calibration was performed according to the manufacturer's recommendation using tin, indium, zinc, bismuth, and lead in normal conditions and operating conditions for both samples' calibration measurements were similar. For each sample, the measurement was carried out at least twice to verify the repeatability or more if the difference between the obtained boiling points from thermoanalytical curve exceeded 0.1 K.
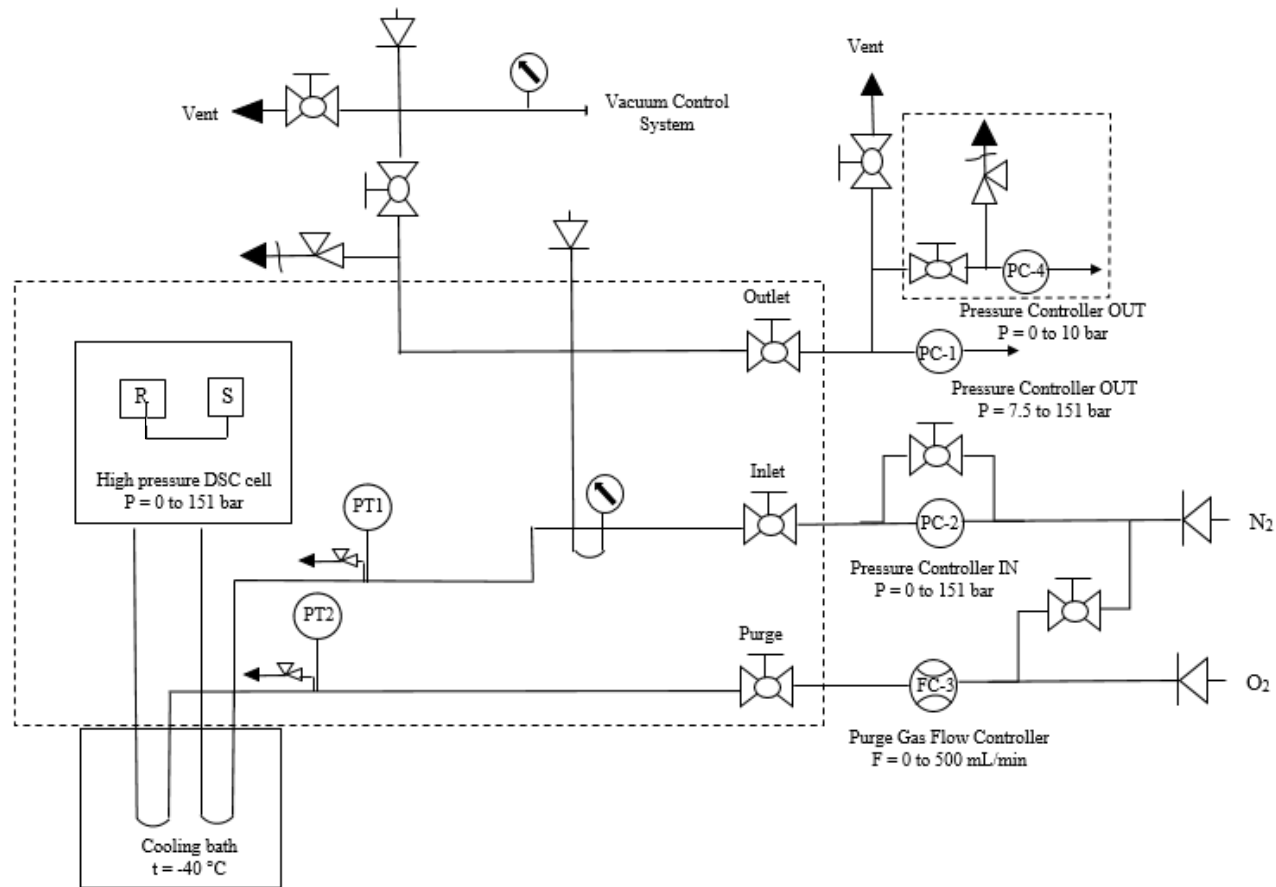
Figure 1. Modified DSC for vapor pressure measurement

Applicability of vapor pressure measurements

Techniques used to measure the vapor pressure of phenolic compounds and gasoline fractions were evaluated prior to experiment. For narrow boiling range gasoline fractions, static vapor pressure tester ERAVAP was used and vapor pressure of phenolic compounds was measured by differential scanning calorimeter (DSC) Performance of these instruments was assessed using several pure compounds. Table 3 provides general information regarding all the compounds used with objective of performance check for vapor pressure instruments. Reference data were rather correlated from the references or Antoine equation constants provided in the references, were used.

As shown in Figure 2, data are in good agreement with references. Average absolute relative deviation for all references is independently below 1%. For most of the compounds, references with various measurement techniques were used. For distilled water, cubic equation of state introduced by Wagner & Pruß, was used. The uncertainty of the equation of state withtin experimental range in the reference article was reported to be about 0.02%. For the compound, while all absolute devations are below or around 0.1 kPa, the vapor pressure measurement error for experiment at atmospheric condition was around 1.5 kPa. And, as a matter of convneince, this point just reported in here and removed from the figure.

Among all experimental data compared for biphenyl, the maximum deviation from the references were seen for atmospheric pressure which shows deviation of less than 0.4 kPa. However, consdiering the rest of data points of this compound, the deviations fall below 0.1 kPa except three data points where the error is approximately 0.15 kPa on average.

On the other hand, most of vapor pressues ARD% were about 0.30% for toluene and 0.55% for benzene and most of the references used in here, reported only the Anotine equation constants. The absolute error values for these compounds is maximum 0.3 kPa. Figure 2 presents the absolute deviation of measured DSC and ERAVAP vapor pressures. Because the error values for benzene and toluene for all the references, one common reference selected for comparison in Figure 2.

Table 3. Pure compounds used for performance evaluation of vapor pressure measurement methods

| Pure compounds	Measurement range in the article (kPa)	Reference	Average absolute relative deviation (ARD %)	Explanation for reference
Differential Scanning Calorimetry (DSC) – II article				
Distilled water	49.88 – 100.92	(Wagner & Pruß, 2002)	0.47%	EoS based on selected data
Biphenyl	0.90-100.40	(Chirico et al., 1989)	0.71%	Ebulliometric method
		(Chipman & Peltier, 1929)	0.44%	Modified isoteniscope-manometer method
		(Garrick, 1927)	0.31%	Modified manometric method
ERAVAP vapor pressure tester – I article				
Benzene	24.1-135.8	(Dreisbach, 1955)	0.30%	Antoine Eq. from API data
		(Boublik et al., 1984)	0.31%	From reported extrapolated data of (Ambrose, 1981)
		(Wilhoit & Zwolinski, 1971)	0.30%	Antoine Eq. from data
		(Ambrose et al., 1990)	0.30%	Ebulliometric
		(Connolly & Kandalic, 1962)	0.30%	Static method
Toluene	18.6-54.1	(Dreisbach, 1955)	0.56%	Antoine Eq. from API data
		(Wilhoit & Zwolinski, 1971)	0.55%	Antoine Eq. from data
		(Dean, 1992)	0.56%	Antoine Eq. from data
		(Willingham et al., 1945)	0.55%	Static method
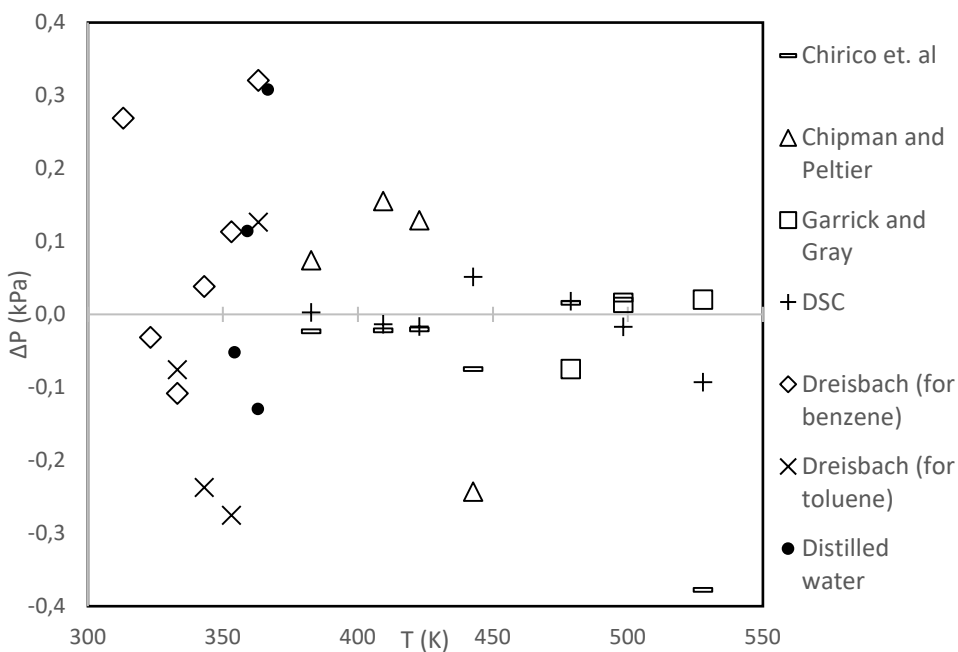
Figure 2. Deviation plot for vapor pressure of pure compounds used for performance check. ΔP is the difference between experimental pressure and reference pressure: [ΔP = P_{reference} − P_{measurement}]

Overall, these insturments showed reliable results to perform vapor pressure measurment for narrow boiling range gasoline fractions as well pyrolysis oil phenolic compounds.

Data processing
Measured samples and compounds were fitted and deviation of experimental were checked with literature values when available.

Data analysis
Experimental vapor pressure data of phenolic compounds were fitted to a tested against Antoine equation:

$$\ln(P) = A + \frac{B}{T + C} \tag{2.1}$$

Where A, B and C are Antoine parameters, T is temperature (K), P is vapor pressure (kPa), R is gas constant and ΔH_{vap} is vaporization enthalpy (kJ mol^{-1}) And, vaporization enthalpy (ΔH_{vap}) at normal boiling point is calculated from the slope of linear Clausius-Clapeyron regression of ln(P) vs 1/T plot:

$$\frac{d(\ln(P))}{d\left(\frac{1}{T}\right)} = \frac{\Delta H_{vap}}{R} \tag{2.2}$$

In order to determine Antoin equation constants, POLYMATH software was used.

For shale gasoline fractions, integrated form of the Clausius-Clapeyron equation was used. Therefore:

$$\ln(P) = -\frac{A}{T} + B \tag{2.3}$$

or,

$$\ln(P) = -\frac{\Delta H_{vap}}{RT} + B \tag{2.4}$$

Where A and B are Antoine parameters, T is temperature (K), P is vapor pressure (kPa), R is gas constant and ΔH_{vap} is vaporization enthalpy (kJ mol^{-1}). These parameters were obtained from linear regression equation plotted for each fraction. (R = 8.314 J mol^{-1} K^{-1}).

Error analysis
Relative deviation and average absolute relative deviation (ARD) of experimental data are expressed as below.
Relative deviation:

$$RD\ \% = \frac{X_e - X_{ref}}{X_e} * 100 \tag{2.5}$$

Average relative deviation:

$$ARD\ \% = \frac{1}{n} \sum \left| \frac{X_e - X_{ref}}{X_{ref}} \right| \times 100 \tag{2.6}$$

Where, X_e represents experimental value measured, X_{ref} is reference value and n is number of experiment data points.

Furthermore, measured gasoline fraction data were compared with several vapor pressure correlations using root mean square error (RMSE) and the absolute deviation between calculated value and measure value denoted with r:

$$RMSE = \sqrt{\frac{\sum(\theta_p - \theta_m)^2}{n}} \tag{2.7}$$

$$r = \theta_m - \theta_p \tag{2.8}$$

Where n is number of data points and θ_P and θ_m are predicted and measured values, respectively.

Kukersite shale oil modelling
Detailed data analysis presented by Gubergrits (Gubergrits et al., 1989) was the main source to be considered for analysis of chemical classes of compounds for shale gasoline fractions. This procedure was thoroughly described in article III. In general, each chemical class of compound were separately estimated for different temperature range (from 40 to 150 °C and from 150 to 180 °C). The Mass percent values were estimated such that they are consistent with the FTIR analysis (Zachariah Steven Baird, 2017). Having estimated these properties, the amount of each class of compound was fitted to boiling point and density values. The result of the fitting were correlations that can be used to estimate the composition of a fraction based on its density and boiling point.

In short, the amount of each chemical class of compound were separately estimated for different temperature range. From around 40 °C to 150 °C and from 150 °C to 180 °C. The Mass percent values were estimated such that they are consistent with the FTIR analysis (Zachariah Steven Baird, 2017). This Analysis was done on data obtained for narrow boiling range fractions. Having estimated these properties, the amount of each class of compound was fitted to boiling point and density values. The result of the fitting were correlations that can be used to estimate the composition of a fraction based on its density and boiling point.

Correlation for neutral oxygen compounds were fitted using literature parameters for pure compounds. Having considered generalized equation for n-alkane suggested by Gross and Sadowski (Gross & Sadowski, 2001) and correlation for 1-alkene proposed by Ghosh et al. (Ghosh et al., 2003). These Three correlations were fitted to experimental shale oil data to develop PC-SAFT non-associating parameters correlations. Therefore, the correlations for aromatic and phenolic classes of compounds obtained by fitting all data to correlations.

3 Results and discussions

In this section, approaches that described earlier, were applied in which, data were either experimentally measured such as vapor pressure gasoline fractions or collected using the properties of all available fractions that had been distilled for the objective of model development.

3.1 Evaluation of petroleum correlations for shale oil gasoline fractions

Vapor pressure experiments carried out for broad range of temperature and static vapor pressure device was used for measuring the vapor pressure of gasoline fractions. There are several correlations and methods that have been widely used to measure the vapor pressure of petroleum fractions. For vapor pressure prediction, the commonly used methods are correlations or graphs. Correlations usually require basic properties of compounds. The applicability of the use of correlations may also be extended to narrow boiling fractions (or pseudocomponents) (M R Riazi, 2005).

Several existing correlations are available to predict the vapor pressure of petroleum fractions. Some of these correlations require information regarding pseudocritical properties such as correlations proposed by Lee and Kesler (B. I. Lee & Kesler, 1975), or Ambrose and Walton (Poling et al., 2000), or modified Riedel equation (Tsonopoulos, C, Heidman, J L, & Hwang, 1986; Wilson et al., 1981).

In the article I, three correlations were selected to calculate the vapor pressure of Estonian Kukersite shale oil narrow boiling gasoline fractions. Correlation proposed by Van Nes and Van Westen (Van Nes & Van Westen, 1951) is the simplest form of vapor pressure correlation with accuracy of 1% for pure hydrocarbons. Correlations suggested by Wilson et al. (Wilson et al., 1981), Maxwell and Bonnell (MB) (Maxwell & Bonnell, 1955, 1957), and modified MB suggested by Tsonopoulos et al. (Maxwell & Bonnell, 1957) and are another alternatives that were chosen for calculation of vapor pressure of gasoline fractions. It has been seen that when the modified Maxwell and Bonnell correlation used, the error was about 4.6% (Tsonopoulos, C, Heidman, J L, & Hwang, 1986) These correlations were selected because of their simplicity in which input parameters were easy to measure or calculate.

Table 4 provides the calculated root mean square error (RMSE) of each correlation.

Table 4. RMSE of correlations used for vapor pressure prediction of shale oil gasoline fractions

Correlation	RMSE (%)	Reference
Van Kranen and Van Westen	3.4	(Van Nes & Van Westen, 1951)
Maxwell and Bonnell	2.9	(Maxwell & Bonnell, 1955, 1957)
Modified Maxwell and Bonnell	2.9	(Tsonopoulos, C, Heidman, J L, & Hwang, 1986; Wilson et al., 1981)

In general, it was seen that behavior of these correlations are comparable to each other while, the estimated vapor pressure value difference between these correlations is not significant, Maxwell and Bonnell as well as modified Maxwell and Bonnell correlation showed slightly better performance compared with Van Kranen and Van Westen. However, possibly one advantage of Van Kranen and Van Westen is that the correlation could be immediately used when only normal boiling point of the fraction is available and hence, no further parameter or properties is required for quick calculation of vapor pressure. While, for vapor pressure prediction using the other two correlations, specific gravity (or density) is needed. Moreover, Van Kranen and Van Westen showed also high accuracy of vapor pressure estimation when used for temperature near boiling points and this deviation increased when temperature exceeds normal boiling point. While, other correlations showed great accuracy for temperature around boiling point, the simplicity of Van Kranen and Van Westen correlation could also be advantage for quick prediction of vapor pressure at temperatures close to the boiling point of the fraction.

In general, it was observed that when these correlations are used to estimate the vapor pressure of shale oil gasoline fractions, the relative error is about 5%. Therefore, these correlations could be collectively used to estimate the vapor pressure of these types of oil.

Watson Characterization factor

One of the most commonly used characterization methods are Watson characterization factor (K_w). Here, the characterization factor of shale oil gasoline fractions was plotted against average boiling point of gasoline fractions. This factor correlates specific gravity and normal boiling point of oil fractions and it could be used to predict the specific gravity or density of oil at 15.5 °C when the K_w value is available. Moreover, it is helpful parameter to classify petroleum fractions and crude oil type (M R Riazi, 2005). Average boiling point in here refers to the average temperature of distillation data.

Generally, Watson characterization factor (Watson K) helps to define oil fractions. This factor has been applied to conventional crude oil in the past decades. Watson K range is usually from 10 to 13 and high Watson K refers to more paraffinic and less aromaticity of the structure of the compound while high Watson K value denotes decrease in aromaticity. On the other hand, Kukersite shale oil is rich in aromatic compounds and therefore, by increase in boiling temperature, it is expected that aromatic content increases. Therefore, it could be the reason for such steep downward trend which is shown in figure below. In Figure 3, this trend was shown for calculated K_w value of each gasoline shale oil fractions (Article I).

Overall, while the correlations for crude oils were seen to be applicable to shale oil fractions, Watson factor could simply emphasize on that by observing similar behavior in Watson K change for both shale oil and crude oil fractions.
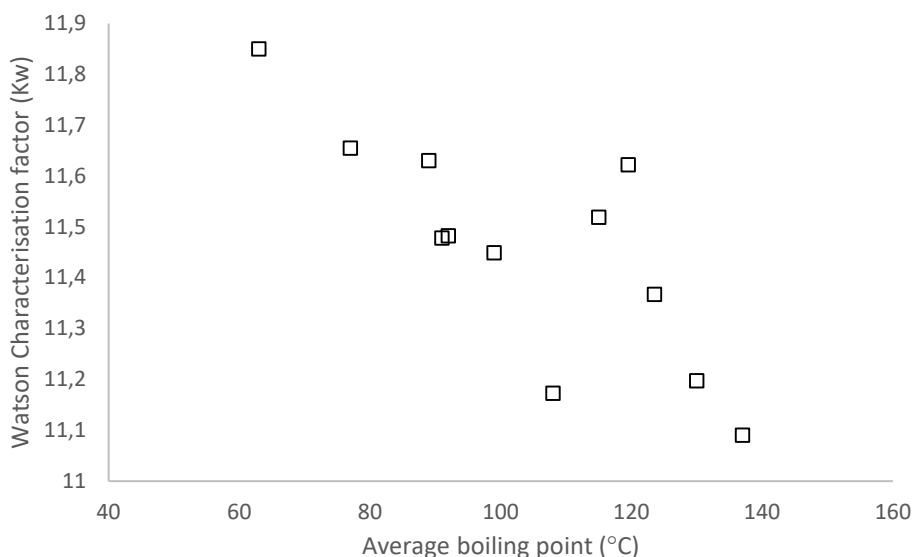
Figure 3. Watson characterization factor for gasoline fractions

3.2 Phenolic compounds in pyrolysis oil

Vapor pressure of two pure compounds extracted from pyrolysis oil, 5-methylresorcinol and 4-ethyl-2methoxyphenol, as well as a phenolic mixture as shale oil by-product were measured by Differential Scanning Calorimetry technique up to atmospheric pressure. The measured data and other calculated properties are available in article II.

Using this technique, the ln(P) as a function of reciprocal T for these fractions provided good linearity of at least R^2=0.9994. Therefore, normal boiling points of these compounds obtained from the fit. Among these compounds measured, very few data for 5-methylresorcinol could be found in the literature. The previous vapor pressure measurements were made at lower temperature range from 322. K to 338.1 K (Ribeiro da Silva & Lobo Ferreira, 2009). It was concluded that because in our work measurement was done at higher temperature, the comparative enthalpy of vaporization was expected to be lower in which the logical trend was seen to be followed (Article II). Information regarding these data is provided in Table 5.

Table 5. Properties data for 5-methylresorcinol available in the literature

Reference	Information
(Ribeiro da Silva & Lobo Ferreira, 2009)	Mass-loss Knudsen effusion method was used for vapor pressure measurement. The experimental conditions are 322.2–328.1 K and 0.153–0.935 Pa. The calculated pressure at T = 293.15 K is (1.5 ±1.4) 10^2 and ΔH_{vap} at normal boiling point is approximately 102.4 kJ mol^{-1}
(Weast et al., 1989)	Normal boiling point is T_b = 562.7 K
(Stephenson & Malanowski, 1987)	For temperature range 402–468 K, Enthalpy of vaporization at normal boiling point was reported to be ΔH_{vap} = 76.6 kJ mol^{-1}
Our work	DSC technique was used (ΔH_{vap} (T_b) = 69.6 kJ mol^{-1}, T_b = 564.4 K)

Phenolic compounds in shale oil are in abundance. However, the richness of these compounds is dependent on the type of oil and process used. Many phenolic fractions were separated from Estonian Kukersite shale oi (Järvik et al., 2021) and properties of these compounds were compared with phenolic compound used in article II (Honeyol, 4-ethyl-2-methoxyphenol and 5-methylresorcinol). Phenolic fractions were separated from shale oil following the method suggested by Kogerman. In brief, benzene was added to shale oil followed by 10% sodium hydroxide (NaOH)) solution in order to make the phenol part separable. Lastly, distilled water was added to oil to remove NaOH (Kogerman, 1931).

In article II analysis, fractions with boiling point of up to 620 K were used. It was seen that 4-ethyl-2-methyoxyphenol could possibly be used as model compound for this type of pyrolysis oil due to having similar properties. Figure 4 graphically describes the possibility of the use of 4-ethyl-2-methyoxyphenol to perform as model compound. This compound was shown in orange. This could also be looked upon so that the compound located within the margins of the trendline associated with all fractions. In Figure 4, all phenolic fractions extracted from Estonian Kukersite shale oil.
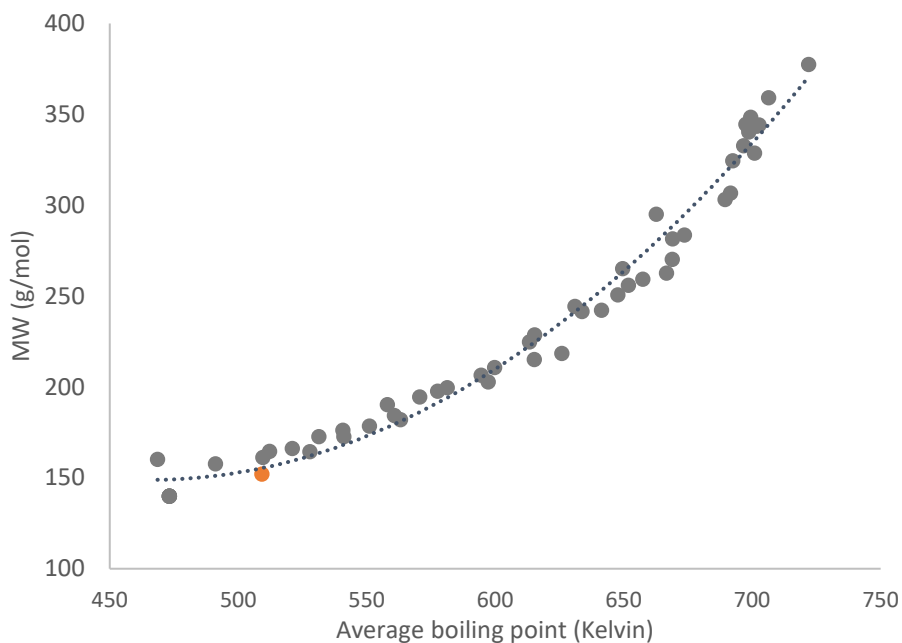
Figure 4. Behavior of molecular weight of 4-ethyl-2-methoxyphenol (orange dot) as well as phenolic fractions extracted from Kukersite shale oil as a function of average boiling point

For simplicity, a polynomial correlation was developed for phenolic fractions. This was done in order to evaluate the applicability of phenolic compounds to behave as model compound for phenolic fraction pyrolysis oil. For this, empirical correlation, R^2 was seen to be approximately 0.98.

$$MW = 0.00341ABP^2 - 1.32017ABP + 277.03507 \qquad (3.1)$$

Where, MW is molecular weight in g mol^{-1} and ABP is average boiling point of phenolic compounds in Kelvin. The average absolute relative deviation of correlation was found to be less than 5%. However, with few data points, the relative deviation (RD%) reached as high as 12%.

Applicability of Estonian Kukersite shale oil model
As explained in the methods and procedure section as well as article III, phase behavior modelling of shale oil gasoline samples was done using PC-SAFT equation of state. Experimental vapor pressure and liquid density of gasoline fractions were used to fit non-associating parameters. The average absolute relative deviation of the fit was near 11%.

The composition of each class of compound for gasoline fractions were estimated up to 180 °C. Although Kukersite shale oil is rich in phenolic compounds the FTIR analysis of the samples showed that these compounds appear in fractions at normal boiling temperatures around 200 °C. Therefore, possibility of very small presence prior to this temperature was negligible for current analysis. In general, for shale oil fractions, with increase in boiling temperature, the amount of olefin and paraffin decreases, while aromaticity follows reverse fashion. This relies partly on the increase in phenolic compounds which was observed for temperature above 200 °C approximately.

Figure 5 presents the trend obtained to explain the behavior of H/C atomic ratio as a function of boiling temperature. In order to evaluate the correctness of estimated compositions, true hydrogen to carbon atomic ratio were fitted polynomial to the normal boiling point of all gasoline fractions.
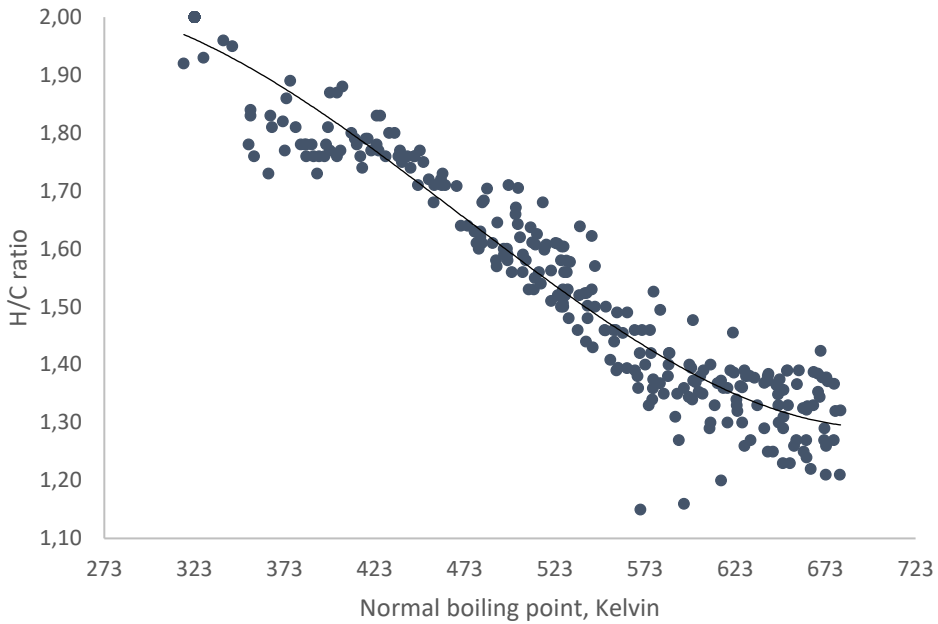

Figure 5. Measured hydrogen to carbon atomic ratio as a function of boiling point of all fractions

Hence, for H/C atomic ratio comparison, the correlation below was used.

$$\frac{H}{C} = 1.4612 * 10^{-8} T_b^3 - 2.0622 * 10^{-5} T_b^2 + 0.0073\ T_b + 1.2534 \qquad (3.2)$$

Where, H/C refers to Hydrogen to Carbon atomic ratio and T_b is normal boiling point of all Kukersite fractions in Kelvin. The R^2 for hydrogen to carbon atomic ratio for estimated contents were 0.93. This correlation could be applicable for estimating the atomic ratio of Kukersite shale oil when normal boiling is available.

Property prediction of Kukersite shale oil
Having modeled the properties of lighter portions of Kukersite shale oil fractions (gasoline fractions), the work was extended to the modelling of Kukersite shale oil fractions up to about 450 °C. The properties of fractions with boiling points higher than 180 °C were provided in the work published by (Järvik et al., 2020). In this work, wide fractions were distilled to narrow boiling range fractions and a number of fractions up to 450 °C were collected and the basic properties of these samples were measured. Having considered these data, the study of the modeling of gasoline fractions was extended to consider higher boiling fractions. To do so, the aromatic correlations obtained from the fit compounds were additionally applied to the alkane and 1-alkene correlations. For this, generalized correlations for phenolic compounds were obtained so that, the presence of the phenolic compounds could also be considered for modelling of all fractions. The correlations for phenolic compounds are as follows:

$$\frac{m_i}{M_i} = q_{01} + q_{11}\frac{M_i - M_{CH_4}}{M_i} \tag{3.3}$$

$$\sigma_i = q_{02} + q_{12}\frac{M_i - M_{CH_4}}{M_i} \tag{3.4}$$

$$\frac{\varepsilon_i}{k} = q_{03} + q_{13}\frac{M_i - M_{CH_4}}{M_i} \tag{3.5}$$

$$k^{AB} = q_{04} + q_{14}\frac{M_i - M_{CH_4}}{M_i} \tag{3.6}$$

$$\varepsilon^{AB}/k = q_{05} + q_{15}\frac{M_i - M_{CH_4}}{M_i} \tag{3.7}$$

Additionally, two more relations were included (equations 3.6 and 3.7) for these types of compounds which correspond to association parameters (association energy and association volume). The error of the fit was seen to be 11.2%. Table 6 implies the coefficients obtained for phenolic compounds from the fit. For modelling of all fractions, binary interaction parameters for all classes of compounds were set to zero except for phenolic compounds in which this value was found through optimization and obtained to be 5.9397. To summarize, correlations for paraffins and olefins are presented in article III equations 2–4, correlations for aromatic were provided in article III equations 6–8 and correlations for phenolic compounds were presented above (equations 3.3–3.7).

Table 6. Coefficients for phenolic compounds present in Kukersite shale oil

Correlation constants	Unit	Phenolic
q_{01}		0.5854
q_{11}	Å	-0.5913
q_{21}		
q_{02}		-5.2050
q_{12}	mol g^{-1}	4.4963
q_{22}		
q_{03}		361.551
q_{13}	K	4978.353
q_{23}		
q_{04}		0.3243
q_{14}	–	-0.5446
q_{05}		49830.1
q_{15}	K	-16776.9

It should be noted that the coefficients for alkane and alkene published by Gross and Sadowsky (Gross & Sadowski, 2001) and Ghosh et al. (Ghosh set al., 2003), respectively along with coefficients for aromatics obtained in our work were presented in Article III.

Overall, two separate models were developed for predicting the properties of Kukersite shale fractions. Primarily, fractions with boiling points up to 180 °C were analyzed and furthermore, fractions with boiling points up to 450 °C were taken into account considering the achieved result from low boiling fractions. As a matter of fact, it can be seen that these models could be used to predict the properties of gasoline fractions individually and the results could just be with little difference.

The models were developed in general in order to observe the behavior of shale oil fractions as a system. In spite of analyzing the behavior of the predicted vapor pressure values (as provided in article III), plotting density curves in a similar manner could also be discussed further as forthcoming investigation. Besides, more studies could be performed in detail in different paths. For instance; the calculations of heat of vaporization or viscosity could be another means to understand the change of these properties for different fractions. Another approach to implement these models is to calculate some properties of a wide gasoline fraction such as gasoline samples that are produced by the oil shale processing plant.

In a different way, creating a mixture of the different fractions in shale gasoline or possibly fractions with higher boiling points based on the mass fractions obtained from the distillations may be cooperative to further calculate the average properties of shale gasoline. One example might be calculating how the vapor pressure changes as progressively more and more of the wide fraction is vaporized.

In a larger scale, the path to creating the model could be the ground for developing a separate model for shale oil of different deposits as well as bio-oil.

4 Conclusions

In this study, multiple property prediction methods were evaluated or developed to estimate the thermodynamic and transport properties of Kukersite shale oil fractions.

Results for vapor pressure prediction correlations indicate that once basic characteristics of fractions such as normal boiling point and/or density are experimentally measured, they could be used as input parameters to suitably predict the vapor pressure of Kukersite shale oil fractions. While accuracy of these vapor pressure models was observed to be within few percent, it was found that this accuracy is improved when the property of oil mixture at approximate normal boiling point is required.

For Kukersite shale oil specifically, using PC-SAFT equation of state, properties of these types of oils could be estimated when several basic properties are available, such as normal boiling point, density and molecular weight. The error for these types of oil was acceptable considering the fact that several industrial wide fractions were obtained within prolonged period of time and also, these fractions were distilled into narrow boiling range fractions using various distillation methods. This could lead to the idea that the presented model would be applicable to diverse range of shale oil samples. Although, the applicability of these samples could be checked for different variety of shale oil samples from other resources, it is likely that it results larger error, possibly because of the structure of Kukersite shale oil, which most probably cannot be widely found in oil shale deposits around the globe. For that, suggestion could be that the initial composition of shale oil fractions to be investigated. The proposed model could be used to estimate the properties and phase behavior of shale oil primarily in Estonia where process design and environmental assessment is of interest.

Finally, the properties of phenolic compounds could be similar to those fractions obtained from distillations. This also hint that these compounds could also be used as model compounds to analyze the behavior of pyrolysis oil. However, it may be advisable to investigate the structure and well along, wider number of basic properties for these model compounds, but some of the compounds obtained from pyrolysis oil appear to be favorable when used for behavior prediction.

List of figures

List of tables

References

Aarna, Agu, & Kask, K. (1953). About the determination of the group composition of middle oil fractions of shale oil by chromatographic analysis (Об определении группового состава средних фракций сланцевой смолы методом хроматографического анализа) [in Russian]. In *in Proceedings of Tallinn University of Technology, Series A* (p. 51).

Akalin, E., Kim, Y. M., Alper, K., Oja, V., Tekin, K., Durukan, I., Siddiqui, M. Z., & Karagöz, S. (2019). Co-hydrothermal Liquefaction of Lignocellulosic Biomass with Kukersite Oil Shale. *Energy and Fuels*, *33*(8), 7424–7435.

Akash, B. A. (2010). *Energy Sources Characterization of Shale Oil as Compared to Crude Oil and Some Refined Petroleum Products*. *25*(12), 1171–1182.

Ambrose, D. (1981). Reference values of vapour pressure the vapour pressures of benzene and hexafluorobenzene. *The Journal of Chemical Thermodynamics*, *13*(12), 1161–1167.

Ambrose, D., Ewing, M. B., Ghiassee, N. B., & Sanchez Ochoa, J. C. (1990). The ebulliometric method of vapour-pressure measurement: vapour pressures of benzene, hexafluorobenzene, and naphthalene. *The Journal of Chemical Thermodynamics*, *22*(6), 589–605.

Andersen, V. F., Anderson, J. E., Wallington, T. J., Mueller, S. A., & Nielsen, O. J. (2010). Vapor pressures of alcohol-gasoline blends. *Energy and Fuels*, *24*(6), 3647–3654.

ASTM. (2003). *ASTM E 1782-03. Standard Test Method for Determining Vapor Pressure by Thermal Analysis*. ASTM International.

ASTM D2224. (1983). *Method of Test for Mean Molecular Weight of Mineral Insulating Oils by the Cryscopic Method*. ASTM International.

ASTM D2892-15. (2015). *ASTM D2892-15. Standard Test Method for Distillation of Crude Petroleum(15-Theoretical Plate Column).* ASTM International.

ASTM D6378-10. (2016). *ASTM D6378-10. Standard Test Method for Determination of Vapor Pressure (VPX) of Petroleum Products, Hydrocarbons, and Hydrocarbon-Oxygenate Mixtures (Triple Expansion Method).* ASTM International.

Baird, Zachariah, S., Oja, V., & Järvik, O. (2015). Distribution of hydroxyl groups in kukersite shale oil: Quantitative determination using fourier transform infrared (FT-IR) spectroscopy. *Applied Spectroscopy*, *69*, 555–562.

Baird, Zachariah S., Uusi-Kyyny, P., Järvik, O., Oja, V., & Alopaeus, V. (2018). Temperature and Pressure Dependence of Density of a Shale Oil and Derived Thermodynamic Properties. *Industrial and Engineering Chemistry Research*, *57*(14), 5128–5135.

Baird, Zachariah S, Uusi-Kyyny, P., Oja, V., & Alopaeus, V. (2017). Hydrogen solubility of shale oil containing polar phenolic compounds. *Industrial & Engineering Chemistry Research*, *56*(30), 8738–8747.

Baird, Zachariah Steven. (2017). *Predicting Fuel Properties From Infrared Spectra*. TUT Press.

Baird, Zachariah Steven, Oja, V., & Järvik, O. (2015). Prediction of pour points of kukersite shale oil: influence of phenols on pour point. *10th European Congress of Chemical Engineering*, 1466.

Baird, Zachariah Steven, Rang, H., & Oja, V. (2021). *Desulfurization, denitrogenation and deoxygenation of shale oil*. *38*(2), 137–154.

Barschevski, M. M., Bezmozgin, E. S., & Shapiro, R. N. (1963). *Handbook of Oil Shale Processing (Справочник по переработке горючих сланцев) [in Russian]*.

Blinova, E. A., Veldre, I. A., & Jänes, H. J. (1974). Toxicology of shale oils and phenols (Токсикология сланцевых смол и фенолов) [in Russian]. In *Institute of Experimental and Clinical Medicine*.

Boublik, T., Fried, V., & Hala, E. (1984). *The Vapor Pressure of Pure Substances* (2nd revise). Elsevier.

Brozena, A. (2013). Vapor pressure of 1-octanol below 5 kPa using DSC. *Thermochimica Acta*, *561*, 72–76.

Butrow, A. B., & Seyler, R. J. (2003). Vapor pressure by DSC: Extending ASTM E 1782 below 5 kPa. *Thermochimica Acta*, *402*, 145–152.

Chipman, J., & Peltier, S. B. (1929). Vapor Pressure and Heat of Vaporization of Diphenyl. *Industrial and Engineering Chemistry*, *21*, 1106–1108.

Chirico, R. D., Knipmeyer, S. E., Nguyen, A., & Steele, W. V. (1989). The thermodynamic properties of biphenyl. *The Journal of Chemical Thermodynamics*, *21*, 1307–1331.

Connolly, J. F., & Kandalic, G. A. (1962). Saturation Properties and Liquid Compressibilities for Benzene and n-Octane. *Journal of Chemical and Engineering Data*, *7*(1), 137–139.

Dean, J. A. (Ed.). (1992). *Lang's Handbook of Chemistry* (14th ed.). McGraw-Hill.

Derenne, S., Largeau, C., Casadevall, E., Sinninghe Damsté, J. S., Tegelaar, E. W., & de Leeuw, J. W. (1990). Characterization of Estonian Kukersite by spectroscopy and pyrolysis: Evidence for abundant alkyl phenolic moieties in an Ordovician, marine, type II/I kerogen. *Organic Geochemistry*, *16*(4–6), 873–888.

Dreisbach, R. R. (1955). *Physical Properties of Chemical Compounds: Advances in Chemistry series 15*. American Chemical Society.

Dyni, J. R. (2003). Geology and resources of some world oil-shale deposits: U.S. Geological Survey Scientific Investigations Report 2005–5294. In *Oil Shale Developments*.

Effendi, A., Gerhauser, H., & Bridgwater, A. V. (2008). Production of renewable phenolic resins by thermochemical conversion of biomass: A review. *Renewable and Sustainable Energy Reviews*, *12*, 2092–2116.

Eldermann, M., Siirde, A., & Gusca, J. (2016). Prospects for Hydrogen Production in Oil Shale Processing Industry in Estonia: Initial Aspects of Life Cycle Analysis. *Energy Procedia*, *95*, 536–539.

Elenurm, A., Oja, V., Tali, E., Tearo, E., & Yanchilin, A. (2008). Thermal processing of dictyonema argillite and kukersite oil shale: Transformation and distribution of sulfur compounds in pilot-scale galoter process. *Oil Shale*, *25*(3), 328–334.

Garrick, F. J. (1927). The vapour pressures of diphenyl and of aniline. *Transactions of the Faraday Society*, *23*, 560–563.

Ge, X., Wang, S., & Jiang, X. (2019a). Catalytic effects of shale ash with different particle sizes on characteristics of gas evolution from retorting oil shale. *Journal of Thermal Analysis and Calorimetry*, *138*, 1527–1540.

Ge, X., Wang, S., & Jiang, X. (2019b). Catalytic effects of shale ash with different particle sizes on characteristics of gas evolution from retorting oil shale. *Journal of Thermal Analysis and Calorimetry*, *138*, 1527–1540.

Ghosh, A., Chapman, W. G., & French, R. N. (2003). Gas solubility in hydrocarbons - a SAFT-based approach. *Fluid Phase Equilibria*, *209*(2), 229–243.

Golubev, N. (2003). Solid Oil Shale Heat Carrier Technology For Oil Shale Retorting. *Oil Shale*, *20*(3), 324–332.

Gross, J., & Sadowski, G. (2001). Perturbed-chain SAFT: An equation of state based on a perturbation theory for chain molecules. *Industrial and Engineering Chemistry Research*, *40*, 1244–1260.

Gubergrits, M. J., Rohtla, I., Elenurm, A., & Myasoyedov, A. M. (1989). Comparison of light oil products from oil shale retorting in solid heat carrier units UTT-3000 and UTT-500 [in Russian]. *Oil Shale*, *6*(2), 189–194.

Guo, S. H. (2009). The chemistry of shale oil and its refining. In *Coal, Oil Shale Natural Bitumen, Heavy Oil and Peat – Vol. II* (Vol. 2, pp. 94–106). Publishers Company Limited.

Hruljova, J., & Oja, V. (2015). Application of DSC to study the promoting effect of a small amount of high donor number solvent on the solvent swelling of kerogen with non-covalent cross-links in non-polar solvents. *Fuel*, *147*, 230–235.

Järvik, O., Baird, Z. S., Rannaveski, R., & Oja, V. (2020). *Properties of kukersite shale oil. Part 1: Experimental data*.

Järvik, O., Baird, Z. S., Rannaveski, R., & Oja, V. (2021). *Properties of kukersite shale oil*.

Järvik, O., & Oja, V. (2017). Molecular weight distributions and average molecular weights of pyrolysis oils from oil shales: Literature data and measurements by SEC and ASAP MS for oils from four different deposits. *Energy & Fuels*, *31*(1), 328–339.

Järvik, O., Rannaveski, R., Roo, E., & Oja, V. (2014). Evaluation of vapor pressures of 5-Methylresorcinol derivatives by thermogravimetric analysis. *Thermochimica Acta*, *590*, 198–205.

Johannes, I., Luik, H., Bojesen-Koefoed, J. A., Tiikma, L., Vink, N., & Luik, L. (2012). Effect of organic matter content and type of mineral matter on the oil yield from oil shales. *Oil Shale*, *29*(3), 206–221.

Kahru, A., Maloverjan, A., Sillak, H., & Põllumaa, L. (1994). The toxicity and fate of phenolic pollutants in the contaminated soils associated with the oil-shale industry. *Environmental Science and Pollution Research International*, *Spec No 1*, 27–33.

Knaus, E., Killen, J., Biglarbigi, K., & Crawford, P. (2010). An Overview of Oil Shale Resources. In *Oil Shale: A Solution to the Liquid Fuel Dilemma* (pp. 3–20).

Kogerman, P. N. (1931). *On the chemistry of the Estonian oil shale "Kukersite"*. *10*, 59–141.

Kogerman, P. N., & Kõll, A. (1930). *Physical properties of Estonian shale oil*.

Kollerov, D. K. (1951). *Physicochemical properties of oil shale and coal liquids (Fiziko-khimicheskie svojstva zhidkikh slantsevykh i kamenougol'nykh produktov)*.

Lee, B. I., & Kesler, M. G. (1975). A generalized thermodynamic correlation based on three-parameter corresponding states. *AIChE Journal*, *21*(3), 510–527.

Lee, S. (1990). *Oil shale technology*. CRC Press.

Lille, U. (2004). Behavior of Estonian kukersite kerogen in molecular mechanical force field. *Oil Shale*, *21*(2), 99–114.

Lille, Ü., Heinmaa, I., & Pehk, T. (2003). Molecular model of Estonian kukersite kerogen evaluated by 13C MAS NMR spectra. *Fuel*, *82*(7), 799–804.

Luts, K. (1934). *The Estonian oil shale Kukersite, its chemistry, technology and analysis (Der estländische brennschiefer-Kukersit, seine chemie, tehnologie und analyse)*. K. Mattiesens Buchdruckerei Ant.-Ges.

Lyu, G., Wu, S., & Zhang, H. (2015). Estimation and comparison of bio-oil components from different pyrolysis conditions. *Frontiers in Energy Research*, *3*, 28.

Maxwell, J. B., & Bonnell, L. S. (1955). *Vapor Pressure Charts for Petroleum Hydrocarbons*. Esso Research and Engineering Company.

Maxwell, J. B., & Bonnell, L. S. (1957). Derivation and Precision of a New Vapor Pressure Correlation for Petroleum Hydrocarbons. *Industrial & Engineering Chemistry*, *49*(7), 1187–1196.

Neshumayev, D., Pihu, T., Siirde, A., Järvik, O., & Konist, A. (2019). Solid heat carrier oil shale retorting technology with integrated CFB technology. *Oil Shale*, *36*(2S), 99–113.

Nji, G. N., Svrcek, W. Y., Yarranton, H. W., & Satyro, M. A. (2008). Characterization of heavy oils and bitumens. 1. Vapor pressure and critical constant prediction method for heavy hydrocarbons. *Energy and Fuels*, *22*(1), 455–462.

O. G. Eisen, & Rang, S. A. (1968). *Individual composition of shale oil hydrocarbons*. Institute of Chemistry, Academy of Sciences of Estonian SSR.

Oja, V., Rooks, I., Elenurm, A., Martins, A., Uus, E., & Milk, A. (2006). *An Evaluation of the Potential for Application of Gasification Technology for Oil Shale Production in Estonia (Gaasistamistehnoloogiate Rakendusvõimaluste Hindamineeestis) Põlevkiviümbertöötlemiseks*.

Oja, Vahur. (2007). Is it time to improve the status of oil shale science? In *Oil Shale*.

Oja, Vahur. (2015). Examination of molecular weight distributions of primary pyrolysis oils from three different oil shales via direct pyrolysis Field Ionization Spectrometry. *Fuel*, *159*, 759–765.

Oja, Vahur, Rooleht, R., & Baird, Z. S. (2016). Physical and thermodynamic properties of Kukersite pyrolysis shale oil: literature review. *Oil Shale*, *33*(2), 184–197.

Oja, Vahur, & Suuberg, E. M. (2012). Oil shale processing , Chemistry and Technology. In *Encyclopedia of Sustainability Science and Technology* (pp. 47–83).

Perez-Caballero, F., Peikolainen, A.-L., Koel, M., Herbert, M., Galindo, A., & Montilla, F. (2008). Preparation of the Catalyst Support from the Oil-Shale Processing By-Product. *The Open Petroleum Engineering Journal*, *1*(1), 42–46.

Pichler, H., & Lutz, J. (2014). Why Crude Oil Vapor Pressure Should Be Tested Prior to Rail Transport. *Advances in Petroleum Exploration and Development*, *7*, 58–63.

Poling, B. E., Prausnitz, J. M., O'connell, J. P., York, N., San, C., Lisbon, F., Madrid, L., City, M., Delhi, M. N., & Juan, S. (2000). *The Propeties of Gases and Liquids* (5th ed.). McGraw-Hill Education.

Qian, J., & Yin, L. (2010). *Oil Shale - Petroleum Alternative*. China Petrochemical Press.

Quann, R. J. (1998). Modeling the chemistry of complex petroleum mixtures. *Environmental Health Perspectives*, *106*(SUPPL. 6), 1441–1448.

Raj, P. K. (2016). A flammability (risk) index for use in transportation of flammable liquids. *Journal of Loss Prevention in the Process Industries*, *44*, 755–763.

Rannaveski, R, & Listak, M. (2018). Flash points of gasoline from Kukersite oil shale: Prediction from vapor pressure. *Agronomy Research*, *16*(S1), 1218–1227.

Rannaveski, Rivo. (2018). *Developing a novel method for using thermal analysis to determine average boiling points of narrow boiling range continuous mixtures.* TalTech.

Rannaveski, Rivo, Listak, M., & Oja, V. (2018). ASTM D86 distillation in the context of average boiling points as thermodynamic property of narrow boiling range oil fractions. *Oil Shale*, *35*(3), 254–264.

Raukas, A., & Siirde, A. (2012). New trends in estonian oil shale industry. In *Oil Shale* (Vol. 29, Issue 3).

Reinik, J., Irha, N., Steinnes, E., Piirisalu, E., Aruoja, V., Schultz, E., & Leppänen, M. (2015). Characterization of water extracts of oil shale retorting residues form gaseous and solid heat carrier processes. *Fuel Processing Technology*, *131*, 443–451.

Riazi, M R. (2005). *Characterization and Properties of Petroleum Fractions*. ASTM International.

Riazi, Mohammad R., & Al-Enezi, G. A. (1999). Modelling of the rate of oil spill disappearance from seawater for Kuwaiti crude and its products. *Chemical Engineering Journal*, *73*, 161–172.

Ribeiro da Silva, M. A. V., & Lobo Ferreira, A. I. M. C. (2009). Experimental standard molar enthalpies of formation of some methylbenzenediol isomers. *Journal of Chemical Thermodynamics*, *41*, 1096–1103.

Savest, N., & Oja, V. (2013). Heat Capacity of Kukersite Oil Shale: Literature Overview. *Oil Shale*, *30*(2), 184–192.

Seitmaganbetov, N., Rezaei, N., & Shafiei, A. (2021). Characterization of crude oils and asphaltenes using the PC-SAFT EoS: A systematic review. *Fuel*, *291*, 120180.

Siirde, A., Eldermann, M., Rohumaa, P., & Gusca, J. (2013). Analysis of greenhouse gas emissions from Estonian oil shale based energy production processes. life cycle energy analysis Perspective. *Oil Shale*, *30*(2 SUPPL.), 268–282.

Siitsman, C., & Oja, V. (2016). Application of a DSC based vapor pressure method for examining the extent of ideality in associating binary mixtures with narrow boiling range oil cuts as a mixture component. *Thermochimica Acta*, *637*, 24–30.

Sillak, S., & Kanger, L. (2020). Global pressures vs. local embeddedness: the de- and restabilization of the Estonian oil shale industry in response to climate change (1995–2016). *Environmental Innovation and Societal Transitions*, *34*, 96–115.

Skrynnikova, G. N. (1954). Experimental investigation of thermal conductivity coef-ficients of oil shale pyrolysis liquids (Eksperimental'noe issledovanie koéffitsienta teploprovodnosti zhidkikh slantsevykh produktov). In G. N. Kollerov, D. K. Zelenin, N. Ya. Garnovskaya (Ed.), *Chemistry and technology of products of oil shale processing (Khimiya i tekhnologiya pro-duktov pererabotki slantsev)* (pp. 242–268).

Speight, J. G. (2014). The Chemistry and Technology of Petroleum. In *The Chemistry and Technology of Petroleum*.

Stephenson, R. M., & Malanowski, S. (1987). Handbook of the Thermodynamics of Organic Compounds. In *Handbook of the Thermodynamics of Organic Compounds*. Elsevier.

Tissot, B. P., Welte, D. H., Tissot, B. P., & Welte, D. H. (1978). Oil Shales: A Kerogen-Rich Sediment with Potential Economic Value. In *Petroleum Formation and Occurrence* (pp. 225–236). Springer Berlin Heidelberg.

Tsonopoulos, C, Heidman, J L, & Hwang, S. (1986). *Thermodynamic and Transport Properties of Coal Liquids*.

Tumakaka, F., Gross, J., & Sadowski, G. (2005). Thermodynamic modeling of complex systems using PC-SAFT. *Fluid Phase Equilibria*, *228–229*, 89–98.

Urov, K., & Sumberg, A. (1999). Characteristics of oil shales and shale-like rocks of known deposits and outcrops: monograph. In *Oil shale Special*. Estonian Acad. Publ.

Van Nes, K., & Van Westen, H. A. (1951). *Aspects of the Constitution of Mineral Oils*. Elsevier Publishing Company.

Wagner, W., & Pruß, A. (2002). The IAPWS formulation 1995 for the thermodynamic properties of ordinary water substance for general and scientific use. *Journal of Physical and Chemical Reference Data*, *31*, 387–535.

Watson, K. M., & Nelson, E. F. (1933). Improved Methods for Approximating Critical and Thermal Properties of Petroleum Fractions. *Industrial and Engineering Chemistry*, *25*(8), 880–887.

Weast, R. C., Grasselli, J. G., & Lide, D. R. (1989). *Handbook of data on organic compounds*. CRC Press.

Wilhoit, R. C., & Zwolinski, B. J. (1971). *Handbook of vapor pressures and heats of vaporization of hydrocarbons and related compounds*. Thermodynamics Research Center,College Station, TX.

Willingham, C. B., Taylor, W. J., Pignocco, J. M., & Rossini, F. D. (1945). Vapor pressures and boiling points of some paraffin, alkylcyclopentane, alkylcyclohexane, and alkylbenzene hydrocarbons. *Journal of Research of the National Bureau of Standards*, *35*(3), 219–244.

Wilson, G. M., Johnston, R. H., Hwang, S. C., & Tsonopoulos, C. (1981). Volatility of Coal Liquids at High Temperatures and Pressures. *Industrial and Engineering Chemistry Process Design and Development*, *20*(1), 94–104.

Xiu, S., & Shahbazi, A. (2012). Bio-oil production and upgrading research: A review. *Renewable and Sustainable Energy Reviews*, *16*, 4406–4414.

Yang, Y., Gilbert, A., & Xu, C. (Charles). (2009). Hydrodeoxygenation of bio-crude in supercritical hexane with sulfided CoMo and CoMoP catalysts supported on MgO: A model compound study using phenol. *Applied Catalysis A: General*, *360*, 242–249.

Ye, Y., Zhang, Y., Fan, J., & Chang, J. (2012). Selective production of 4-ethylphenolics from lignin via mild hydrogenolysis. *Bioresource Technology*, *118*, 648–651.

Yu, X., Luo, Z., Li, H., Zhang, J., & Gan, D. (2019). The diffusion and separation of the oil shale in the compound dry beneficiation bed. *Powder Technology*, *355*, 72–82.

Zelenin , N. I. , Fainberg , V. S. , Chernysheva, K. B. (1968). Physicochemical properties (Fiziko-khimicheskie svojstva). In *Chemistry and technology of oil shale tars (Khimiya i tekhnologiya slantsevoj smoly)* (pp. 132–179).

Zhang, X., Zhang, Q., Wang, T., Ma, L., Yu, Y., & Chen, L. (2013). Hydrodeoxygenation of lignin-derived phenolic compounds to hydrocarbons over Ni/SiO2-ZrO2 catalysts. *Bioresource Technology*, *134*, 73–80.

Acknowledgements

All the way through, I was given lots of support. For that, I could keep up with all the ups and downs I encountered throughout the work.

I express my gratitude to my supervisors, Oliver and Zach for their advice and patience. To Prof. Oja who laid the foundation of this journey for me. To the head of the department, Andres, who was always supportive. To all the colleagues who shared their experiences with me and to my family and friends who were with me. Thank you for all these years of what I say tremendously challenging but it became more enjoyable for me with you.

Abstract

Phase Equilibria of Complex Mixture in the Context of Unconventional Fuel Resources

Predicting various thermodynamic, physical and transport properties of hydrocarbon mixtures is crucial to oil operations and related industries to be used for oil unit design, separation processes etc. While characterization of oil is important, these data are not always widely available or measured, and therefore, developing reliable approaches with suitable accuracy has continuously been requisite for vapor-liquid phase equilibria calculations. Property prediction methods were mostly defined for conventional oils and effectiveness of these methods yet to be thoroughly evaluated for shale oils. Besides, outcome could vary for the reason that shale oil resources are different in composition and other properties. While Estonian Kukersite shale oil has been fairly utilized and studied in the last century, there has been inadequate data for them. Moreover, despite having distinctive structure, applicability of predictive methods for petroleum yet to be investigated or further, separate model to be independently introduced for these types of oils.

The goal of this thesis was to present an additional dataset for Kukersite shale oil and then introduce an additional applicable model, which could be used as predictive tool for these types of oils. This was done using existing correlations that have been previously developed for petroleum, and creating several equations with respect to properties of oil fractions to model Kukersite shale oil.

Therefore, narrow boiling range gasoline fractions distilled from wide fraction as well as several compounds derived from pyrolysis oil were studied. Gasoline fractions were used to evaluate the applicability of vapor pressure prediction correlations and pyrolysis oil derived phenolic compounds were used to observe the relevance of such compounds if they can be used as a model compound for phenolic part of Kukersite shale oil. Using an extensive database of measured Kukersite shale oil properties, PC-SAFT equation of state was develop to model Kukersite shale oil.

This study led to realize that petroleum vapor pressure correlations for light fractions were applicable to shale oil gasoline fractions and furthermore, the developed model for Kukersite shale oil in this work could be used to predict and model the characteristics of shale oil in general with reasonable accuracy.

Lühikokkuvõte

Komplekssete segude faaside tasakaalud mittekonventsionaalsete energiaallikate tehnoloogiates

Süsivesinike põhiste multikomponentsete segude termodünaamilisi, füüsikalisi ja transpordiomadusi kasutatakse naftatööstuses ja sellega seotud tööstusharudes erinevate protsesside, sealhulgas separatsiooniprotsesside projekteerimisel. Kuigi nimetatud omaduste teadmine on oluline, ei ole need andmed alati avalikult kättesaadavad või teada. Seetõttu on näiteks faasitasakaalu andmete usaldusväärset hindamist võimaldavate meetodite väljatöötamine jätkuvalt oluline. Meetodid erinevate omaduste hindamiseks on tavaliselt välja töötatud naftafraktsioonide jaoks, mistõttu tuleb nende meetodite sobivust mittekonventsionaalsete õlide puhul põhjalikult kontrollida. Põlevkiviõlide kui mittekonventsionaalsete õlide korral tuleb arvestada sellega, et nende koostis ja omadused olenevad põlevkivi leiukohast. Kuigi kukersiitset põlevkiviõli on viimasel sajandil põhjalikult uuritud ja see on leidnud laialdast kasutust, siis andmed termodünaamilised omaduste kohta on puudulikud. Veelgi enam, kuna kukersiitsel põlevkiviõlil on iseloomulik koostis, siis naftafraktsioonidel põhinevad ennustusmudelite rakendatavust tuleb veel uurida ja enamasti tuleb seda tüüpi õlide jaoks võtta kasutusele eraldi mudelid.

Käesoleva doktoritöö eesmärgiks oli luua kukersiitse põlevkiviõli omaduste kohta täiendav andmestik ning nende andmete abil pakkuda välja mudelid, mida saaks kasutada seda tüüpi õlide omaduste hindamiseks. Mudelid loodi kas varem nafta jaoks välja töötatud korrelatsioonide põhjal või töötati välja olekuvõrrandid kukersiitse põlevkiviõli modelleerimiseks.

Mudelite koostamiseks uuriti nii laia keemispiiriga bensiinifraktsioonist destilleerimise teel saadud kitsaste keemispiiridega bensiinifraktsioone kui ka mitmeid pürolüüsiõlides esinevaid ühendeid. Bensiinifraktsioone kasutati aururõhu hindamiseks kasutatavate korrelatsioonide rakendatavuse kontrollimiseks. Pürolüüsiõlis leiduvaid fenoolseid ühendeid kasutati hindamaks selliste ühendite kasutatavust kukersiitse põlevkiviõli fenoolse osa modelleerimist võimaldavate mudelühenditena (pseudokomponentidena). Kasutades kukersiitse põlevkiviõli omaduste mõõtetulemuste andmebaasi, töötati välja PC-SAFT olekuvõrrand kukersiitse põlevkiviõli modelleerimiseks.

Töö tulemusena jõuti järeldusele, et nafta kergete fraktsioonide jaoks välja töötatud aururõhkude hindamiseks kasutatav korrelatsioon sobivad ka põlevkiviõlist saadud bensiinifraktsiooni aururõhkude hindamiseks. Lisaks, käesolevas töös väljatöötatud mudelit kukersiitsele põlevkiviõlile saab kasutada selleks, et mõistliku täpsusega arvutada põlevkiviõli omadusi üldiselt.

Appendix

Publication I
Mozaffari, P.; Baird, Z. S.; Listak, M.; Oja, V. (2020). Vapor pressures of narrow gasoline fractions of oil from industrial retorting of Kukersite oil shale. Oil Shale. 37(4), 288–303.

Vapor pressures of narrow gasoline fractions of oil from industrial retorting of Kukersite oil shale

Parsa Mozaffari, Zachariah Steven Baird, Madis Listak, Vahur Oja*

Department of Energy Technology, School of Engineering, Tallinn University of Technology, Ehitajate tee 5, 19086 Tallinn, Estonia

Abstract. *This study presents vapor pressure data for narrow boiling range fractions, viewed as pseudocomponents, prepared by rectification from a wide Kukersite oil shale retort oil gasoline fraction, a straight-run fraction with a boiling range from about 40 to about 200 °C. This technical gasoline fraction was produced in a commercial solid heat carrier retort. Vapor pressures were measured according to the ASTM D6378 standard with a commercial ERAVAP vapor pressure tester using a vapor-liquid ratio of 4:1. The vapor pressure curves were derived by fitting the experimental data using the integrated form of the Clausius-Clapeyron equation. From this equation heats of vaporization and atmospheric boiling points were calculated. The suitability of three easy-to-use conventional oil vapor pressure correlations for predicting the vapor pressure of narrow boiling range fractions of Kukersite oil shale retort oil gasoline was evaluated.*

Keywords: *Kukersite oil shale, oil shale retort oil, gasoline fraction, pseudocomponents, vapor pressure, vapor pressure correlations.*

1. Introduction

Vaporization properties are important to be taken into account in transporting, handling and storing liquid oil products or evaluating their environmental risks [1–3]. This information can be used in calculations for designing processes and equipment and in modelling the spread of oil in the environment. For conventional oils, vapor pressure correlations are available for predicting vapor pressures from the basic properties of oils [4–7]. However, there is less information available for alternative oils, including oils produced via retorting (or pyrolysis) from oil shales from various deposits [8–11]. Many of these alternative oils contain polar compounds, which can make prediction more difficult due to the increased complexity of the intermolecular interactions in these oils [12–17].

---

* Corresponding author: e-mail *vahur.keemteh@outlook.com*

In general, our literature review indicated that only a small amount of data existed on the thermodynamic and transport properties of oils produced via retorting from oil shales, especially for their narrow boiling range fractions [18, 19]. For example, Estonian Kukersite oil shale retort oil is one of the most extensively studied oils of this type [12, 20, 21], but only limited information can be found in the literature [18, 19, 22–24]. A recent literature review by Oja et al. [19] on the thermodynamic properties of Kukersite oil shale retort oil showed that the publicly available information was spotty and poorly suitable for evaluating the applicability of the existing thermodynamic property prediction methods, even for evaluating the simplest approaches based on "undefined" pseudocomponents [5, 6]. Concerning the vaporization characteristics of Kukersite oil shale retort oil, Kollerov [18] presented data on the vapor pressures at different vapor-liquid ratios, including for some samples in the boiling range of gasoline and diesel. Also, data for a few narrow boiling range gasoline fractions were provided by Siitsman and Oja [16, 25]. At the same time, the studies by Siitsman et al. [26] and Astra and Oja [27] were focused only on evaluating the applicability of a differential scanning calorimetry method to measuring the vapor pressures of complex mixtures such as narrow boiling range oil fractions, while no vapor pressure data for the Kukersite straight-run gasoline sample was presented. It should be noted that in practice, there are various techniques for measuring the vapor pressure of oil-like compounds and complex mixtures depending on the volatility of the sample [28–33]. In the current study, the vapor pressures of the gasoline samples (narrow boiling fractions with boiling points of about 60 to 130 ℃) were measured according to the ASTM D6378-10 standard [34], using a commercial ERAVAP analyzer (Eralytics GmbH, Vienna, Austria).

The purpose of this study was to provide the vapor pressure data for the Kukersite gasoline narrow boiling range fractions (distillation cuts that can be viewed as pseudocomponents). This information can be used for calculations related to handling, storage and risk assessment. Also, the applicability of the existing petroleum based easy-to-use vapor pressure correlations for these Kukersite gasoline fractions was evaluated [6, 35–38]. Lighter (i.e. lower boiling) fractions of Kukersite oil are known to contain more olefins and aromatic hydrocarbons than those of conventional oils [12, 19].

2. Experimental and methods

2.1. Sample preparation

The Kukersite oil shale gasoline fraction, a wide straight-run fraction with a boiling range from about 40 to about 200 °C, was obtained from Eesti Energia's Narva Oil Plant (Narva, Estonia). The plant uses solid heat carrier technology to convert oil shale organic matter into oil [39, 40]. In this

technology, pyrolysis vapors are fed from a retort to a distillation/separation column that separates oil into three broad industrial fractions: gasoline, fuel oil and heavy oil. The wide straight-run gasoline fraction used in the current study had a density of 0.7904 g/cm^3 and a refractive index of 1.4445 at 20 °C. Literature-based elemental composition data show that usually up to 3% of the Kukersite straight-run gasoline fractions consist of heteroatoms, most of which are likely sulfur and oxygen compounds [12, 13].

The wide straight-run gasoline fraction was further separated into fractions with narrow boiling ranges using rectification in accordance with ASTM D2892 [41]. For rectification, a packed distillation column with 24 theoretical plates and a 6:1 reflux ratio was used. The rectification was largely by volume, collecting approximately 18 to 20 ml of sample. During sample collection, the vapors were condensed in a glass condenser at about –10 °C and the liquid gasoline was then collected in pre-cooled vials (to about –10 °C) to ensure no loss of volatiles.

2.2. Vapor pressure measurements and data analysis

Vapor pressure was measured according to ASTM D6378-10 [34] with said ERAVAP analyzer using a vapor-liquid ratio of 4:1. The instrument had a temperature range of 273–393 K and a pressure range from a few kPa to 1000 kPa. Based on experience, the device was best suited for samples with vapor pressures between 10 and 150 kPa at 310.95 K. The accuracy of the measurements made with the apparatus was checked by measuring the vapor pressure of benzene between 40 and 90 °C and that of toluene between 60 and 90 °C. The measured data together with selected reference data are given in Table 1 for benzene and in Table 2 for toluene. Based on this data (the difference between the measured and reference data points), the standard uncertainty of the vapor pressure measurements presented here was found to be better than 0.3 kPa.

Table 1. Accuracy of vapor pressure values of benzene (boiling point 80.1 °C) measured using the ERAVAP analyzer

T, °C	P, kPa	P^1, kPa	ΔP^1, kPa	P^2, kPa	ΔP^2, kPa	P^3, kPa	ΔP^3, kPa	P^4, kPa	ΔP^4, kPa	P^5, kPa	ΔP^5, kPa
40.0	24.1	24.4	–0.3	24.4	–0.3	24.4	–0.3	24.4	–0.3	24.4	–0.3
50.0	36.2	36.2	0.0	36.2	0.0	36.2	0.0	36.2	0.0	36.2	0.0
60.0	52.3	52.2	0.1	52.2	0.1	52.2	0.1	52.2	0.1	52.2	0.1
70.0	73.4	73.4	0.0	73.5	–0.1	73.4	0.0	73.5	–0.1	73.4	0.0
80.0	100.9	101.0	–0.1	101.0	–0.1	101.0	–0.1	101.0	–0.1	101.0	–0.1
90.0	135.8	136.1	–0.3	136.1	–0.3	136.1	–0.3	136.1	–0.3	136.1	–0.3

Note: [1] is reference [42], [2] is reference [43], [3] is reference [44], [4] is reference [46], [5] is reference [47].

Table 2. Accuracy of vapor pressure values of toluene (boiling point 110.6 °C) measured using the ERAVAP analyzer

T, °C	P, kPa	P^1, kPa	ΔP^1, kPa	P^2, kPa	ΔP^2, kPa	P^3, kPa	ΔP^3, kPa	P^4, kPa	ΔP^4, kPa
60.0	18.6	18.5	0.1	18.5	0.1	18.5	0.1	18.5	0.1
70.0	27.4	27.2	0.2	27.2	0.2	27.2	0.2	27.2	0.2
80.0	39.1	38.8	0.3	38.8	0.3	38.8	0.3	38.8	0.3
90.0	54.1	54.2	−0.1	54.2	−0.1	54.2	−0.1	54.2	−0.1

Note: [1] is reference [42], [2] is reference [48], [3] is reference [44], [4] is reference [49].

Comparison of measured data with easy-to-use conventional oil vapor pressure correlations was performed using the root mean squared error (RMSE) and residual (a simple difference between predicted and measured values, r):

$$RMSE = \sqrt{\frac{\Sigma(\theta_p - \theta_m)^2}{n}}, \qquad (1)$$

$$r = \theta_m - \theta_p, \qquad (2)$$

where θ_p is the predicted value, θ_m is the measured value and n is the number of data points.

2.3. Determination of fraction properties

The characteristic properties of the fractions used in this study (density at 20 °C, refractive index at 20 ° C, average boiling point, K_W factor) are given in Table 3. The density at 20 °C was measured using a DMA 5000M density meter (Anton Paar GmbH, Graz, Austria). The instrument has a reproducibility of 0.00005 g/cm³. For gasoline samples, the standard uncertainty was found to be 0.00015 g/cm³. The refractive index at 20 °C was measured on an Abbemat HT refractometer (Anton Paar GmbH, Graz, Austria) at a wavelength of 589.592 nm. For gasoline samples, the standard uncertainty was found to be 0.0011. The average boiling point of narrow boiling range fractions was determined as the arithmetic mean of the lower and upper temperature limits of the fraction collected during rectification (provided that the fraction had a Gaussian boiling point distribution), with a measurement uncertainty of 1 °C. For fraction 4 alone, the average boiling point was not calculated because, due to an experimental error in collecting this fraction, its initial boiling point was higher than the final boiling point. The K_W factor, also called the Watson characterization factor or the Universal Oil Products Company (UOP) characterization factor, was calculated from measured density and average boiling point values according to the following equation:

Table 3. Properties of narrow boiling gasoline fractions

Fraction	T_{av}, °C	ρ, g/cm³	RI	K_W
1	63	0.71033	1.4053	11.9
2	77	0.73005	1.4161	11.7
3	92	0.74776	1.4235	11.5
4		0.74978	1.4254	11.5*
5	89	0.74188	1.4210	11.6
6	99	0.76079	1.4299	11.5
7	108	0.78518	1.4420	11.2
8	115	0.76604	1.4314	11.5
9	119.5	0.76254	1.4298	11.6
10	123.5	0.77531	1.4359	11.4
11	130	0.79599	1.4466	11.2
12	137	0.80901	1.4524	11.1

Note: T_{av} – average boiling point, ρ – density at 20 °C, *RI* – refractive index at 20 °C, K_W – Watson characterization factor.
* Indicative K_w value, calculated using the normal boiling point calculated from the integrated Clausius-Clapeyron equation (integrated Clausius-Clapeyron equation constants are reported in Table 5).

$$K_w = \frac{\sqrt[3]{T_{av}}}{S},$$ (3)

where T_{av} is the fraction's average boiling point, R, and *S* is the specific gravity at 60 °F. (However, in this study we used the density at 20 ° C, instead of 15.5 °C, to calculate specific gravity because the corresponding error was judged to be insignificant in our calculations). For fraction 4, the indicative value of K_w was calculated using the normal boiling point (estimated through the integrated Clausius-Clapeyron equation, Eq. (4)).

3. Results and discussion

3.1. Vapor pressure data

The experimental vapor pressure data for the twelve Kukersite oil shale retort oil narrow boiling range gasoline fractions is given in Table 4 and is shown graphically in Figure 1. The vapor pressures of all the fractions exhibited a linear trend on the ln(*P*) versus 1/*T* plot, and the R² correlation coefficient values were greater than 0.9995 for all the samples. Therefore, the integrated form of the Clausius-Clapeyron equation (Eq. (4)) was used to fit the

Table 4. Vapor pressure values (kPa) for the Kukersite oil shale derived gasoline fractions (Fr.) measured at different temperatures (T, °C)

T, °C	Fr. 1	Fr. 2	Fr. 3	Fr. 4	Fr. 5	Fr. 6	Fr. 7	Fr. 8	Fr. 9	Fr. 10	Fr. 11	Fr. 12
40.0	53.5	37.6	27.1	25.7	21.9							
50.0	75.7	53.5	39.7	36.9	32.1	22.5						
60.0	104.2	74.4	56.6	51.9	45.9	33.6	25.4					
70.0	140.8	101.3	77.8	71.3	64.4	47.2	36.7	30.1	23.8			
80.0	185.9	135.5	104.1	95.9	88.2	64.7	50.8	41.8	34.5	41	26.3	21.3
90.0	241.7	178.0	136.8	126.9	118.5	87.3	69	56.9	47.8	58	36.9	30.2
100.0	309.7	230.2	176.9	165.2	156.6	115.8	92.5	76.3	65.5	78.5	51.8	42.4
110.0	391.4	293.0	225.7	211.7	203.3	151.5	122.6	101.3	88.5	106.2	72.4	57.8
120.0	489	368.8	285.3	268.2	260.6	198.3	159.7	135.1	117.1	141.6	97.1	77.4

Table 5. Regression parameters A and B, heats of vaporizations (ΔH) and normal boiling points (T_b) for the Kukersite oil shale derived gasoline fractions studied

Fraction	A	B	ΔH, kJ/mol	T_b, °C
1	3398.5 ± 22.0	14.8 ± 0.1	28.3 ± 0.2	59.2
2	3513.1 ± 14.6	14.9 ± 0.0	29.2 ± 0.1	70.1
3	3601.9 ± 60.6	14.8 ± 0.2	29.9 ± 0.5	79.7
4	3607.3 ± 17.3	14.8 ± 0.0	30.0 ± 0.1	82.1
5	3812.2 ± 19.2	15.3 ± 0.1	31.7 ± 0.2	84.8
6	3906.6 ± 62.2	15.2 ± 0.2	32.5 ± 0.5	95.1
7	3995.7 ± 38.4	15.2 ± 0.1	33.2 ± 0.3	103.1
8	4032.0 ± 77.9	15.1 ± 0.2	33.5 ± 0.6	109.7
9	4286.4 ± 54.0	15.7 ± 0.1	35.6 ± 0.4	114.7
10	4283.5 ± 77.5	15.8 ± 0.2	35.6 ± 0.6	108.3
11	4563.6 ± 116.3	16.2 ± 0.3	37.9 ± 1.0	121.4
12	4486.9 ± 55.3	15.8 ± 0.1	37.3 ± 0.5	129.4

experimental data of the fractions as follows:

$$\ln P = -\frac{A}{T} + B = \frac{-\Delta H_{vap}}{RT} + B,$$ (4)

where P is the vapor pressure, kPa; ΔH_{vap} is the heat of vaporization, J mol^{-1}; T is the temperature, K; A and B are fitting constants and R is the ideal gas constant (8.314 J mol^{-1} K^{-1}). For each fraction the values of fitting constants A and B, together with the calculated heat of vaporization (from the fitting constant A) and atmospheric boiling point values (calculated at pressure 101.3 kPa) are given in Table 5.
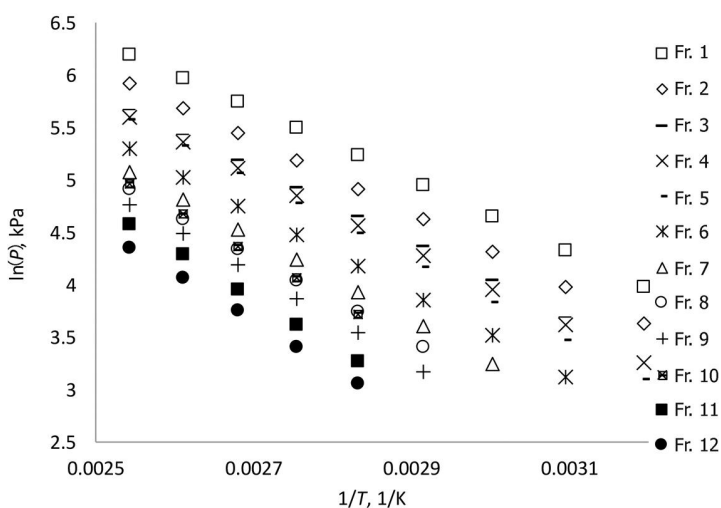
Fig. 1. Vapor pressures of Kukersite oil shale derived gasoline fractions on a $1/T$ vs $\ln(P)$ plot.

3.2. Evaluation of the applicability of prediction methods to oil shale gasoline

Various prediction methods, such as equations and graphs of varying degrees of complexity, have been developed to predict the vapor pressure of liquid fuels [5, 6]. In this study only easy-to-use methods, i.e. those based on conveniently measureable input parameters, were selected for evaluation. Correlations requiring critical temperature, critical pressure and acentric factor, i.e. parameters estimated by conventional oil-based empirical correlations, remained beyond consideration. The selected correlations were the following: a correlation from Van Nes and Van Westen [35], the Maxwell and Bonnell correlations [36, 37] and the modification to the Maxwell and Bonnell correlations presented by Tsonopoulos et al. [6] and Wilson et al. [38].

The correlation from Van Nes and Van Westen [35] is expressed by Equation (5) as follows:

$$log_{10}P_T = 3.2041\left(1 - 0.998 \cdot \frac{T_b - 41}{T - 41} \cdot \frac{1393 - T}{1393 - T_b}\right), \tag{5}$$

where P_T is the vapor pressure, bar, at temperature T, K, and T_b is the normal boiling point, K.

The Maxwell and Bonnell correlations [36, 37] are written as:

$$log_{10}P^{vap} = \frac{3000.538Q - 6.761560}{43Q - 0.987672} \text{ for } Q > 0.0022 \ (P^{vap} < 2 \text{ torr}), \tag{6}$$

$$log_{10}P^{vap} = \frac{2663.129Q - 5.994296}{95.76Q - 0.972546} \text{ for } 0.0013 \le Q \le 0.0022 \ (2 \text{ torr} \le P^{vap} \le 760 \text{ torr}), \tag{7}$$

$$log_{10}P^{vap} = \frac{2770.085Q - 6.412631}{36Q - 0.989679} \text{ for } Q < 0.0013 \ (P^{vap} > 760 \text{ torr}), \tag{8}$$

$$Q = \frac{\frac{T'_b}{T} - 0.00051606T'_b}{748.1 - 0.3861T'_b}, \tag{9}$$

$$T'_b = T_b - \Delta T_b, \tag{10}$$

$$\Delta T_b = 1.3889F(K_W - 12)log_{10}\frac{P^{vap}}{760}, \tag{11}$$

$$F = 0 \quad \text{if } T_b < 367\text{K if } T_b < 367\text{K}, \tag{12}$$

$$F = -3.2985 + 0.009T_b \text{ if } T_b \ge 367\text{K}, \tag{13}$$

where P^{vap} is the vapor pressure, Torr; T is the temperature at which the vapor pressure is to be calculated, K; T_b is the normal boiling point, K; $T_b{}'$ is the normal boiling point corrected to the Watson characterization factor $K_W = 12$, K; F is the correction factor for the fractions with a K_W different than 12 (crude oils are classified as paraffinic with K_W between 11 and 12.9).

The modification to the Maxwell and Bonnell correlations presented by Tsonopoulos et al. [6] and Wilson et al. [38] gives equations which replace Equations (11)–(13):

$$\Delta T_b = F_1 F_2 F_3, \tag{14}$$

$$F_1 = \begin{cases} 0, & T_b \le 366.5K \\ -1 + 0.009(T_b - 255.37), & T_b > 366.5K \end{cases}, \tag{15}$$

$$F_2 = (K_W - 12) - 0.01304(K_W - 12)^2, \tag{16}$$

$$F_3 = \begin{cases} 1.47422 log_{10} P^{vap}, & P^{vap} \leq 1atm \\ 1.47422 log_{10} P^{vap} + 1.190833(log_{10} P^{vap})^2, & P^{vap} > 1atm \end{cases}, \tag{17}$$

where P^{vap} is in the units of atm.

The RMSEs (3.4, 2.9 and 2.9 kPa, respectively) of the predicted vapor pressure values for each correlation show that, overall, the three selected correlations performed similarly, although the Maxwell and Bonnell correlations were slightly more accurate than the Van Nes and Van Westen correlation. Also the trend in the residuals was similar for all the correlations. The residuals of each point of the Maxwell and Bonnell correlations and the Van Nes and Van Westen correlation are shown in Figure 2 (individual fractions are not distinguished). The corresponding relative deviation of the predicted values was typically less than 5%.
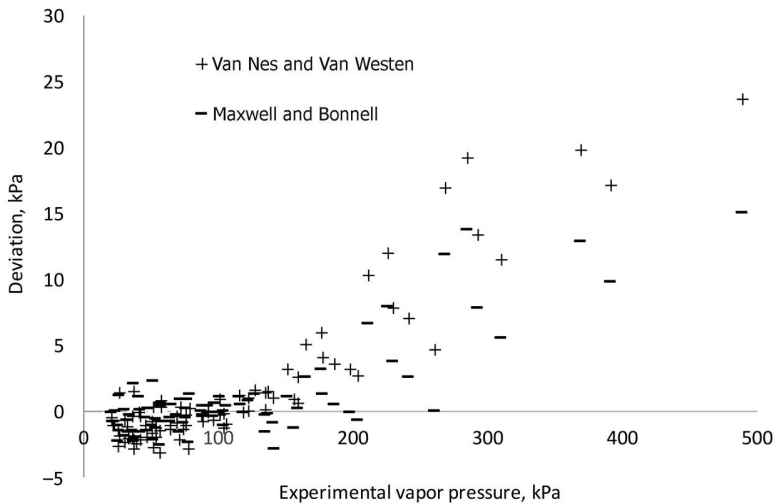

Fig. 2. Deviation of predicted vapor pressure values from the experimental values (given as predicted value minus measured value).

Due to the fixed temperature range of the measuring apparatus, 273–393 K, and the different volatilities of the fractions, their measured vapor pressure ranges varied significantly, the vapor pressure of fraction 1 was measured between 53.5 and 489 kPa, and that of fraction 12 between 21.3 and 77.4 kPa. Therefore, to better illustrate the performance of easy-to-use conventional
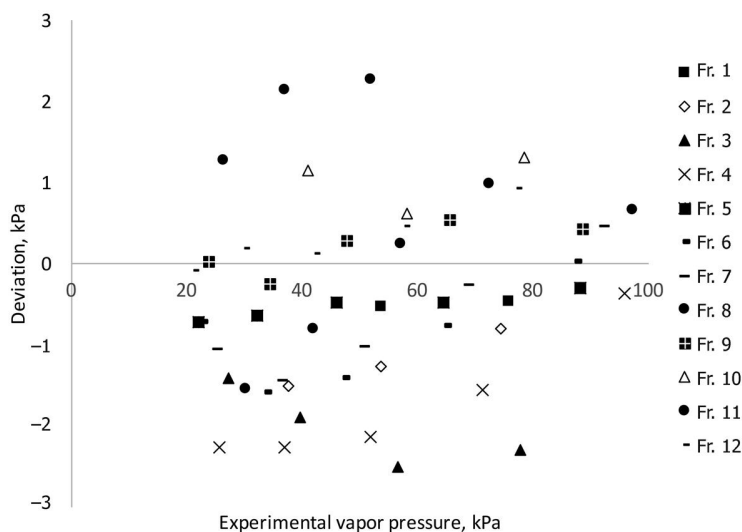
Fig. 3. Deviation of vapor pressure values predicted by the Maxwell and Bonnell correlations, from the experimental values, illustrated for all fractions at pressures up to 100 kPa.
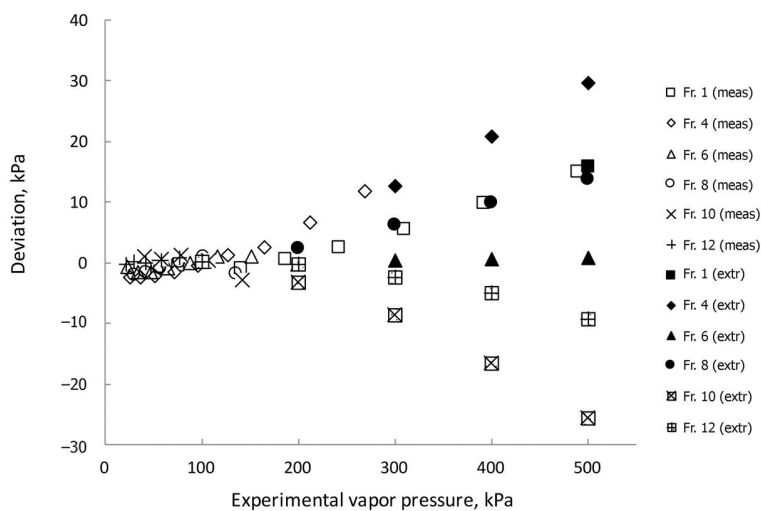

Fig. 4. Deviation of vapor pressures predicted by the Maxwell and Bonnell equation from the experimental values, illustrated for selected fractions at pressures up to 500 kPa. Experimental data-based residuals are shown as open points and extrapolated data-based residuals as solid points. (Abbreviations: meas – measured, extr – extrapolated.)

oil equations, the Maxwell and Bonnell correlations-based comparison is presented somewhat differently in Figures 3 and 4. Figure 3 shows the residuals, distinguishing each fraction specifically, up to a pressure of 100 kPa. It can be seen from Figure 3 that the residues vary quite randomly by fraction, the behavior of fractions exhibiting random variation around the average deviation trend. At the same time, the predicted vapor pressure values have a deviation of ± 2.5 kPa, while the relative deviation at 50 kPa is less than 5%. Some explanations for this, more like random variation, can be derived from the data in Table 3. Table 3, which contains characteristic data, shows that as the fraction number increases, there is no strictly monotonic increase in density or refractive index; rather, slight local minima and maxima can be seen in the generally increasing behavior with an increase in the initial boiling point. Assuming that the uncertainty associated with distillation is not so significant, this may indicate that the rectification results in the dominance of different classes of compounds among the boiling regions of the fractions. Figure 4 shows residuals for six selected fractions up to 500 kPa, displaying both experimental data-based residuals (open points) and extrapolated data-based residues (solid points). The extrapolation beyond the measurement region is done here for illustrative purposes only. Again, the residuals vary quite randomly by fraction and the corresponding relative deviations of the predicted values fall below 5%.

In summary, the easy-to-use vapor pressure correlations, which were evaluated in this study, can be used to get reasonable estimates of the vapor pressure for these types of shale oil gasoline fractions and a choice between them could be merely a matter of convenience.

4. Conclusions

This article presented vapor pressure data for the narrow boiling fractions (or pseudocomponents) prepared by rectification from a wide technical gasoline fraction, which in turn was produced from Kukersite oil shale by using solid heat carrier retorting technology. Basic characteristics information (specific gravity, refractive index, average boiling point) was also measured for these fractions. It was found that the three examined easy-to-use correlations (which were based on conveniently measureable input parameters, either atmospheric boiling point or atmospheric boiling point and the characterization K_W factor calculable on the basis of density and average boiling point) provided reasonable estimates of the vapor pressure of the gasoline fractions studied, while the choice between them could be merely a matter of convenience. In general, the performance of the different correlations was similar, although the Maxwell and Bonnell correlations were a little more accurate than the Van Nes and Van Westen correlation. The relative deviation of the predicted values was below 5% on average.

Acknowledgement

REFERENCES

1. Riazi, M. R., Al-Enezi, G. A. Modelling of the rate of oil spill disappearance from seawater for Kuwaiti crude and its products. *Chem. Eng. J.*, 1999, **73**(2), 161–172.
2. Raj, P. K. A flammability (risk) index for use in transportation of flammable liquids. *J. Loss Prevent. Proc.*, 2016, **44**, 755–763.
3. Pichler, H., Lutz, J. Why crude oil vapor pressure should be tested prior to rail transport. *Adv. Petrol. Explor. Dev.*, 2014, **7**(2), 58–63.
4. Andersen, V. F., Anderson, J. E., Wallington, T. J., Mueller, S. A., Nielsen, O. J. Vapor pressures of alcohol−gasoline blends. *Energ. Fuel.*, 2010, **24**(6), 3647–3654.
5. Riazi, M. R. *Characterization and Properties of Petroleum Fractions*. ASTM International, 2005.
6. Tsonopoulos, C., Heidman, J. L., Hwang, S.-C. *Thermodynamic and Transport Properties of Coal Liquids*. Wiley, 1986.
7. Nji, G. N., Svrcek, W. Y., Yarranton, H. W., Satyro, M. A. Characterization of heavy oils and bitumens. 1. Vapor pressure and critical constants prediction methods for heavy hydrocarbons. *Energ. Fuel.*, 2008, **22**(1), 455–462.
8. Oja, V., Suuberg, E. M. Oil shale processing, chemistry and technology. In: *Encyclopedia of Sustainability Science and Technology* (Meyers, R. A., ed.). Springer, 2012, 7457−7491.
9. Lee, S. *Oil Shale Technology*. CRC Press, 1990.
10. Ge, X., Wang, S., Jiang, X. Catalytic effects of shale ash with different particle sizes on characteristics of gas evolution from retorting oil shale. *J. Therm. Anal. Calorim.*, 2019, **138**, 1527−1540.
11. Yu, X., Luo, Z., Li, H., Zhang, J., Gan, D. The diffusion and separation of the oil shale in the compound dry beneficiation bed. *Powder Technol.*, 2019, **355**, 72−82.
12. Qian, J. L., Yin, L., Wang, J. Q., Li, S. Y., Han, F., He, Y. G. *Oil Shale – Petroleum Alternative*. China Petrochemical Press, Beijing, 2010.
13. Urov, K., Sumberg, A. Characteristics of oil shales and shale-like rocks of known deposits and outcrops. Monograph. *Oil Shale*, 1999, **16**(3S), 1−64.
14. Akalin, E., Kim, Y. M., Alper, K., Oja, V., Tekin, K., Durukan, I., Siddiqui, M. Z., Karagöz, S. Co-hydrothermal liquefaction of lignocellulosic biomass with Kukersite oil shale. *Energ. Fuel.*, 2019, **33**(8), 7424−7435.

15. Oja, V. Examination of molecular weight distributions of primary pyrolysis oils from three different oil shales via direct pyrolysis Field Ionization Spectrometry. *Fuel*, 2015, **159**, 759−765.

16. Siitsman, C., Oja, V. Application of a DSC based vapor pressure method for examining the extent of ideality in associating binary mixtures with narrow boiling range oil cuts as a mixture component. *Thermochim. Acta*, 2016, **637**, 24−30.

17. Akash, B. A., Characterization of shale oil as compared to crude oil and some refined petroleum products. *Energ. Source.*, 2003, **25**(12), 1171–1182.

18. Kollerov, D. K. *Physicochemical Properties of Oil Shale and Coal Liquids.* Moscow, 1951 (in Russian).

19. Oja, V., Rooleht, R., Baird, Z. S. Physical and thermodynamic properties of kukersite pyrolysis shale oil: literature review. *Oil Shale*, 2016, **33**(2), 184–197.

20. Oja, V. Is it time to improve the status of oil shale science? *Oil Shale*, 2007, **24**(2), 97−100.

21. Johannes, I., Luik, H., Bojesen-Koefoed, J. A., Tiikma, L., Vink, N., Luik, L. Effect of organic matter content and type of mineral matter on the oil yield from oil shales. *Oil Shale*, 2012, **29**(3), 206–221.

22. Baird, Z. S., Uusi-Kyyny, P., Järvik, O., Oja, V., Alopaeus, V. Temperature and pressure dependence of a shale oil and derived thermodynamic properties. *Ind. Eng. Chem. Res.*, 2018, **57**(14), 5128–5135.

23. Baird, Z. S., Uusi-Kyyny, P., Oja, V., Alopaeus, V. Hydrogen solubility of shale oil containing polar phenolic compounds. *Ind. Eng. Chem. Res.*, 2017, **56**(30), 8738–8747.

24. Rannaveski, R., Listak, M., Oja, V. ASTM D86 distillation in the context of average boiling points as thermodynamic property of narrow boiling range oil fractions. *Oil Shale*, 2018, **35**(3), 254–264.

25. Siitsman, C., Oja, V. Extension of the DSC method to measuring vapor pressures of narrow boiling range oil cuts. *Thermochim. Acta*, 2015, **622**, 31–37.

26. Siitsman, C., Kamenev, I., Oja, V. Vapor pressure data of nicotine, anabasine and cotinine using differential scanning calorimetry. *Thermochim. Acta*, 2014, **595**, 35–42.

27. Astra, H.-L., Oja, V. Vapour pressure data for 2-n-propylresorcinol, 4-ethyl-resorcinol and 4-hexylresorcinol near their normal boiling points measured by differential scanning calorimetry. *J. Chem. Thermodyn.*, 2019, **134**, 119–126.

28. Gray, J. A., Holder, G. D., Brady, C. J., Cunningham, J. R., Freeman, J. R., Wilson, G. M. Thermophysical properties of coal liquids. 3. Vapor pressure and heat of vaporization of narrow boiling coal liquid fractions. *Ind. Eng. Chem. Proc. Des. Dev.*, 1985, **24**(1), 97–107.

29. Oja, V., Suuberg, E. M. Development of a nonisothermal Knudsen effusion method and application to PAH and cellulose tar vapor pressure measurement. *Anal. Chem.*, 1997, **69**(22), 4619–4626.

30. Castellanos-Diaz, O., Schoeggl, F. F., Yarranton, H. W., Satyro, M. A. Measurement of heavy oil and bitumen vapor pressure for fluid characterization. *Ind. Eng. Chem. Res.*, 2013, **52**(8), 3027–3035.

31. Oja, V., Suuberg, E. M. Measurements of the vapor pressures of coal tars using the nonisothermal Knudsen effusion method. *Energ. Fuel.*, 1998, **12**(6), 1313–1321.

32. Spencer, W. F., Cliath, M. M. Measurement of pesticide vapor pressures. In: *Residue Reviews* (Gunther, F. A., Gunther, J. D., eds.), Springer, New York, 1983, 57–71.

33. Rannaveski, R., Oja, V. A new thermogravimetric application for determination of vapour pressure curve corresponding to average boiling points of oil fractions with narrow boiling ranges. *Thermochim. Acta*, 2020, **683**, Article 178468.

34. ASTM D6378-10. *Standard Test Method for Determination of Vapor Pressure (VPX) of Petroleum Products, Hydrocarbons, and Hydrocarbon-Oxygenate Mixtures (Triple Expansion Method)*. ASTM International, West Conshohocken, PA, USA, 2016.

35. Van Nes, K., Van Westen, H. A. *Aspects of the Constitution of Mineral Oils*. Elsevier Publishing Company, 1951.

36. Maxwell, J. B., Bonnell, L. S. *Vapor Pressure Charts for Petroleum Hydrocarbons*. Esso Research and Engineering Company, 1955.

37. Maxwell, J. B., Bonnell, L. S. Derivation and precision of a new vapor pressure correlation for petroleum hydrocarbons. *Ind. Eng. Chem.*, 1957, **49**(7), 1187–1196.

38. Wilson, G. M., Johnston, R. H., Hwang, S. C., Tsonopoulos, C. Volatility of coal liquids at high temperatures and pressures. *Ind. Eng. Chem. Proc. Des. Dev.*, 1981, **20**(1), 94–104.

39. Golubev, N. Solid oil shale heat carrier technology for oil shale retorting. *Oil Shale*, 2003, **20**(3S), 324–332.

40. Elenurm, A., Oja, V., Tali, E., Tearo, E., Yanchilin, A. Thermal processing of dictyonema argillite and kukersite oil shale: Transformation and distribution of sulfur compounds in pilot-scale Galoter process. *Oil Shale*, 2008, **25**(3), 328−334.

41. ASTM D2892-15. *Standard Test Method for Distillation of Crude Petroleum (15-Theoretical Plate Column)*. ASTM International, West Conshohocken, PA, 2015.

42. Dreisbach, R. R. *Physical Properties of Chemical Compounds*. Advances in Chemistry Series, **15**, Am. Chem. Soc., Washington, D. C, 1955.

43. Boublik, T., Fried, V., Hala, E. *The Vapor Pressure of Pure Substances*, 2nd revised Edition. Elsevier, Amsterdam, The Netherlands, 1984.

44. Zwolinski, B. J., Wilhoit, R. C. *Handbook of Vapor Pressures and Heats of Vaporization of Hydrocarbons and Related Compounds*. API-44, TRC Publication No. 101, Texas A&M University, College Station, TX, 1971.

45. Stephenson, R. M., Malanowski, S. *Handbook of the Thermodynamics of Organic Compounds*. Elsevier, New York, 1987.

46. Ambrose, D., Ewing, M. B., Ghiassee, N. B., Sanchez Ochoa, J. S. The ebulliometric method of vapour-pressure measurement: vapour pressures of benzene, hexafluorobenzene, and naphthalene. *J. Chem. Thermodyn.*, 1990, **22**(6), 589−605.

47. Connolly, J. F., Kandalic, G. A. Saturation properties and liquid compressibilities for benzene and n-octane. *J. Chem. Eng. Data*, 1962, **7**(1),137−139.

48. Dean, J. A., Ed. *Lange's Handbook of Chemistry*. 14th Edition, McGraw-Hill, New York, 1992.

49. Willingham, C. B., Taylor, W. J., Pignocco, J. M., Rossini, F. D. Vapor pressures and boiling points of some paraffin, alkylcyclopentane, alkylcyclohexane, and alkylbenzene hydrocarbons. *J. Res. Natl. Bur. Stand.*, 1945, **35**, 219−244.

Publication II
Mozaffari, P.; Järvik, O.; Baird, Z. S. (2020). Vapor Pressures of Phenolic compounds Found in Pyrolysis Oil. Journal of Chemical & Engineering data, 65 (11), 5559–5566.

Vapor Pressures of Phenolic Compounds Found in Pyrolysis Oil

Parsa Mozaffari,* Oliver Järvik, and Zachariah Steven Baird

ACCESS | Metrics & More | Article Recommendations | Supporting Information

ABSTRACT: Oil produced from pyrolysis of Kukersite oil shale and lignocellulosic biomass contains significant amounts of phenolic compounds. Here, we present new experimental vapor pressure data for two such compounds (4-ethyl-2-methoxyphenol and 5-methylresorcinol) and also for a mixture of phenolic compounds extracted from pyrolysis oil (Honeyol). Vapor pressure data were measured by differential scanning calorimetry, in accordance with the ASTM E 1782 standard test method. The measurements were conducted in the pressure range from 0.89 kPa to atmospheric pressure. The measured temperature ranges for the vapor pressure were 374.5−509.1 K for 4-ethyl-2-methoxyphenol, 428.0−565.0 K for Honeyol, and 429.4−565.8 K for 5-methylresorcinol. Density data for 4-ethyl-2-methoxyphenol were also measured at 293.15−363.15 K. The experimental vapor pressure and density

data for 4-ethyl-2-methoxyphenol were fitted using the PC-SAFT equation of state, and the vapor pressure data for the other compounds were fit using the Antoine equation. Enthalpies of vaporization were also calculated. The properties of these compounds were then compared to the literature data for other pure phenolic compounds and mixtures of the phenolic compounds from Kukersite shale oil. This comparison indicates that some pure compounds, such as 4-ethyl-2-methoxyphenol, could be used as model compounds for estimating the properties of the phenolic portion of pyrolysis oil.
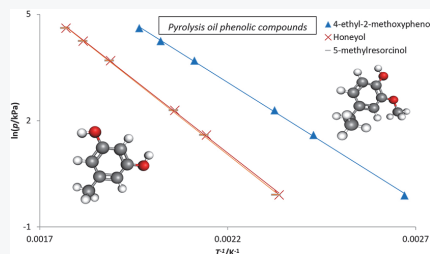
1. INTRODUCTION

Continuous fossil fuel production to meet worldwide energy demands has led to large emissions of greenhouse gases, and climate change resulting from this has spurred interest in producing fuels from biomass. Some countries continue to show interest in using their local oil shale resources, even though it is a fossil fuel, as a way to ensure domestic energy security. Hence, renewable energy resources as well as unconventional energy resources, such as oil produced from oil shale or wastes such as plastics and tires, have drawn substantial attention in the past decades.[1] Oil shale is an organic-rich sedimentary rock from which oil is produced through pyrolysis. The main organic component of oil shale is an insoluble solid macromolecular structure called kerogen.[2−6] The properties of the shale oil produced vary depending on the type of kerogen (i.e., oil shale) and the conversion process used. Therefore, the concentration of phenolic compounds in shale oil varies. In shale oil produced from Kukersite oil shale, there is a high concentration of phenolic compounds.[6] Although shale oil has not seen widespread commercial use, it is an important fuel in some regions, such as Estonia, Brazil, and China.[7]

Alternatively, biomass can also be converted to bio-oil through pyrolysis.[8,9] Generally plant biomass is used, the major components of which are lignin, hemicellulose, and cellulose. Because such lignocellulosic biomass contains large amounts of oxygen, the resulting bio-oil also generally contains many oxygenated compounds. Lignin often decomposes into

phenolic compounds, and these can be utilized to produce fine phenolic chemicals.[10] Furthermore, because the lignin in biomass contains aromatic structures, it is an important element for replacement of petroleum crude oil with biomass.[11,12]

Additionally, these phenolic compounds can be valuable chemicals and are often less desirable in fuel because of problems with thermal instability, chemical instability, and hydrocarbon immiscibility.[13−15] Therefore, information on their properties can also be useful for designing systems to separate or convert these phenols (such as hydrodeoxygenation).

Phenolic compounds from shale oil and bio-oil are used by various industries. For example, water-soluble phenols are extracted from shale oil, fractionated, and crystallized to yield products for chemical industries. These water-soluble compounds are mainly a mixture of alkylresorcinols, and 5-methylresorcinol is the primary component. Pure 5-methylresorcinol is used as a raw material to synthesize cosmetic dyes, fungicides, and drugs, among other products, or as a reagent for analytical chemistry.[16] Honeyol—a mixture of resorcinols

Table 1. Molecular Weight, CAS Number, Empirical Formula, Supplier, Measured Purities of Verification Compounds, and Phenolic Compounds Studied

compound	supplier	CAS RN	empirical formula	molecular weight (MW)/g mol^{-1}	Analytical method	Purity[a]
4-ethyl-2-methoxyphenol	ACROS Organics	2785-89-9	$C_9H_{12}O_2$	152.2	GC[b]	98.6%
5-methylresorcinol	VKG	504-15-4	$C_7H_8O_2$	124.1	GC	99.9%
Honeyol™	VKG	799275-41-5		142.8		
Biphenyl	Alfa Aesar	92-52-4	$C_{12}H_{10}$	154.2		99.0%
Water			H_2O	18.0		bi-distilled

[a]Purity given as mass percent. [b]Gas chromatography.

produced and sold by Viru Keemia Grupp (VKG)—contains minimum 48% of 5-methylresorcinol. This product is of interest to various industries and is used as a substitute for resorcinol and phenols in the rubber, wood processing, construction, and oil industries. Compared with resorcinol, the alkyl substituent in the alkylresorcinol molecular structure improves resin adhesion as well as heat and water resistance.

Vaporization properties of oil and oil products, including phenolic compounds, are important for production, storage, transportation, and environmental risk assessment.[17−19] Therefore, modeling the volatile characteristic of oil compounds in a simple form is crucial to characterize their thermodynamic behavior. One possible approach to estimate such vaporization parameters is to utilize pure compounds or compounds derived from oil with similar characteristics, as pseudocomponents.[20] However, the data regarding thermodynamic properties of phenolic compounds are scarce. Existing correlations are not sufficient to model the thermodynamic and physical properties of phenolic compounds, so new experimental data on their properties are critical to produce and handle these compounds.

Therefore, in this work, three phenolic compounds that are often present in pyrolysis oil were chosen for vapor pressure measurements: 4-ethyl-2-methoxyphenol (4-ethylguaiacol), Honeyol, and 5-methylresorcinol. 4-Ethyl-2-methoxyphenol (4-ethylguaiacol) was selected as a lignin-derived phenolic monomer. This compound is widely used as a chemical intermediate for preparation of polymers, medicines, resins, and pesticides and is also produced from petroleum sources. As a replacement for fossil fuel utilization, this compound can also be produced from a renewable source, lignin, which is noticeably more environmentally favorable.[12] Among the compounds studied here, the only available literature data were for 5-methylresorcinol in the work by Da Silva and Ferreira[21] in which the vapor pressure of 5-methylresorcinol was measured in the temperature range of 322.2−338.1 K. Moreover, density values for phenolic compounds at different temperatures, and more specifically for 4-ethyl-2-methoxyphenol, are scarce.

Honeyol and 5-methylresorcinol were selected as alkylresorcinols derived from Kukersite shale oil. The vapor pressures of these compounds were measured using differential scanning calorimetry (DSC). Additional information regarding the application of DSC for measuring vapor pressures is provided in refs.[22−24] In addition, the density of 4-ethyl-2-methoxyphenol, as a bio-based phenolic compound, was measured at temperatures from 293.15 to 363.15 K.
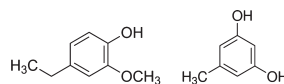
2. EXPERIMENTAL METHODS

2.1. Chemicals. The phenolic compounds used in this work are 4-ethyl-2-methoxyphenol (CAS RN: 2785-89-9; $C_9H_{12}O_2$), Honeyol, and anhydrous 5-methylresorcinol (CAS RN: 504-15-4; $C_7H_8O_2$). 4-Ethyl-2-methoxyphenol was

purchased from ACROS Organics with a reported minimum purity of 98%. Honeyol and 5-methylresorcinol were provided by Viru Keemia Grupp (VKG). All the compounds in this study were used as received without further purification. Information about the compounds [molecular weight, CAS RN, empirical formula, compound suppliers, and purity verified by gas chromatography (GC)] are provided in Table 1. Honeyol composition analyzed by GCMS is given in Table 2. The chemical structures of the compounds are also presented in Figure 1.

Table 2. Honeyol Compositions Measured by GC[a]

compound	mass %
5-methylresorcinol	62.4
4,5-dimethylresorcinol	11.4
2,5-dimethylresorcinol	6.7
5-ethylresorcinol	9.4
other alkylresorcinols	10.1
total	100

[a]The expanded uncertainty (for 0.95 confidence interval) was estimated to be $U_r(m) = 0.014$.

Figure 1. Chemical structures of phenolic compounds studied. (Left to right: 4-ethyl-2-methoxyphenol and 5-methylresorcinol).

The experimental vapor pressure was measured within the range from 0.89 kPa to atmospheric pressure. The corresponding temperature ranges were 428.0−565.0 K for Honeyol, 429.4−565.8 K for 5-methylresorcinol, and 374.5−509.1 K for 4-ethyl-2-methoxyphenol.

2.2. Apparatus. Vapor pressure measurements were carried out using a NETZSCH 204HP Phoenix DSC, in accordance with the standard test method ASTM E 1782, " the standard test method for determining vapor pressure by thermal analysis".[25]

The density of 4-ethyl-2-methoxyphenol was measured using a DMA 5000M density meter (Anton Paar GmbH) from 293.15 to 363.15 K. The expanded uncertainty of the instrument is 0.05 kg m^{-3}. When taking into account the purity of the 4-ethyl-2-methoxyphenol, the expanded uncertainty ($k = 2$) was estimated to be 1 kg m^{-3}. Furthermore, water (double distilled) was used for calibration and performance of check of the density meter.

The molecular weight of Honeyol was measured by vapor pressure osmometry using a KNAUER K-7000 vapor pressure osmometer (Wissenschaftliche Gerätebau Dr. Ing. Herbert KNAUER GmbH, Germany). In this technique, water was

Table 3. Comparison of Experimental Vapor Pressure of Liquid Biphenyl with Literature Data

T^a/K	P/kPa	$U(p)^b$/kPa	$P_{ref}{}^c$/kPa[32]	ΔP/kPa	$P_{ref}{}^d$/kPa[33]	ΔP/kPa	$P_{ref}{}^e$/kPa[34]	ΔP/kPa
382.7	0.90	0.01	0.8779	0.0229				
409.4	2.89	0.04	2.8708	0.0216				
422.7	4.88	0.07	4.8639	0.0201				
442.7	9.95	0.14	9.8723	0.0747	10.0213	0.0742	9.8723	0.0747
478.9	29.88	0.42	29.8930	0.0162	30.0323	0.1554	29.8930	0.0162
498.2	49.87	0.70	49.8930	0.0205	50.0019	0.1294	49.8930	0.0205
527.8	100.40	1.41	100.0186	0.3775	100.1531	0.2429	100.0186	0.3775

[a]The combined expanded uncertainty (0.95 confidence interval) for experimental temperature is 0.25 K. [b]The combined expanded uncertainty of experimental vapor pressure for 0.95 confidence interval. [c]The uncertainty of the reference was 0.0003−0.0043 kPa. [d]The uncertainty of the reference values was calculated to be 0.001−0.010 kPa. [e]No uncertainty was reported.

used as the solvent for measurement and an aqueous solution of NaCl with a molality of 433.8 mmol $(Na^+ + Cl^-)$ kg^{-1} (H_2O) was used as the calibration standard. The measurement was performed at 333.15 K. The accuracy of this method was thoroughly described earlier by Järvik and Oja.[26] The expanded uncertainty ($k = 2$) was approximately U_r (MW) = 0.07 (i.e. 7%).

2.3. Calibration. Temperature calibration of DSC was performed at atmospheric conditions with tin (T_{fus} = 505.05 K, T_{exp} = 504.25 K), indium (T_{fus} = 429.75 K, T_{exp} = 429.25 K), zinc (T_{fus} = 692.75 K, T_{exp} = 691.55 K), bismuth (T_{fus} = 544.55 K, T_{exp} = 543.75 K), and lead (T_{fus} = 600.65 K, T_{exp} = 599.55 K) standards. One organic compound, naphthalene (99% purity, CAS RN: 91-20-3), was also measured as a performance check (T_{fus} = 353.25 K[27]), and a fusion temperature of 353.15 K was obtained. The calibration measurement procedure is similar to that used for the studied compounds, except that for metals, larger sample mass was used (10−15 mg). The vacuum sensor (MKS Baratron 626B) with a reported full-scale error of $U_r(p)$ = 0.00008 was calibrated at the Metrosert AS metrological center which is traceable to the Finnish VTT Mikes measurement pressure standard and CMI (Czech metrology center) measurement pressure standard. The vacuum sensor's operating range was 0.0133−130 kPa, and the accuracy of the reading is $U_r(p)$ = 0.0025 for measurements below atmospheric pressure. The distance between the outlet pressure sensors and DSC cell was measured to be 47 cm, and therefore, the pressure drop at atmospheric conditions between the sensor and the measurement chamber was estimated to be 0.003 kPa.[28]

2.4. Procedures. The experimental procedure was thoroughly described in earlier articles from our research group by Siitsman et al.[19,28,29]

The sample mass was weighed on a microanalytical balance (Sartorius Cubis Micro Balances 6.6S) with ±0.001 mg precision. For the measurements, a sample mass between 1 and 4 mg (or 1−4 μL) was used for experiments above 5 kPa, while a mass of 4−9 mg (or 4−9 μL) was used for experiments below 5 kPa to prevent mass depletion during preboiling.

40 μL aluminum crucibles and lids with different pinhole diameters were used. The heating rate was 5 K min⁻¹. For measurement above 5 kPa, lids with 50 μm laser-drilled pinholes were cold welded to the crucibles using a sealing press and placed inside the DSC furnace. However, for experiments below 5 kPa, a 180 μm microdrill was used to make the pinholes to avoid self-pressurization and, therefore, peak broadening which lowers the accuracy of onset temperature analysis.[30] Butrow and Seyler[31] suggested earlier that using larger pinholes from 175 μm up to 375 μm for vapor pressure

measurements below 5 kPa improves measurement accuracy to the point at which it is comparable to that of experimental values above 5 kPa.

The melting point of the solid compounds was determined as the onset temperature of the melting peak where the tangent lines of the baseline and melting peak intersect.

For the present study, the DSC performance was validated using water and biphenyl (99% purity, CAS RN: 92-52-4). Biphenyl was measured within the pressure range of 0.89 kPa to atmospheric pressure, and the boiling temperature of water was measured from 50 kPa to atmospheric pressure. Comparison between biphenyl experimental results and the literature values is given in Table 3, and the graph ln P versus 1/T is provided in Figure S1 in the Supporting Information. The data points in Table 3 are the average values of the repeated DSC experiments and comparison with the average values obtained from the literature.

For water, the obtained values were compared with the IAPWS95 equation of state[35] which is implemented in CoolProp.[36] The measured and reference values are given in Table 4.

Table 4. Deviation of Experimental Values of Water Vapor Pressure from the IAPWS95 Equations of State[35]

P^a/kPa	T^b/K	P^c/kPa[35]	$ΔP^d$%
49.88 ± 0.70	354.4	49.83	0.10%
59.92 ± 0.84	359.1	60.03	0.19%
69.91 ± 0.98	363.0	69.78	0.19%
79.91 ± 1.12	366.7	80.22	0.38%
100.93 ± 1.41	373.4	102.44	1.47%

[a]The combined expanded uncertainty for experimental vapor pressure was given for 0.95 confidence interval. [b]The combined expanded uncertainty (0.95 confidence interval) for experimental temperature is 0.25 K. [c]The relative expanded uncertainty of the literature was reported to be 0.0001−0.0002. [d]$ΔP = \left| \frac{P_e - P_{lit}}{P_e} \right| \times 100$

The vapor pressure of biphenyl has been previously studied for liquid[32−34,37] and solid phases.[37−39] A deviation plot of experimental DSC values is also presented in the Supporting Information (Figure S2). It was observed that DSC vapor pressure values are in excellent agreement with the values obtained by Chirico et al.,[32] Chipman and Peltier,[33] and Garrick and Gray.[34] Compared to those measured by Chirico et al. (350 K to 578 K),[32] our experimental values deviate by a mere 0.07 kPa for subatmospheric pressures and slightly less than 0.4 kPa for atmospheric pressure. Chipman and Peltier[33] reported vapor pressures from 436 to 595 K, and Garrick and Gray[34] reported their values in the range from 426 to 527 K.

The absolute average deviation between the reported values was 0.4 and 0.3%. Therefore, good agreement was obtained for a wide range of experimental pressures.

2.5. PC-SAFT Optimization. The properties of 4-ethyl-2-methoxyphenol were modeled using the PC-SAFT equation of state,[40] and therefore, vapor pressure curves were fit to the experimental data using the PC-SAFT equation of state. The PC-SAFT parameters were determined using the differential evolution optimizer implemented in the Scipy package for Python.[41,42] Our PC-SAFT code can be found on Github[43] and is also available as a package on the Python Package Index.[44] The vapor pressure and density data were used for optimization. Because there was no available density data for the solid compounds (5-methylresorcinol and Honeyol), PC-SAFT parameters were not optimized.

2.6. Uncertainty Analysis. For uncertainty calculations, a coverage factor of 2 ($k = 2$) was used. The estimated expanded uncertainty of the temperature measurement was 0.25 K.[6] For pressure measurement uncertainty, the expanded uncertainty was determined based on data from the performance check with water. Based on the deviation between the measured values and the IAPWS95 equation of state,[35] the expanded uncertainty of vapor pressures measured was $U_r(p) = 0.014$. Because the pressure sensor has a resolution of 0.01 Torr (0.001 kPa), for measurements at low pressures, a minimum expanded uncertainty of 0.07 kPa was assumed. The effect of impurities was also included for pressure uncertainty calculations. This was calculated by estimating the likely relative deviation of the vapor pressures of the impurities and multiplying that by the concentration of the impurities (i.e. ideal mixing was assumed). For 5-methylresorcinol, the impurity concentration was negligible and therefore was not considered.

3. RESULTS AND DISCUSSION

Table 5 provides the liquid density of 4-ethyl-2-methoxyphenol at 293.15–363.15 K, and the PC-SAFT parameters for 4-ethyl-2-methoxyphenol are given in Table 6.

Table 5. 4-Ethyl-2-Methoxyphenol Liquid Density Values from 293.15 to 363.15 K ($P = 100.01 \pm 0.05$ kPa)

temperature[a]/K	density[b]/kg m^{-3}
293.15	1064
303.15	1055
313.15	1046
323.15	1037
333.15	1028
343.15	1018
353.15	1009
363.15	1000

[a]Standard uncertainty was 0.01 K (based on manufacturer's specification). [b]Expanded uncertainty ($k = 2$) was 1 kg m^{-3}.

Table 6. 4-Ethyl-2-Methoxyphenol PC-SAFT Parameters[a]

compound	m	σ	ϵ/k (Å)	ϵ^{AB}/k (K)	κ^{AB}
4-ethyl-2-methoxyphenol	4.7776	3.4799	284.44	1004.12	0.0266

[a]m is segment number, σ is segment diameter (Å), ϵ/k is dispersion energy divided by Boltzmann constant (k), ϵ^{AB}/k is association energy divided by Boltzmann constant (k), and κ^{AB} is association volume.

Vapor pressure data for 4-ethyl-2-methoxyphenol, Honeyol, and 5-methylresorcinol were measured within the range of 0.89 kPa to atmospheric pressure using DSC.

Endotherms of 5-methylresorcinol and Honeyol at 700 mbar are provided in Figure S3 in the Supporting Information. Experimental vapor pressure data for these compounds are provided in Table 7. Additionally, ln P versus $1/T$ of studied

Table 7. Experimental Vapor Pressure Data of the Measured Phenolic Compounds in the Liquid Phase

4-ethyl-2-methoxyphenol		5-methylresorcinol		Honeyol™	
T/K^a	P/kPa^c	T/K^a	P/kPa^b	T/K^a	P/kPa^b
374.5	0.90	429.4	0.91	428.0	0.91
412.0	4.92	467.8	4.93	466.6	4.93
430.1	9.91	486.3	9.90	485.4	9.90
473.6	39.88	530.4	39.85	529.5	39.88
494.5	69.87	551.0	69.91	550.6	69.89
509.1	100.01	565.8	100.37	565.0	99.69

[a]Combined expanded uncertainty ($k = 2$) for temperature is $U(T) = 0.25$ K. [b]Combined expanded uncertainty ($k = 2$) for pressure is $U_r(p) = 0.014$ of the pressure value or $U(p) = 0.07$ kPa, whichever is greater. [c]Combined expanded uncertainty ($k = 2$) for the vapor pressure of 4-ethyl-2-methoxyphenol is $U_r(p) = 0.016$, except for the 0.9 kPa experiment where the expanded uncertainty is $U_r(p) = 0.078$.

compounds in addition to the normal boiling point of 5-methylresrcinol obtained from Weast et al.[45] and vapor pressure data provided by da Silva and Ferreira[21] are given in Figure 2. For other studied compounds, no available vapor pressure data was found in the literature.

Vapor pressure curves were fit using the Antoine equation (eq 1).

$$\log_{10} P = A - \frac{B}{T + C} \quad (1)$$

where P is the vapor pressure (kPa), T is the temperature (K), and A, B, and C are Antoine equation constants. To estimate the Antoine coefficients, along with 95% confidence intervals, POLYMATH software (version 6.1) was used.

The enthalpy of vaporization (ΔH_{vap}) at the normal boiling point was calculated from the slope of the linear Clausius–Clapeyron equation (eq 2). Therefore, from the ln$P$ versus $1/T$ plot

$$\frac{d(\ln P)}{d\left(\frac{1}{T}\right)} = \frac{\Delta H_{vap}}{R} \quad (2)$$

where ΔH_{vap} is the enthalpy of vaporization (kJ mol^{-1}) and R is the universal gas constant ($R = 8.314$ J mol^{-1} K^{-1}). Although vapor pressures were experimentally obtained at atmospheric conditions, the normal boiling points of the compounds ($P = 101.325$ kPa) were calculated from the vapor pressure curves.

Melting points of the solid compounds were obtained from the onset temperature of the melting peak of the thermoanalytical curve. For 5-methylresorcinol, the average value of repeated measurements was calculated and is provided in Table 8. Because Honeyol is a mixture of different compounds, the boiling points at different experimental pressures can be also be viewed as an average boiling point and therefore, the thermogram obtained by DSC corresponds to the boiling point curve as it was also explained thoroughly in
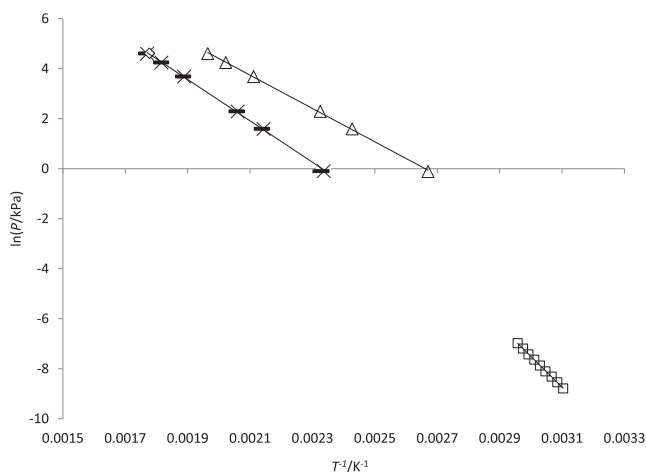
Figure 2. Vapor pressure curves for phenolic compounds measured by DSC: Honeyol (×; R^2 = 0.9994), 4-ethyl-2-methoxyphenol (△; R^2 = 0.9995), and 5-methylresorcinol (−; R^2 = 0.9994) and the normal boiling point of 5-methylresorcinol from Weast et al.[45] (◇) and 5-methylresorcinol vapor pressure data from da Silva and Ferreira[21] (□; R^2 = 0.9996).

Table 8. Experimental Temperature Ranges, Antoine Constants, Enthalpies of Vaporization, and Melting Points for the Phenolic Compounds

compound	temperature range/K	Antoine constants (eq 1)			normal boiling point K/T_b	ΔH_{vap} (T_b)/kJ mol^{-1}	melting point/K
		A	*B*	*C*			
4-ethyl-2-methoxyphenol	374.5−509.1	6.373 ± 0.137	1847.263 ± 95.572	−86.711 ± 8.894	508.2 ± 1.0	55.4 ± 1.3	
Honeyol^{TM}	428.0−565.0	6.701 ± 0.108	2128.279 ± 82.022	−112.376 ± 7.198	564.0 ± 1.3	68.8 ± 1.8	323.15 to 353.15
5-methylresorcinol	429.4−565.8	6.721 ± 0.170	2127.539 ± 128.069	−114.845 ± 11.200	564.4 ± 1.1	69.6 ± 1.9	382.15 ± 0.23

ref 46. For Honeyol, the melting range is given instead of a melting point because Honeyol is a mixture and, therefore, the sharp endotherm was not obtained; thus, the melting range was estimated.

It should be noted that the composition of Honeyol varies, as seen from comparing with the compositions in other articles.[47,48] However, the properties of Honeyol, such as vapor pressures values and boiling points, are similar to those of 5-methylresorcinol. Therefore, the presence of other resorcinol derivatives does not significantly affect the properties of Honeyol in general, which is likely because different resorcinols have quite similar structures.

The experimental temperature range, Antoine parameters obtained from eq 1, boiling point at 101.325 kPa, and vaporization enthalpy of the studied compounds, along with expanded uncertainties (k = 2), are given in Table 8.

For the compounds measured, only a few data are available in the literature for comparison. Based on the data from Weast et al.,[45] the normal boiling point of 5-methylresorcinol is 562.7 K, which is 1.7 K lower than the value from our vapor pressure curve (relative deviation within 0.3%). From the data reported by Stephenson and Malanowski,[49] the enthalpy of vaporization of 5-methylresorcinol within the temperature range of 402 to 468 K is 76.6 kJ mol^{-1}. Furthermore, it was observed that the enthalpy of vaporization calculated from our data is smaller than that of the value calculated from the data published by da Silva and Ferreira[21] (ΔH_{vap} = ~102.4 kJ mol^{-1}). Because, in our work, experiments were carried out at higher temperature range, the temperature-dependent vaporization enthalpy was

expected to be lower. Therefore, compared to the enthalpy of vaporization result obtained by da Silva and Ferreira,[21] it could be concluded that our data follow the logical trend that enthalpy of vaporization decreases as temperature increases.

We can also compare the enthalpy of vaporization results with some phenolic compounds containing 2 OH groups. Astra and Oja[6] measured the enthalpies of vaporization of 4-ethylresorcinol and 2-n-propylresorcinol by DSC, and the ΔH_{vap} obtained were 60.9 and 58.6 kJ mol^{-1}, correspondingly. 5-MR has a structure similar to these compounds, containing one methyl group (−CH$_3$) attached to the benzene ring, while this is instead an ethyl group (−C$_2$H$_5$) for 4-ethylresorcinol and a propyl group (−C$_3$H$_7$) for 2-n-propylresorcinol. The value for resorcinol with no functional group attached to the benzene ring is reported to be 78.4 kJ mol^{-1}.[50] 4-Ethyl-2-methoxyphenol contains one OH group, an ethyl group, and a methyl ether group (−OCH$_3$) attached to the benzene ring. From our DSC measurements, the enthalpy of vaporization of 4-ethyl-2-methoxyphenol was 55.4 kJ mol^{-1}. Therefore, substitution of various functional groups attached to benzene ring in phenolic compounds affects the enthalpy of vaporization to a certain extent. The comparison between 5MR, 4-ethylresorcinol, and 2-n-propyl resorcinol shows that a functional group with longer chain length attached to the benzene ring decreases the heat of vaporization.

3.1. Comparison with Boiling Points of Phenolic Fractions. Phenols are one of the main classes of compounds in Kukersite shale oil.[6] Furthermore, phenolic compounds are
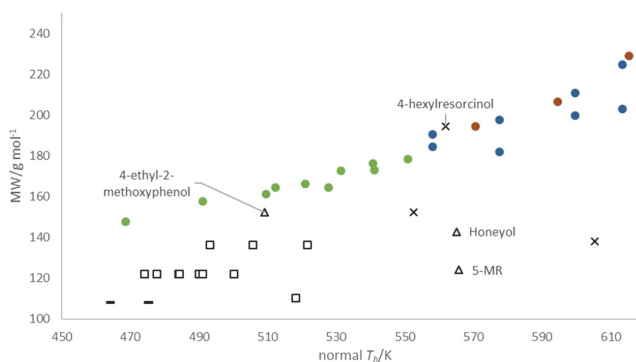
E

Figure 3. Comparison of the properties of various phenolic compounds. (● green) Phenolic oil fractions—0.1−0.64 OH per molecule,[56] (● blue) phenolic oil fractions—0.64−1.30 OH per molecule,[56] (● red) phenolic fractions—>1.30 OH per molecule,[56] (Δ) studied compounds, (−) Cresol isomers,[55] (✕) disubstituted phenolic compound,[6] and (□) other phenolic compounds.[52]
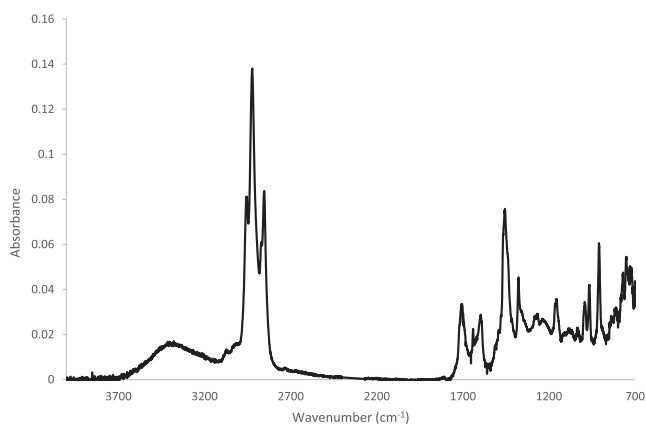

Figure 4. Infrared spectrum of a light phenolic fraction of kukersite shale oil.

one of the main classes of organic components of bio-oils, produced from woods, which comprises about 20−30%.[51]

The normal boiling points (normal T_b) of the phenolic compounds studied in this article were compared with those of other phenolic compounds obtained from the book of reference data[52] and the characteristics of phenolic shale oil fractions measured earlier by our research group (soon to be published). The phenolic fractions were prepared from the shale oil using the method suggested by Kogerman[53] and described in refs 5 and 54.

For the purpose of the analysis, fractions with normal boiling points below 620 K, phenolic compounds with two hydroxyl groups,[6] and three isomeric methylphenols (cresol)[55] were considered for comparison.

Molecular weights and normal boiling points of the disubstituted phenolic compounds (containing two hydroxyl groups) were from the data obtained by Astra and Oja.[6] Properties of other phenolic compounds were also obtained from a chemical and physical data reference book.[52] The other phenolic compounds include six dimethylphenol isomers (xylenol), two trimethylphenol isomers, two ethylphenol isomers, catechol, and 4-propylphenol.

Figure 3 presents the normal boiling points of different phenolic compounds as a function of their molecular weight. Based on the number of OH groups per molecule, phenolic shale oil fractions were divided into three categories: fractions with fewer OH groups per molecule (below 0.64), fractions with higher OH content (0.64−1.30 OH groups per molecule), and a third group with the most OH groups (>1.30 per molecule). For the fractions with higher OH contents, clearly some molecules have more than one OH group.

The OH content of the phenolic oil fractions was determined from the infrared spectra of the phenolic fractions.[5] The infrared spectrum of one light phenolic fraction was provided in Figure 4 as a reference. According to the approach introduced by Coates,[57] peaks related to the OH functional group appear at approximately 3200 and 1200 cm⁻¹.

The normal boiling point of 4-ethyl-2-methoxyphenol was measured to be 508.2 K. Two fractions had similar normal boiling points (normal T_b = 509.5 K and MW = 161.3 g mol⁻¹, T_b = 512.2 K and MW = 164.6 g mol⁻¹) and could be directly compared. The OH contents of these fractions were measured to be 3.4 and 4.0 wt %, and their densities at 293.15 K (d_{20}) were 906.65 and 923.86 kg m⁻³, respectively. Despite having

slightly lower densities than 4-ethyl-2-methoxyphenol (d_{20} = 1063.55 kg m^{-3}), these fractions have higher molecular weights. Furthermore, as shown in Figure 1, 4-ethyl-2-methoxyphenol also contains one methoxy group ($-OCH_3$) and one ethyl group ($-CH_2H_3$). However, OH analysis of these fractions indicates that, on average, molecules in these oil samples had less than one OH group per molecule, so some of the molecules were not phenolic compounds. 4-Hexylresorcinol is also in the neighborhood of some phenolic fractions for which the normal boiling points and molecular weights are near 562 K and 195 g mol^{-1}. The 4-hexylresorcinol structure contains one OH group and one long hydrocarbon chain attached to the phenol unit.

Overall, as shown in Figure 3, compounds 4-ethyl-2-methoxyphenol and 4-hexylresorcinol behave similarly to the phenolic fractions and, therefore, are in line with the trend of phenolic fractions. These compounds have longer hydrocarbon side chains in their molecular structure [$-OCH_3$ chain for 4-ethyl-2-methoxyphenol and $-CH_3(CH_2)_4CH_2$ chain for 4-hexylresorcinol] compared with the other phenolic compounds considered here. In addition, 4-ethyl-2-methoxyphenol has only one hydroxyl group. Most of the oil fractions shown here also had closer to 1 OH group per molecule, and therefore, 4-ethyl-2-methoxyphenol could likely behave similarly to phenolic fractions.

Other compounds used in this study, as well as other phenolic compounds that contained one phenol unit, differed more from the properties of the phenolic oil fractions, and therefore, these compounds would probably not be useful for modeling the phenolic compounds in pyrolysis oil.

4. CONCLUSIONS

DSC was used to measure the vapor pressures of the phenolic compounds 4-ethyl-2-methoxyphenol, Honeyol, and 5-methylresorcinol from 0.89 kPa to atmospheric pressure. To the best of our knowledge, these are the first published vapor pressure curves for Honeyol and 4-ethyl-2-methoxyphenol and the first vapor pressure data for 5-methylresorcinol in this pressure range. The normal boiling points and heats of vaporization of the phenolic compounds were calculated using the obtained vapor pressure curves. Also, properties of these and other pure phenolic compounds were compared to those of the phenolic portion of pyrolysis oil (Kukersite shale oil). This allowed us to identify the compounds that could potentially be used as model compounds for predicting the behavior of pyrolysis oil. While 4-ethyl-2-methoxyphenol could likely be used as a model compound, 5-methylresorcinol and Honeyol did not appear to be useful for modeling oil.

■ ASSOCIATED CONTENT

ⓢ Supporting Information

The Supporting Information is available free of charge at https://pubs.acs.org/doi/10.1021/acs.jced.0c00675.

Experimental vapor pressure graph of biphenyl compared with literature data; deviation plot for vapor pressure of biphenyl compared with literature values; and endotherms of Honeyol and 5-methylresorcinol obtained from DSC (PDF)

■ AUTHOR INFORMATION

Corresponding Author

   Parsa Mozaffari − *School of Engineering, Department of Energy Technology, Tallinn University of Technology, Tallinn 19086, Estonia;* ⓘ orcid.org/0000-0001-6021-042X; Email: parsa.mozaffari@taltech.ee

Authors

   Oliver Järvik − *School of Engineering, Department of Energy Technology, Tallinn University of Technology, Tallinn 19086, Estonia;* ⓘ orcid.org/0000-0001-8530-2582

   Zachariah Steven Baird − *School of Engineering, Department of Energy Technology, Tallinn University of Technology, Tallinn 19086, Estonia;* ⓘ orcid.org/0000-0002-4327-3469

Complete contact information is available at:
https://pubs.acs.org/10.1021/acs.jced.0c00675

Notes
The authors declare no competing financial interest.

■ REFERENCES

(1) Kılıç, M.; Pütün, A. E.; Uzun, B. B.; Pütün, E. Converting of Oil Shale and Biomass into Liquid Hydrocarbons via Pyrolysis. *Energy Convers. Manag.* **2014**, *78*, 461−467.

(2) Oja, V.; Suuberg, E. M. Oil Shale Processing , Chemistry and Technology. *Encyclopedia of Sustainability Science and Technology*, 2012; pp 47−83.

(3) Savest, N.; Oja, V.; Kaevand, T.; Lille, Ü. Interaction of Estonian Kukersite with Organic Solvents: A Volumetric Swelling and Molecular Simulation Study. *Fuel* **2007**, *86*, 17−21.

(4) Tissot, B. P.; Welte, D. H.; Tissot, B. P.; Welte, D. H. Oil Shales: A Kerogen-Rich Sediment with Potential Economic Value. In *Petroleum Formation and Occurrence*; Springer Berlin Heidelberg, 1978; pp 225−236.

(5) Baird, Z. S.; Oja, V.; Järvik, O. Distribution of Hydroxyl Groups in Kukersite Shale Oil: Quantitative Determination Using Fourier Transform Infrared (FT-IR) Spectroscopy. *Appl. Spectrosc.* **2015**, *69*, 555−562.

(6) Astra, H.-L.; Oja, V. Vapour Pressure Data for 2-n-Propylresorcinol, 4-Ethylresorcinol and 4-Hexylresorcinol near Their Normal Boiling Points Measured by Differential Scanning Calorimetry. *J. Chem. Thermodyn.* **2019**, *134*, 119−126.

(7) Oja, V. Vaporization Parameters of Primary Pyrolysis Oil from Kukersite Oil Shale. *Oil Shale* **2015**, *32*, 124−133.

(8) Effendi, A.; Gerhauser, H.; Bridgwater, A. V. Production of Renewable Phenolic Resins by Thermochemical Conversion of Biomass: A Review. *Renew. Sustain. Energy Rev.* **2008**, *12*, 2092−2116.

(9) Xiu, S.; Shahbazi, A. Bio-Oil Production and Upgrading Research: A Review. *Renew. Sustain. Energy Rev.* **2012**, *16*, 4406−4414.

(10) Wahyudiono; Sasaki, M.; Goto, M. Recovery of Phenolic Compounds through the Decomposition of Lignin in near and Supercritical Water. *Chem. Eng. Process.* **2008**, *47*, 1609−1619.

(11) Schuler, J.; Hornung, U.; Kruse, A.; Dahmen, N.; Sauer, J. Hydrothermal Liquefaction of Lignin. *J. Biomater. Nanobiotechnol.* **2017**, *08*, 96−108.

(12) Ye, Y.; Zhang, Y.; Fan, J.; Chang, J. Selective Production of 4-Ethylphenolics from Lignin via Mild Hydrogenolysis. *Bioresour. Technol.* **2012**, *118*, 648−651.

(13) Yang, Y.; Gilbert, A.; Xu, C. Hydrodeoxygenation of Bio-Crude in Supercritical Hexane with Sulfided CoMo and CoMoP Catalysts Supported on MgO: A Model Compound Study Using Phenol. *Appl. Catal., A* **2009**, *360*, 242−249.

(14) Zhang, X.; Zhang, Q.; Wang, T.; Ma, L.; Yu, Y.; Chen, L. Hydrodeoxygenation of Lignin-Derived Phenolic Compounds to Hydrocarbons over Ni/SiO2-ZrO2 Catalysts. *Bioresour. Technol.* **2013**, *134*, 73−80.

(15) Lyu, G.; Wu, S.; Zhang, H. Estimation and Comparison of Bio-Oil Components from Different Pyrolysis Conditions. *Front. Energy Res.* **2015**, *3*, 28.

(16) Järvik, O.; Rannaveski, R.; Roo, E.; Oja, V. Evaluation of Vapor Pressures of 5-Methylresorcinol Derivatives by Thermogravimetric Analysis. *Thermochim. Acta* **2014**, *590*, 198−205.

(17) Baird, Z. S.; Uusi-Kyyny, P.; Järvik, O.; Oja, V.; Alopaeus, V. Temperature and Pressure Dependence of Density of a Shale Oil and Derived Thermodynamic Properties. *Ind. Eng. Chem. Res.* **2018**, *57*, 5128−5135.

(18) Pichler, H.; Lutz, J. Why Crude Oil Vapor Pressure Should Be Tested Prior to Rail Transport. *Adv. Pet. Explor. Dev.* **2014**, *7*, 58−63.

(19) Siitsman, C.; Oja, V. Extension of the DSC Method to Measuring Vapor Pressures of Narrow Boiling Range Oil Cuts. *Thermochim. Acta* **2015**, *622*, 31−37.

(20) Phillips, J. *The Structure and Reaction Processes of Coal*. In Smith, K. L., Smoot, L. D., Fletcher, T. H.; Pugmire, R. J., Eds.; Plenum Press: New York, 1994; p 471; *AIChE J.* 1996, 42, 2399−2400.

(21) da Silva, M. A. V. R.; Ferreira, A. I. M. C. L. Experimental Standard Molar Enthalpies of Formation of Some Methylbenzenediol Isomers. *J. Chem. Thermodyn.* **2009**, *41*, 1096−1103.

(22) Seyler, R. J. Parameters Affecting the Determination of Vapor Pressure by Differential Thermal Methods. *Thermochim. Acta* **1976**, *17*, 129−136.

(23) Jones, K.; Seyler, R. Differential Scanning Calorimetry for Boiling Points and Vapor Pressure. *NATAS Notes* **1994**, *26*, 61−69.

(24) Tilinski, D.; Puderbach, H. Experiences with the Use of DSC in the Determination of Vapor Pressure of Organic Compounds. *J. Therm. Anal.* **1989**, *35*, 503−513.

(25) *American Society for Testing and Materials Method E 1782−03. Standard Test Method for Determining Vapor Pressure by Thermal Analysis*; ASTM International: West Conshohocken, PA.

(26) Järvik, O.; Oja, V. Molecular Weight Distributions and Average Molecular Weights of Pyrolysis Oils from Oil Shales: Literature Data and Measurements by SEC and ASAP MS for Oils from Four Different Deposits. *Energy Fuels* **2017**, *31*, 328−339.

(27) Miller, G. A. Vapor Pressure of Naphthalene. Thermodynamic Consistency with Proposed Frequency Assignments. *J. Chem. Eng. Data* **1963**, *8*, 69−72.

(28) Siitsman, C.; Kamenev, I.; Oja, V. Vapor Pressure Data of Nicotine, Anabasine and Cotinine Using Differential Scanning Calorimetry. *Thermochim. Acta* **2014**, *595*, 35−42.

(29) Siitsman, C.; Oja, V. Application of a DSC Based Vapor Pressure Method for Examining the Extent of Ideality in Associating Binary Mixtures with Narrow Boiling Range Oil Cuts as a Mixture Component. *Thermochim. Acta* **2016**, *637*, 24−30.

(30) Brozena, A. Vapor Pressure of 1-Octanol below 5 KPa Using DSC. *Thermochim. Acta* **2013**, *561*, 72−76.

(31) Butrow, A. B.; Seyler, R. J. Vapor Pressure by DSC: Extending ASTM E 1782 below 5 KPa. *Thermochim. Acta* **2003**, *402*, 145−152.

(32) Chirico, R. D.; Knipmeyer, S. E.; Nguyen, A.; Steele, W. V. The Thermodynamic Properties of Biphenyl. *J. Chem. Thermodyn.* **1989**, *21*, 1307−1331.

(33) Chipman, J.; Peltier, S. B. Vapor Pressure and Heat of Vaporization of Diphenyl. *Ind. Eng. Chem.* **1929**, *21*, 1106−1108.

(34) Garrick, F. J.; Gray, R. W. The Vapour Pressures of Diphenyl and of Aniline. *Faraday Soc. Trans.* **1927**, *23*, 560−563.

(35) Wagner, W.; Pruß, A. The IAPWS Formulation 1995 for the Thermodynamic Properties of Ordinary Water Substance for General and Scientific Use. *J. Phys. Chem. Ref. Data* **2002**, *31*, 387−535.

(36) Bell, I. H.; Wronski, J.; Quoilin, S.; Lemort, V. Pure and Pseudo-Pure Fluid Thermophysical Property Evaluation and the Open-Source Thermophysical Property Library Coolprop. *Ind. Eng. Chem. Res.* **2014**, *53*, 2498−2508.

(37) Sasse, K.; N'guimbi, J.; Jose, J.; Merlin, J. C. Tension de Vapeur d'hydrocarbures Polyaromatiques Dans Le Domaine 10-3-10 Torr. *Thermochim. Acta* **1989**, *146*, 53−61.

(38) Bradley, R. S.; Cleasby, T. G. The Vapour Pressure and Lattice Energy of Some Aromatic Ring Compounds. *J. Chem. Soc.* **1953**, 1690−1692.

(39) Seki, S.; Suzuki, K. Physico-Chemical Studies on Molecular Compounds. III. Vapor Pressures of Diphenyl, 4, 4'-Dinitrodiphenyl, and Molecular Compound between Them. *Bull. Chem. Soc. Jpn.* **1953**, *26*, 209−213.

(40) Gross, J.; Sadowski, G. Perturbed-Chain SAFT: An Equation of State Based on a Perturbation Theory for Chain Molecules. *Ind. Eng. Chem. Res.* **2001**, *40*, 1244−1260.

(41) Storn, R.; Price, K. Differential Evolution − A Simple and Efficient Heuristic for Global Optimization over Continuous Spaces. *J. Global Optim.* **1997**, *11*, 341−359.

(42) Jones, E.; Oliphant, T.; Peterson, P. *SciPy: Open Source Scientific Tools for Python*, 2001.

(43) Baird, Z. S. *Pcsaft: The PC-SAFT Equation of State; Including Dipole; Association and Ion Terms.*; n.D.

(44) PyPI *PyPI - the Python Package Index.*

(45) Weast, R. C.; Grasselli, J. G.; Lide, D. R. *Handbook of Data on Organic Compounds*; CRC Press, 1989.

(46) Rannaveski, R.; Järvik, O.; Oja, V. A New Method for Determining Average Boiling Points of Oils Using a Thermogravimetric Analyzer. *J. Therm. Anal. Calorim.* **2016**, *126*, 1679−1688.

(47) Peikolainen, A.-L.; Pérez-caballero, F.; Koel, M. Low-Density Organic Aerogels from Oil Shale by-Product 5-Methylresorcinol. *Oil Shale* **2008**, *25*, 348−358.

(48) Siimer, K.; Kaljuvee, T.; Christjanson, P.; Pehk, T.; Saks, I. Effect of Alkylresorcinols on Curing Behaviour of Phenol-Formaldehyde Resol Resin. *J. Therm. Anal. Calorim.* **2008**, *91*, 365−373.

(49) Stephenson, R. M.; Malanowski, S. *Handbook of the Thermodynamics of Organic Compounds*; Elsevier, 1987.

(50) Verevkin, S. P.; Kozlova, S. A. Di-Hydroxybenzenes: Catechol, Resorcinol, and Hydroquinone. Enthalpies of Phase Transitions Revisited. *Thermochim. Acta* **2008**, *471*, 33−42.

(51) Nascimento, M. S.; Maranhao, A. C.; Oliveira, L. S.; Bieber, L. Phenolic Extractives and Natural Resistance of Wood. In *Biodegradation - Life of Science*; Books on Demand, 2013; pp 349−370.

(52) *CRC Handbook of Chemistry and Physics*, 85th ed.; Lide, D. R., Ed.; CRC Press, 2003.

(53) Kogerman, P. N. On the Chemistry of the Estonian Oil Shale "Kukersite". *Oil Shale Res. Lab.* **1931**, *10*, 59−141.

(54) Baird, Z. S. *Predicting Fuel Properties from Infrared Spectra*, 2017.

(55) Biddiscombe, D. P.; Martin, J. F. VAPOUR PRESSURES OF PHENOL AND THE CRESOLS. *Faraday Soc. Trans.* **1958**, *54*, 1316−1322.

(56) Järvik, O.; Baird, Z. S.; Rannaveski, R.; Oja, V. *Properties of Kukersite Shale Oil. Part 1: Experimental Data*, 2020.

(57) Coates, J. Interpretation of Infrared Spectra, A Practical Approach. In *Encyclopedia of Analytical Chemistry*; Meyers, R. A., Ed.; John Wiley & Sons, Ltd, 2001; pp 11498−11520.

Supporting Information

Vapor pressures of phenolic compounds found in pyrolysis oil

Parsa Mozaffari* (parsa.mozaffari@taltech.ee), Oliver Järvik, Zachariah Steven Baird

Tallinn University of Technology, School of Engineering, Department of Energy Technology, Ehitajate tee 5, 19086 Tallinn, Estonia

*corresponding author, phone: +372 58506450

Figure S1. Experimental vapor pressure of biphenyl are shown graphically below: (×) DSC experimental data, (━) Chirico et al [32] (◇) Chipman and Peltier [33], (□) Garrick and Gray[34].
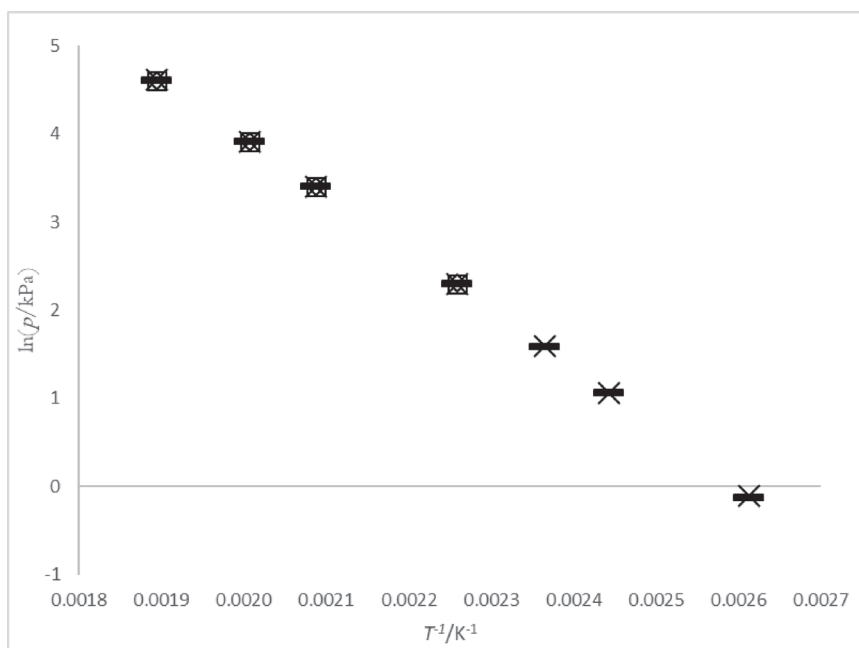
Figure S2. Deviation plot for vapor pressure of biphenyl is provided below. $\Delta p/p = \{(P_{\text{lit}} - P_{\text{e}})\}$ where P_{lit} is the vapor pressure obtained from the literature and P_e is calculated from the Antoine equation fit to the experimental vapor pressure data measured in this work: (+) DSC experimental data, (—) Chirico et al [32], ($\triangle$) Chipman and Peltier [33], ($\square$) Garrick and Gray [34].
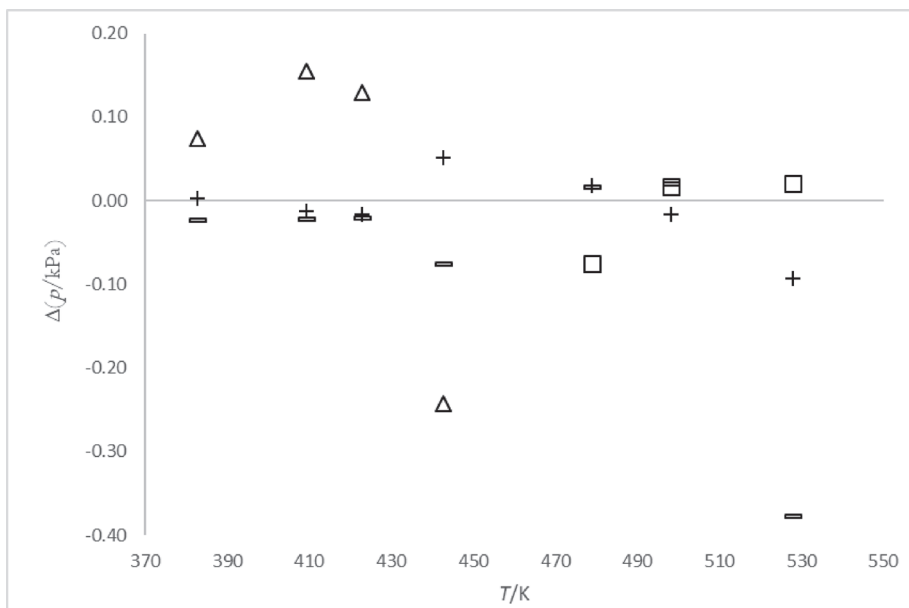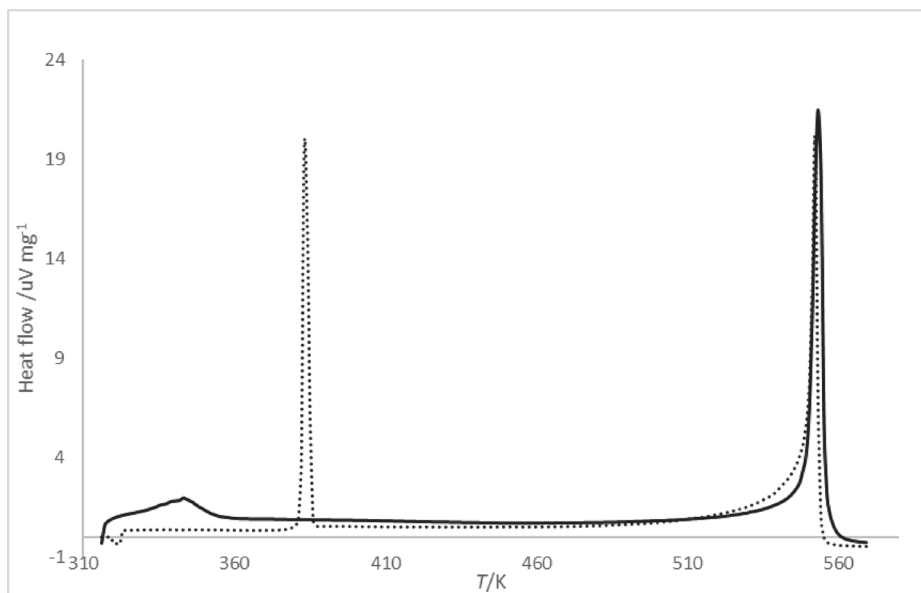
Figure S3. Endotherm of Honeyol™ (solid line) in comparison with 5-methylresorcinol (dashed line) at 700 mbar is shown below. According to Table 2, 62.4% of Honeyol™ is 5-methylresorcinol.

Publication III
Mozaffari, P.; Baird, Z. S, Järvik, O.; (2022). A Predictive Approach towards Using PC-SAFT for Modeling the Properties of Shale Oil. Materials, 15 (12), 4221.

materials

Article

A Predictive Approach towards Using PC-SAFT for Modeling the Properties of Shale Oil

Parsa Mozaffari * [ID]**, Zachariah Steven Baird** [ID] **and Oliver Järvik** [ID]

Department of Energy Technology, School of Engineering, Tallinn University of Technology, Ehitajate tee 5, 19086 Tallinn, Estonia; zachariah.baird@taltech.ee (Z.S.B.); oliver.jarvik@taltech.ee (O.J.)
* Correspondence: parsa.mozaffari@taltech.ee

Abstract: Equations of state are powerful tools for modeling thermophysical properties; however, so far, these have not been developed for shale oil due to a lack of experimental data. Recently, new experimental data were published on the properties of Kukersite shale oil, and here we present a method for modeling the properties of the gasoline fraction of shale oil using the PC-SAFT equation of state. First, using measured property data, correlations were developed to estimate the composition of narrow-boiling-range Kukersite shale gasoline samples based on the boiling point and density. These correlations, along with several PC-SAFT equations of the states of various classes of compounds, were used to predict the PC-SAFT parameters of aromatic compounds present in unconventional oil-containing oxygen compounds with average boiling points up to 180 °C. Developed PC-SAFT equations of state were applied to calculate the temperature-dependent properties (vapor pressure and density) of shale gasoline. The root mean square percentage error of the residuals was 13.2%. The average absolute relative deviation percentages for all vapor pressure and density data were 16.9 and 1.6%, respectively. The utility of this model was shown by predicting the vapor pressure of various portions of the shale gasoline. The validity of this model could be assessed for oil fractions from different deposits. However, the procedure used here to model shale oil gasoline could also be used as an example to derive and develop similar models for oil samples with different origins.

Keywords: Kukersite oil shale; pyrolysis oil; shale oil gasoline fractions; PC-SAFT prediction model

1. Introduction

Models to predict the thermodynamic and transport properties of compounds are of interest to many chemical, oil, and related industries. Models to estimate the phase behavior of fluids in the system are used to design chemical processes and equipment, improve separation processes and product quality, and assess the environmental risks that are inevitably associated with these processes. Therefore, the demand for the use of equations and models applicable to complex mixtures of hydrocarbons has increased considerably [1].

While several predictive correlations for thermodynamic properties of complex mixtures such as oils have been suggested, these models were mainly developed for oils containing small concentrations of heteroatoms with aliphatic and aromatic structures. Therefore, these correlations are not particularly applicable to oils with different structures and compositions. The composition of unconventional oils is different from that of petroleum and varies depending on the source of the oil. As a result, the properties are also different. Shale oil is one such unconventional oil. It is produced by thermally processing organic-rich rocks (oil shale). The conversion technique used for oil shale has been known for a century, and is viewed as the most optimal and efficient thermochemical process to convert shale rock into oil. The advantages of this process have also been extended further for conversion of biomass into biofuel both economically and environmentally [2,3].

Although some basic property prediction correlations developed for petroleum could also be used for shale oil [4], in general, proposed correlations and models developed for

petroleum do not essentially lead to accurate results for shale oil [5–8]. Therefore, these models are usually not suitable for shale oil, and more specifically for Kukersite shale oil, due to differences in composition [9]. Information about the properties of shale oil is limited, and thus, from an engineering point of view, developing such prediction models would be beneficial.

Oils are generally complex mixtures with a large number of different compounds. It is not currently feasible to identify all the compounds and their concentrations in the oil; therefore, simplification for modeling is required. This is generally accomplished by lumping compounds together into groups or classes, which are termed pseudocomponents. Once the pseudocomponent is defined, the properties of all the compounds in the pseudocomponent are described using the average properties of the whole group. The oil as a whole is then modeled as a mixture of these pseudocomponents [10].

One of the simplest methods to define pseudocomponents is to split oil into fractions with narrower boiling points, often through distillation, and measure or estimate the properties of those fractions. These methods are sometimes called bulk property methods, and they do not require any information about the composition of the oil. Because it is a labor-intensive process to measure a full set of properties for many fractions, correlations have been developed for petroleum to estimate a variety of properties from a smaller set of experimental data that are commonly measured for an oil. Generally, only the distillation curve and a second property, such as the density, viscosity, or refractive index, need to be measured to be able to model an oil using these methods [10,11].

A more complex method is to analyze the composition of the oil and then use the data to define the pseudocomponents based on the molecular structure. This is commonly performed by splitting the oil into classes of molecules, for instance, using PNA (paraffins, naphthalenes, aromatics) or SARA (saturates, aromatics, resins, asphaltenes) analysis. These types of the composition analyses refer to characterization methods used to quantitatively determine the amount of each class of compound in an oil. These classes are then further divided by the size of the molecules, i.e., average molar mass or the average number of carbon atoms [10]. The properties of these pseudocomponents can then be estimated based on existing data for pure compounds with the same type of structure. For instance, the properties of paraffin pseudocomponents can be calculated from the properties of pure n-alkanes. For petroleum, there are even correlations that allow the composition of oil to be calculated based simply on the measured properties of an oil and its fractions [10]. Modern analytical techniques, such as gas chromatography and mass spectroscopy, can provide even more detailed data, allowing the pseudocomponents to be defined closer to the level of individual compounds [12]. However, these analytical techniques are expensive and time-consuming, so in industry, the simpler characterization schemes are usually used [11].

If possible, the goal is often to model the pseudocomponents and the oil as a whole using an equation of state. Equations of state allow many of the properties of a mixture to be modeled over a wide range of temperatures and pressures. Correlations for predicting the equation of state parameters for petroleum pseudocomponents have been developed with this goal in mind [10,13]. In the past, cubic equations of state have often been used. However, cubic equations of state require values for the critical properties of a pseudocomponent, and these properties can be difficult to measure or estimate accurately [10]. In the last two decades, it has become more common to use equations of state based on statistical associating fluid theory (SAFT), especially perturbed-chain statistical associating fluid theory (PC-SAFT), for modeling oils, including bio-oils [1,13–18]. Moreover, several studies indicate the importance and applicability of these equations in the energy industry [19–21].

SAFT models do not require critical property values and they can more accurately calculate the liquid density of a system, which means that density data can also be used in fitting PC-SAFT parameters [1]. Indeed, some systems have been modeled using only density data for parameter fitting [22].

Modeling shale oil has received relatively little attention. As previously stated, because shale oil has a much different composition than petroleum, the validity of correlations and

models developed for petroleum is predominantly questionable for shale oil. Based on our literature survey, the only correlations that attempt to provide some sort of systematic modeling framework for shale oil were published in 1930 by Kogerman and Kõll [23], in 1934 by Luts [24], and in 1951 by Kollerov [25]. All three of these publications rely in large part on the experimental data from Kogerman and Kõll [23], which was from only a single distillation of oil from an experimental generator retort. These studies focused mainly on shale oil from Estonian Kukersite oil shale, and shale oils from other deposits have received even less attention.

One of the main obstacles to developing correlations for shale oil has been the lack of data [26]. The new data that have been measured now provide an opportunity to perform this modeling work [27]. Here, we provide correlations that allow gasoline fractions of Kukersite shale oil to be defined in terms of pseudocomponents, and then we present equations for calculating the PC-SAFT parameters of these pseudocomponents. Note that, based on the type of oil shale and the pyrolysis method used, the properties of shale oils can change greatly [28–32]. Therefore, the models developed for Kukersite gasoline shale oil probably cannot be directly used for modeling shale oils from other deposits. However, the approach developed for this purpose could be generally applied to model other shale oils.

2. Modeling Methods

2.1. Industrial Samples

Several wide Kukersite shale oil gasoline fractions with a boiling range from about 40 to about 200 °C were obtained from Eesti Energia's Oil Plant (Narva, Estonia). The technology developed for processing oil shale in this plant was described by Neshumayev et al. [33]. These wide fractions were then separated into narrow-boiling-range fractions using different distillation methods. The sample preparation and distillation methods were previously described by Järvik et al. [34]. These fractions were received from the plant at different times in the hopes of capturing the natural range of variation in the composition of shale gasoline. Over this two-year period, 6 different distillations were performed to fractionate the gasoline samples received. These differences in composition and distillation method should help ensure that the model works for a variety of Kukersite gasoline samples.

2.2. Compositional Analysis

Generally, the properties of oil fractions depend on the chemical composition of these fractions. Obtaining a relationship between chemical composition and the properties of gasoline fractions could allow the composition of a sample to be predicted from basic physical properties. This is important because PC-SAFT models generally require information about the composition.

Several investigations were previously carried out on the composition and characteristics of Kukersite shale oil [35–40]. In these works, the chemical composition of Kukersite shale gasoline was provided for different retorts. Having considered these data, the compositions (mass%) of gasoline fractions used in this work were estimated, mainly based on the detailed data that are partially available in the study published by Gubergrits et al. [34,40]. In this study, the same technology (the Galoter process) was used to obtain shale oil. In Estonia, this technology was developed later than other processes and it is currently the main technology used to produce shale oil.

For the gasoline fractions studied in this work, different properties such as the hydrogen–carbon ratio, infrared spectra, and hydroxyl group content were measured. The behavior of these properties was previously discussed [34]. Almost all the measurements were repeated at least once and if large difference was observed, then additional measurements were carried out for better reliability. Based on these properties, reasonable assumptions about the composition were made so that the changes in the main classes of compounds with average boiling points, up to 180 °C, were carefully defined.

In addition to aromatics, olefins, and paraffins, the rest of the compounds were assumed to be oxygen-containing compounds. Based on the experimental data for gasoline

fractions distilled below 180 °C, the concentration of phenolic compounds is quite low; therefore, phenolic compounds were disregarded for further analysis and modeling. Therefore, for developing the model, four different classes of compounds (olefin, paraffin, aromatic, and oxygen-containing compounds) were considered in total. The oxygen-containing compounds are mostly ketones, aldehydes, and ethers [41]. The change in composition of each class of compound was estimated for different average boiling temperatures. From 40 °C to 180 °C, the amount of each class of compound (i.e., olefin, paraffin, and aromatic and neutral oxygen) was carefully estimated so that these changes were consistent with the FTIR and elemental composition analysis of the studied gasoline fractions. For estimation of the amount of each class of compound, chemical group composition data provided by Luik [42] was also considered. It should be noted that the compositions provided in this work are just estimates and the exact composition is unknown because such detailed data have not been measured before. Although the objective of the present study was to develop a model for Kukersite shale oil gasoline with average boiling points up to 180 °C, the composition was estimated up to 500 °C to facilitate future studies where the modeling of all Kukersite shale oil fractions is of interest. This helps to deliver a systematic and coherent path to extend the study. However, in this study, we focused solely on shale gasoline fraction because additional variables and adjustments are required to model the phenols in the heavier portion of the oil. In other words, the analysis performed in this study is the first step in a multistep process.

It was noticed that numerous fractions have similar boiling points, but differ in other properties, such as density. Because oil samples with the same boiling range can still have different compositions, the effect of density along with boiling point was also included as a second parameter to better model the variations of composition that occur in shale oil. Therefore, the composition of each class of compound was estimated such that these variations were also taken into account. For instance, having considered fractions with similar boiling points, fractions with lower densities are expected to have more olefins and paraffins and fewer aromatic compounds in their composition. To incorporate density into the correlations for composition, first, the densities of all fractions were plotted versus their average boiling point, and this trend was used to calculate the average density at a given boiling point. Compositions were also estimated for fractions with similar boiling points and higher or lower densities. The result was a dataset of fractions with different boiling points and densities along with estimates of their compositions.

The estimated mass percent of each class of compound with respect to average boiling point and density were then fitted using the differential evolution optimizer in the Scipy package for Python [43,44]. All experimental data are available in [27], and the basic correlation considered to fit the variables is as follows:

$$X \;=\; C_0 T_b^2 + C_1 T_b + C_2 + C_3 \rho^2 + C_4 \rho + C_5 T_b \, \rho \qquad (1)$$

In Equation (1), X is the mass percent of the class of compound, T_b is the average boiling point (°C), ρ is the density (kg m^{-3}), and C_0–C_5 are constants obtained from the fitted data. The concentration for neutral oxygen compounds was calculated by difference. Therefore, separate coefficients were not obtained for neutral oxygen compounds.

2.3. Shale Oil Modeling

The shale oil gasoline was modeled using the PC-SAFT equation of state. The PC-SAFT equation of state was thoroughly described by Gross and Sadowsky [1]. This equation is used to predict the thermodynamic behavior of pure and multicomponent systems. For the PC-SAFT equation, the main parameters characterizing a fluid are the segment number (m), segment diameter (σ), and segment energy (ε/k). For neutral oxygen compounds, we also included a polar term, which depends on the dipole moment. The dipole moment for many ketones and aldehydes is 2.7 [45], so this value was used in the model.

These parameters for the aromatic class of compounds were determined by fitting the PC-SAFT equation of state to the measured physical property data, i.e., liquid density, and

the average normal boiling point of the fractions. For data analysis of experimental data and model development, Python (Version 3.9) was used.

For the purpose of developing a model, it was shown by Gross and Sadowsky [1] that Equations (2)–(4) are suitable for correlating parameters for pure compounds with varying molar masses.

The relation for segment diameter (σ_i) as a function of the molecular weight (M_i) is as follows:

$$\sigma_i = q_{01} + q_{11}\frac{M_i - M_{CH_4}}{M_i} + q_{21}\frac{M_i - M_{CH_4}}{M_i}\frac{M_i - 2M_{CH_4}}{M_i} \tag{2}$$

For the chain length to molecular weight ratio, the proposed relation is:

$$\frac{m_i}{M_i} = q_{02} + q_{12}\frac{M_i - M_{CH_4}}{M_i} + q_{22}\frac{M_i - M_{CH_4}}{M_i}\frac{M_i - 2M_{CH_4}}{M_i} \tag{3}$$

In addition, the relationship for the dispersion energy parameter is given as:

$$\frac{\varepsilon_i}{k} = q_{03} + q_{13}\frac{M_i - M_{CH_4}}{M_i} + q_{23}\frac{M_i - M_{CH_4}}{M_i}\frac{M_i - 2M_{CH_4}}{M_i} \tag{4}$$

Here, M_{CH_4} is the molecular weight of methane (M_{CH_4} = 16.043 g mol^{-1}) and q_{jk} are constants to be fitted to pure component parameters (*i* refers to component *i*). For the n-alkane series, these constants were previously published by Gross and Sadowski [1], and these suggested relations were used as a model for paraffins in shale oil. Moreover, Ghosh et al. [46] proposed correlations obtained by fitting the homologous series of 1-alkenes; therefore, these relations were also used for olefin compounds in Kukersite shale gasoline fractions. Correlations for the neutral oxygen compounds (ketones) were obtained from linear regression between PC-SAFT parameters of several pure compounds and their molecular weights. This was implemented to find the line of best fit. Data for neutral oxygen compounds was obtained from the work published by Kleiner and Sadowski [45]. The form of the equation for neutral oxygen compounds and aromatic compounds differed from that of other compounds, for which Equations (2)–(4) were used. Below, the suggested equations for oxygen-containing compounds are shown:

$$f(MW) = \begin{cases} m = C_6\ MW + C_7 \\ \sigma = C_8\ MW + C_9 \\ \frac{\varepsilon}{k} = C_{10}\ MW + C_{11} \end{cases} \tag{5}$$

where C_6 to C_{11} are coefficients obtained from the fit and *MW* is the molecular weight of the pure compounds used (g mol^{-1}).

For aromatic compounds, there are numerous correlations suggested in the literature for pure compounds and petroleum cuts. However, existing correlations yielded poor results when tested for these shale gasoline fractions. This could be expected because aromatic compounds in Kukersite shale oil might not be similar to the pure compounds used for literature correlations. Therefore, although an equation form from the literature was used, the coefficients were optimized to give better results for Kukersite shale oil. The following relations (Equations (6)–(8)) for pure component aromatic compounds were taken from the work published by Gonzalez et al. [47]:

$$m_{aromatic} = q_{01}\ MW + q_{11} \tag{6}$$

$$s_{aromatic} = \frac{q_{02}\ MW + q_{12}}{m_{aromatic}} \tag{7}$$

$$e_{aromatic} = q_{03}\ \log(MW) + q_{13} \tag{8}$$

The coefficients of the correlations for aromatic compounds were fit to experimental data for shale gasoline fractions. The scheme in Figure 1 summarizes the full process

to model shale oil gasoline fractions, including the development of correlations for predicting the composition of shale gasoline samples, which were used in developing the PC-SAFT model.
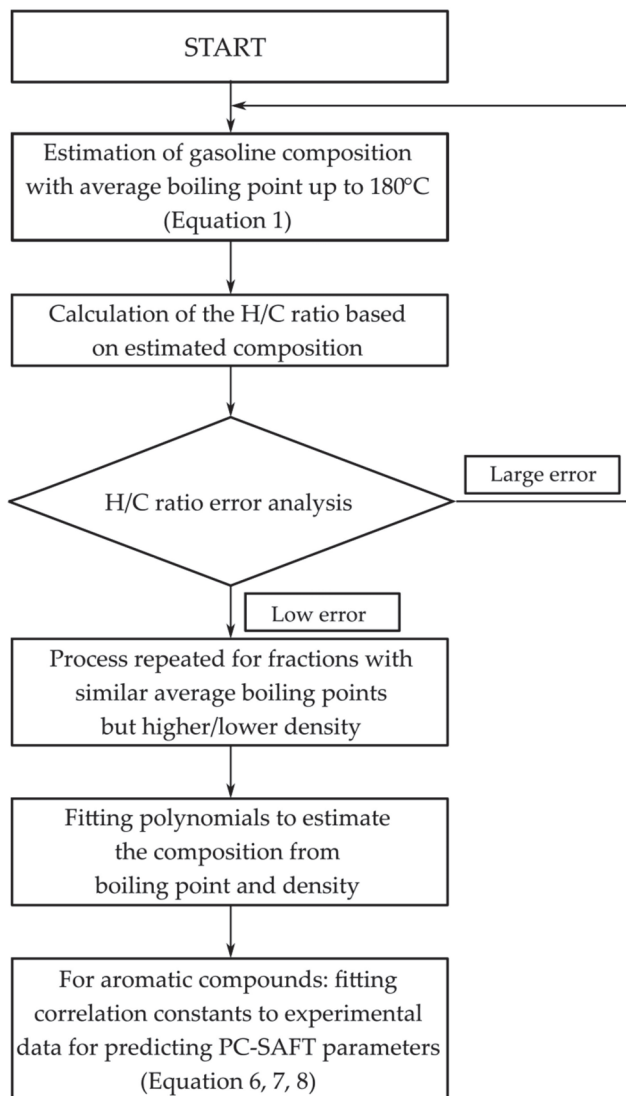

Figure 1. The modeling procedure used in this work for shale oil gasoline fractions.

The estimated hydrogen–carbon ratio was compared with the actual hydrogen–carbon ratio and the average absolute deviation was obtained to be 1.6%.

3. Results and Discussion

Table 1 shows the coefficients for olefins, paraffins, aromatics, and neutral oxygen compounds. These coefficients were used to predict the composition of narrow-boiling-range fractions. Coefficients C_0–C_5 for Equation (1) were regressed for olefin, paraffin, and

aromatic compounds. Then, the content of neutral oxygen compounds was calculated by subtracting the content of other compounds from the total.

Table 1. Correlation constants for predicting the composition of all classes of compounds present in Kukersite shale gasoline fractions.

Classes of Compounds	C_0	C_1	C_2	C_3	C_4	C_5
Olefins	0.00019606	−0.06643364	219.60530800	0.00016198	−0.33551954	−0.00011084
Paraffins	0.00012930	−0.08110412	173.77635700	0.00012325	−0.27158847	−0.00002634
Aromatics	−0.00015131	0.16682950	−52.31917130	−0.00003139	0.10378634	−0.000046658

Using experimental vapor pressure and density data for gasoline fractions up to 180 °C, correlation constants were optimized for predicting the PC-SAFT parameters of aromatic compounds in Kukersite shale gasoline. These constants are shown in Table 2 along with the coefficients from the literature for paraffins and olefins. For most of the fractions, densities were measured at different temperatures, while vapor pressure was only used at the normal boiling point.

Table 2. PC-SAFT correlation constants used for aromatics, paraffins, and olefins.

Correlation Constants	Unit	Aromatic	Olefin *	Paraffin **
q_{01}		0.0230	3.7146	3.7039
q_{11}	Å	0.6411	−0.4797	−0.3226
q_{21}			0.8790	0.6907
q_{02}		0.0823	0.07901	0.06233
q_{12}	mol g^{-1}	3.3062	−0.05266	−0.02236
q_{22}			−0.00175	−0.01563
q_{03}		57.7375	121.09	150.03
q_{13}	K	149.9793	133.62	80.68
q_{23}			15.648	38.96

* The coefficients were published by Gross and Sadowsky [1]. ** The coefficients were published by Ghosh et al. [46].

Coefficients C_6 to C_{11} for oxygen-containing compounds were found from Equation (5), in which PC-SAFT parameters were linearly fit to the molecular weight of several ketones and aldehydes. These coefficients are given in Table 3.

Table 3. Correlation constants for neutral oxygen compounds in Kukersite shale gasoline.

C_6	C_7	C_8	C_9	C_{10}	C_{11}
0.02796	0.90944	0.00244	3.27518	0.05441	242.10097

The root mean square percent error (RMSE) for all compounds was found to be 13.2%. This is a reasonable accuracy for a model for oil samples, especially since the wide fractions were taken at different times from the oil plant; therefore, the properties of these fractions varied. Additionally, different distillation types were used to obtain narrow boiling samples from these wide fractions. These differences ensure that a wide variety of samples and properties were used, and thus they ensure that the model developed for shale gasoline fractions could be used for a broader range of samples. The error for the three-parameter equation of state can be considered reasonable for these types of oils, considering the

complexity of these mixtures and the lack of data on the detailed composition of shale oils. If the results of the prediction model for different properties are considered separately, then the RMSE for density was much lower than that of vapor pressure.

Figures 2 and 3 illustrates the error percent for the vapor pressure and density of all gasoline fractions calculated using the PC-SAFT equation of state. In these figures, the *x*-axis indicates the normal boiling points (nBP) of the gasoline fractions. The smallest errors are mostly for calculated density values. While many errors for individual data points are below 10%, there are several data points that show higher deviations. These outliers comprise 13% of the total data points used for modeling. All these data points with large errors are vapor pressures and for samples with normal boiling points below about 100 °C. For these lower boiling points, one factor contributing to the larger relative errors is that the absolute value of the boiling point is smaller.
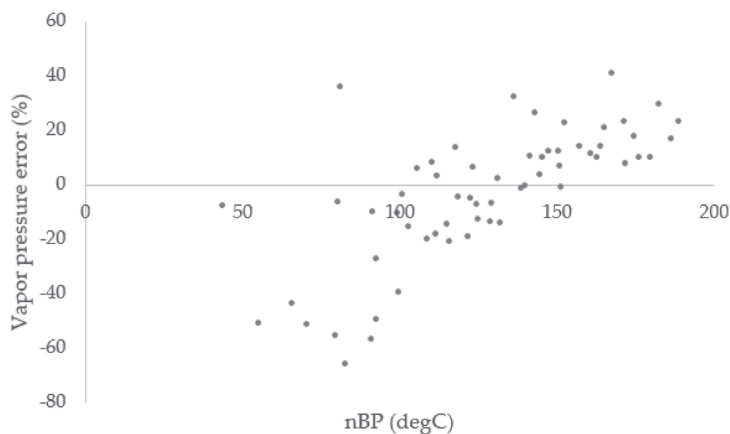

Figure 2. Percent error of the vapor pressure calculated using PC-SAFT for all gasoline fractions analyzed in this work.
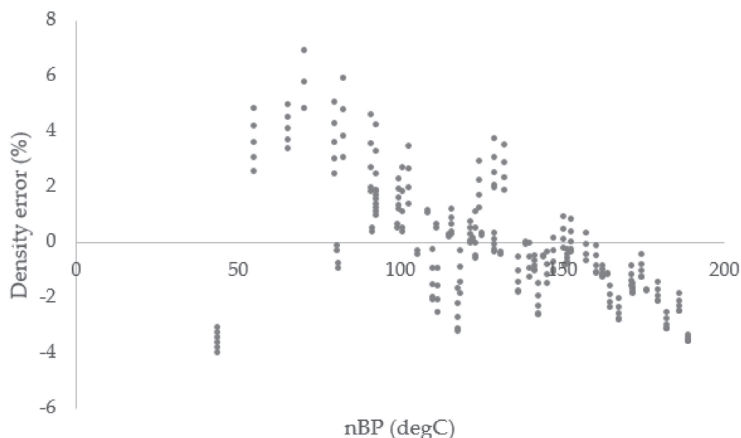

Figure 3. Percent error of the calculated density values.

Using the model, the vapor pressures of gasoline fractions with different average boiling points were predicted and the results are shown in Figure 4. The vapor pressure curves were plotted from approximately 60 to 180 °C. Hypothetical fractions with boiling temperatures were plotted in 20 °C increments in order to present the whole range of light distillates.
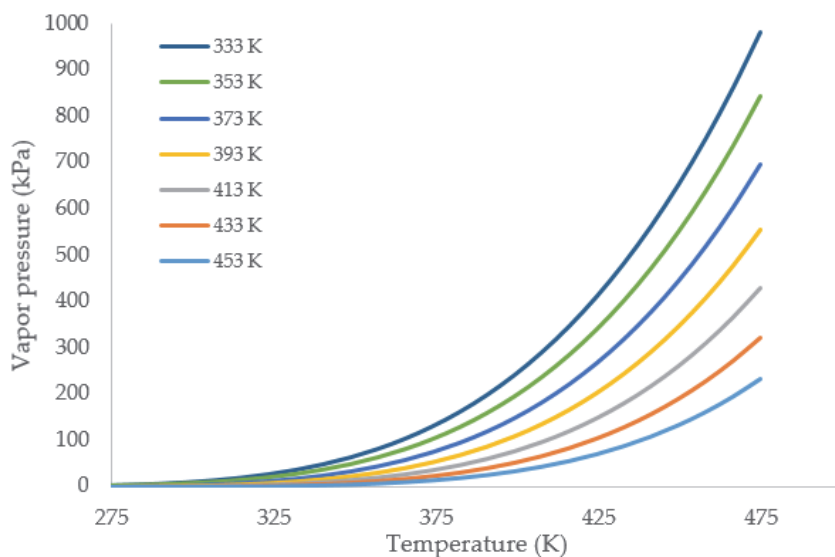
Figure 4. Predicted vapor pressure of gasoline fractions with varying normal boiling points. The values in legends are temperature in Kelvin.

Overall, larger deviation was seen for lower boiling fractions below 100 °C (Figure 2). The average absolute relative deviation percentage (AARD%) between model values and experimental values was calculated using the below equation:

$$AARD\% = \frac{100}{n} \sum_{i=1}^{n} \left(\frac{|x_{exp} - x_{calc}|}{x_{exp}} \right) \tag{9}$$

In Equation (9), x_{calc} is the calculated property value (vapor pressure or liquid density) using the model, x_{exp} is the measured (experimental) value, and n is total number of data points.

The AARD% for all vapor pressure data was 16.9% and this deviation reduced to 11.6% for fractions with average boing points above 100 °C. Additionally, for density prediction, the average absolute deviation was 1.6%, which indicated considerable reliability of the model.

Furthermore, as for comparison with the model, several gasoline fractions were analyzed, and the vapor pressure curves of these fractions were plotted and compared with calculated curve in Figure 5. Some characteristic properties of these fractions were as follows: fraction 1 (T_b = 395 K, ρ = 792.2 kg m^{-3}, MW = 112.4 g mol^{-1}), fraction 2 (T_b = 420 K, ρ = 809.6 kg m^{-3}, MW = 122 g mol^{-1}), fraction 3 (T_b = 425 K, ρ = 818.0 kg m^{-3}, MW = 126 g mol^{-1}). The vapor pressures of these fractions were obtained and compared from about 343 K to 383 K. The expanded uncertainty of vapor pressure measurements at 95% confidence level (k = 2) was found to be 1.5 kPa. Within the experimental temperature range, the largest AARD% for fraction 1 was seen to be 6.8%. However, corresponding absolute deviation was 3.4 kPa. This could be expected due to the low vapor pressure of this fraction. Of all the experimental values for fraction 1, the largest absolute deviation was seen to be at 3.7 kPa. For fractions 2 and 3, the AARD% were 4.8 and 15.8%, respectively. However, despite the larger AARD% for fraction 3, the average absolute deviation was 3.1 kPa.
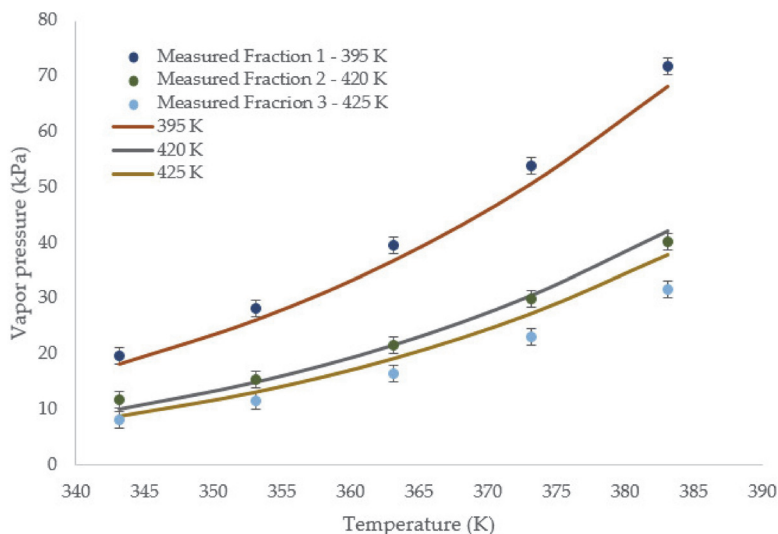
Figure 5. Comparison of measured and calculated vapor pressure of several gasoline fractions. The values in legends are temperature in Kelvin. Error bar shows expanded uncertainty (95% confidence level, k = 2) of measured vapor pressure values.

In general, the developed model showed favorable results when modeling shale oil gasoline fractions. With this analysis as a basis, modeling could be further extended to shale oil fractions with normal boing points above 180 °C [29,34] in the future.

4. Conclusions

In this work, we presented the developed PC-SAFT equation of state model for predicting the 35 gasoline fractions. The model is using normal boiling point and density at 20 °C of a fraction as input parameters. These input parameters were used to estimate the composition of the fraction and consequently to calculate the temperature dependence of vapor pressure and density of shale oil samples. Based on literature data, shale gasoline fractions were assumed to contain four main classes of compounds: olefins, paraffins, aromatics, and oxygen-containing compounds. For estimating the composition, simple polynomial equations were developed using available literature data for the composition of Kukersite shale oil gasoline. Ready-to-use correlations from available literature for olefins and paraffins along with linear equations obtained for oxygen-containing compounds were used to develop respective correlations for aromatic compounds. The resulting model can be used as a property prediction model for shale gasoline samples with normal boiling points below 180 °C.

The suitability of these prediction models for Kukersite shale gasoline was evaluated and the root mean square percent error was 13.2%. Although good results were obtained for Kukersite shale oil, due to the difference in the composition for different shale oils, the applicability of the model could be further assessed once the composition of the main classes of compounds of other shale oils is analyzed.

References

1. Gross, J.; Sadowski, G. Perturbed-chain SAFT: An equation of state based on a perturbation theory for chain molecules. *Ind. Eng. Chem. Res.* **2001**, *40*, 1244–1260. [CrossRef]
2. Li, G.; Hu, R.; Wang, N.; Yang, T.; Xu, F.; Li, J.; Wu, J.; Huang, Z.; Pan, M.; Lyu, T. Cultivation of microalgae in adjusted wastewater to enhance biofuel production and reduce environmental impact: Pyrolysis performances and life cycle assessment. *J. Clean. Prod.* **2022**, *355*, 131768. [CrossRef]
3. Huang, Z.; Zhang, J.; Pan, M.; Hao, Y.; Hu, R.; Xiao, W.; Li, G.; Lyu, T. Valorisation of microalgae residues after lipid extraction: Pyrolysis characteristics for biofuel production. *Biochem. Eng. J.* **2022**, *179*, 108330. [CrossRef]
4. Mozaffari, P.; Baird, Z.S.; Listak, M.; Oja, V. Vapor pressures of narrow gasoline fractions of oil from industrial retorting of Kukersite oil shale. *Oil Shale* **2020**, *37*, 288–303.
5. Rannaveski, R. *Developing a Novel Nethod for Using Thermal Analysis to Determine Average Boiling Points of Narrow Boiling Range Continuous Mixtures*; TalTech: Tallinn, Estonia, 2018.
6. Baird, Z.S.; Uusi-Kyyny, P.; Oja, V.; Alopaeus, V. Hydrogen solubility of shale oil containing polar phenolic compounds. *Ind. Eng. Chem. Res.* **2017**, *56*, 8738–8747. [CrossRef]
7. Baird, Z.S.; Oja, V.; Järvik, O. Prediction of pour Points of kukersite shale oil: Influence of phenols on pour point. In Proceedings of the 10th European Congress of Chemical Engineering, Nice, France, 27 September–1 October 2015; p. 1466.
8. Rannaveski, R.; Listak, M. Flash points of gasoline from Kukersite oil shale: Prediction from vapor pressure. *Agron. Res.* **2018**, *16*, 1218–1227.
9. Mozaffari, P.; Järvik, O.; Baird, Z.S. Vapor pressures of phenolic compounds found in pyrolysis oil. *J. Chem. Eng. Data* **2020**, *65*, 5559–5566. [CrossRef]
10. Riazi, M.R.; Daubert, T.E. Characterization parameters for petroleum fractions. *Ind. Eng. Chem. Res.* **1987**, *26*, 755–759. [CrossRef]
11. Ahmad, M.I.; Zhang, N.; Jobson, M. Molecular components-based representation of petroleum fractions. *Chem. Eng. Res. Des.* **2011**, *89*, 410–420. [CrossRef]
12. Quann, R.J. Modeling the chemistry of complex petroleum mixtures. *Environ. Health Perspect.* **1998**, *106*, 1441–1448. [CrossRef]
13. Rodriguez, G.; Lucia, D. *Modeling of Asphaltene Precipitation and Deposition Tendency Using the PC-SAFT Equation of Etate*; Rice University: Houston, TX, USA, 2008.
14. Chapman, W.G.; Gubbins, K.E.; Jackson, G.; Radosz, M. SAFT: Equation-of-state solution model for associating fluids. *Fluid Phase Equilib.* **1989**, *52*, 31–38. [CrossRef]
15. Saajanlehto, M.; Alopaeus, V. Heavy oil characterization method for PC-SAFT. *Fuel* **2014**, *133*, 216–223. [CrossRef]
16. Saajanlehto, M.; Uusi-Kyyny, P.; Alopaeus, V. Hydrogen solubility in heavy oil systems: Experiments and modeling. *Fuel* **2014**, *137*, 393–404. [CrossRef]
17. Soo, C.-B. *Experimental Thermodynamic Measurements of Biofuel-Related Associating Compounds and Modeling Using the PC-SAFT Equation of State*; École Nationale Supérieure des Mines de Paris: Fontainebleau, France, 2011.
18. Panuganti, S.R.; Vargas, F.M.; Gonzalez, D.L.; Kurup, A.S.; Chapman, W.G. PC-SAFT characterization of crude oils and modeling of asphaltene phase behavior. *Fuel* **2012**, *93*, 658–669. [CrossRef]
19. Nachtergaele, P.; Sin, G.; De Meester, S.; Ruysbergh, E.; Lauwaert, J.; Dewulf, J.; Thybaut, J.W. Simulation of an industrial-scale reactive liquid-liquid extraction tower using polar PC-SAFT toward understanding and improving the hydrolysis of triglycerides. *ACS Sustain. Chem. Eng.* **2021**, *9*, 4735–4743. [CrossRef]
20. Eller, J.; Sauerborn, T.; Becker, B.; Buntic, I.; Gross, J.; Helmig, R. Modeling subsurface hydrogen storage with transport properties from entropy scaling using the PC-SAFT equation of state. *Water Resour. Res.* **2022**, *58*, e2021WR030885. [CrossRef]
21. Ruan, S.-X.; Zhang, X.-B.; Luo, Z.-H. Steady-state and dynamic modeling of the solution polyethylene process based on rigorous PC-SAFT equation of state. *Ind. Eng. Chem. Res.* **2022**, *61*, 6753–6762. [CrossRef]
22. Ji, X.; Held, C.; Sadowski, G. Modeling imidazolium-based ionic liquids with ePC-SAFT. *Fluid Phase Equilib.* **2012**, *335*, 64–73. [CrossRef]
23. Kogerman, P.N.; Kõll, A. *Physical Properties of Estonian Shale Oil*; Oil Shale Research Laboratory: Tartu, Estonia, 1930.
24. Luts, K. *The Estonian Oil Shale Kukersite, Its Chemistry, Technology and Analysis (Der Estländische Brennschiefer-Kukersit, Seine Chemie, Tehnologie und Analyse)*; K. Mattiesens Buchdruckerei Ant.-Ges.: Tartu, Estonia, 1934.
25. Kollerov, D.K. *Physicochemical Properties of Oil Shale and Coal Liquids (физико-химические свойства жидких сланцевых и каменноугольных продуктов)*; State Scientific and Technical Publishing House of Oil and Mining and Fuel Literature: Moscow, Russia, 1951.
26. Oja, V.; Rooleht, R.; Baird, Z.S. Physical and thermodynamic properties of Kukersite pyrolysis shale oil: Literature review. *Oil Shale* **2016**, *33*, 184–197. [CrossRef]
27. Baird, Z.; Järvik, O. Basic Characterization Data. OSF. 2022. Available online: https://osf.io/fqjhd/ (accessed on 27 May 2022).
28. Urov, K.; Sumberg, A. *Characteristics of Oil Shales and Shale-Like Rocks of Known Deposits and Outcrops: Monograph*; Acad. Publ.: Tallinn, Estonian, 1999.
29. Järvik, O.; Oja, V. Molecular weight distributions and average molecular weights of pyrolysis oils from oil shales: Literature data and measurements by SEC and ASAP MS for oils from four different deposits. *Energy Fuels* **2017**, *31*, 328–339. [CrossRef]
30. Guo, S.H. The chemistry of shale oil and Its refining. In *Coal, Oil Shale Natural Bitumen, Heavy Oil and Peat*; EOLSS Publications: Oxford, UK, 2009; Volume 2, pp. 94–106.

31. Oja, V.; Elenurm, A.; Rohtla, I.; Tali, E.; Tearo, E.; Yanchilin, A. Comparison of oil shales from different deposits: Oil shale pyrolysis and co-pyrolysis with ash. *Oil Shale* **2007**, *24*, 101–108.

32. Mozaffari, S.; Järvik, O.; Baird, Z.S. Effect of N_2 and CO_2 on shale oil from pyrolysis of Estonian oil shale. *Int. J. Coal Prep. Util.* **2021**, 1–15. [CrossRef]

33. Neshumayev, D.; Pihu, T.; Siirde, A.; Järvik, O.; Konist, A. Solid heat carrier oil shale retorting technology with integrated CFB technology. *Oil Shale* **2019**, *36*, 99–113. [CrossRef]

34. Järvik, O.; Baird, Z.S.; Rannaveski, R.; Oja, V. Properties of kukersite shale oil. *Oil Shale* **2021**, *38*, 265–294.

35. Agu, A.; Kask, K. About the determination of the group composition of middle oil fractions of shale oil by chromatographic analysis (Об определении группового состава средних фракций сланцевой смолы методом хроматографического анализа). *Proc. Tallinn Univ. Technol. Ser. A.* **1953**, *51*, 1–16. (In Russian)

36. Barschevski, M.M.; Bezmozgin, E.S.; Shapiro, R.N. *Handbook of Oil Shale Processing (Справочник по переработке горючих сланцев)*; Gostopizdat: Leningrad, Russia, 1963. (In Russian)

37. Blinova, E.A.; Veldre, I.A.; Jänes, H.J. *Toxicology of Shale Oils and Phenols (Токсикология сланцевых смол и фенолов)*; Institute of Experimental and Clinical Medicine: Tallinn, Estonia, 1974. (In Russian)

38. Eisen, O.G.; Rang, S.A. *Individual Composition of Shale Oil Hydrocarbons*; Institute of Chemistry, Academy of Sciences of Estonian SSR: Tallinn, Estonia, 1968.

39. Oja, V.; Rooks, I.; Elenurm, A.; Martins, A.; Uus, E.; Milk, A. *An Evaluation of the Potential for Application of Gasification Technology for Oil Shale Production in Estonia (Gaasistamistehnoloogiate Rakendusvõimaluste Hindamineeestis) Põlevkiviümbertöötlemiseks*; Chemical Engineering Department, Tallinn University of Technology: Tallinn, Estonia, 2006. (In Estonian)

40. Gubergrits, M.J.; Rohtla, I.; Elenurm, A.; Myasoyedov, A.M. Comparison of light oil products from oil shale retorting in solid heat carrier units UTT-3000 and UTT-500. *Oil Shale* **1989**, *6*, 189–194. (In Russian)

41. Kekisheva, L.; Krainyukova, N.; Zhirjakov, Y.; Soone, J. A review on basic methods of extraction of neutral oxygen compounds from shale oil, their composition and properties. *Oil Shale* **2004**, *21*, 173–178.

42. Luik, H. Chemical and Other Products from Shale Oil. *Coal Oil Shale Nat. Bitum. Heavy Oil Peat* **2000**, *2*, 107–128.

43. Storn, R.; Price, K. Differential Evolution—A Simple and Efficient Heuristic for global Optimization over Continuous Spaces. *J. Glob. Optim.* **1997**, *11*, 341–359. [CrossRef]

44. Jones, E.; Oliphant, T.; Peterson, P. SciPy: Open Source Scientific Tools for Python. 2001. Available online: https://scipy.org/ (accessed on 24 April 2021).

45. Kleiner, M.; Sadowski, G. Modeling of polar systems using PCP-SAFT: An approach to account for induced-association interactions. *J. Phys. Chem. C* **2007**, *111*, 15544–15553. [CrossRef]

46. Ghosh, A.; Chapman, W.G.; French, R.N. Gas solubility in hydrocarbons—A SAFT-based approach. *Fluid Phase Equilib.* **2003**, *209*, 229–243. [CrossRef]

47. Gonzalez, D.L.; Hirasaki, G.J.; Creek, J.; Chapman, W.G. Modeling of asphaltene precipitation due to changes in composition using the perturbed chain statistical associating fluid theory equation of state. *Energy Fuels* **2007**, *21*, 1231–1242. [CrossRef]

Curriculum vitae

Personal data

Name:	Parsa Mozaffari
Date of birth:	08-09-1992
Place of birth:	Tehran, Iran
Citizenship:	Iranian

Contact data

E-mail:	parsamozaffari@yahoo.com

Education

2017–2022	Tallinn University of Technology – PhD
2014–2016	University of Aberdeen – MSc
2010–2014	Univerity of Indoensia – BSc
2006–2009	Allame Tabatabaei High school

Language competence

Persian	Native
English	Fluent
Estonian	A2

Elulookirjeldus

Isikuandmed

Nimi:	Parsa Mozaffari
Sünniaeg:	08-09-1992
Sünnikoht:	Teheran, Iraan
Kodakondsus:	Iraanlane

Kontaktandmed

E-post:	parsamozaffari@yahoo.com

Hariduskäik

2017–2022	Tallinna Tehnikaülikool – PhD
2014–2016	Aberdeeni Ülikool – MSc
2010–2014	Indoneesia ülikool – BSc
2006–2009	Allame Tabatabaei keskkool – keskharidus

Keelteoskus

Pärsia keel	Emakeel
Inglise keel	Kõrgtase
Eesti keel	Algtase